# Recovery Act: Novel Oxygen Carriers for Coal-fueled Chemical Looping (DE-FE0001808)

# **Final Report**

(January 1<sup>st</sup>, 2010 – February 28<sup>th</sup>, 2013)

#### Submitted to:

#### **Bruce Lani**

U. S. Department of Energy National Energy Technology Laboratory Email: Bruce.Lani@NETL.DOE.GOV

#### Submitted by:

#### Drs. Wei-Ping Pan and Yan Cao

Institute for Combustion Science and Environmental Technology
Western Kentucky University
Bowling Green, KY, 42101

Phone number: (270)792-3776, and (270)779-0202 Email: wei-ping.pan@wku.edu, and yan.cao@wku.edu

Feb 15, 2013

ICSET, WKU December, 2012

#### **DISCLAIMER**

This report was prepared as an account of work sponsored by an agency of the United States Government. Neither the United States Government nor any agency thereof, nor any of their employees, makes any warranty, express or implied, or assumes any legal liability or responsibility for the accuracy, completeness, or usefulness of any information, apparatus, product, or process disclosed, or represents that its use would not infringe privately owned rights. Reference herein to any specific commercial product, process, or service by trade name, trademark, manufacturer, or otherwise does not necessarily constitute or imply its endorsement, recommendation, or favoring by the United States Government or any agency thereof. The views and opinions of authors expressed herein do not necessarily state or reflect those of the United States Government or any agency thereof.

#### **ABSTRACT**

Chemical Looping Combustion (CLC) could totally negate the necessity of pure oxygen by using oxygen carriers for purification of CO<sub>2</sub> stream during combustion. It splits the single fuel combustion reaction into two linked reactions using oxygen carriers. The two linked reactions are the oxidation of oxygen carriers in the air reactor using air, and the reduction of oxygen carriers in the fuel reactor using fuels (i.e. coal). Generally metal/metal oxides are used as oxygen carriers and operated in a cyclic mode. Chemical looping combustion significantly improves the energy conversion efficiency, in terms of the electricity generation, because it improves the reversibility of the fuel combustion process through two linked parallel processes, compared to the conventional combustion process, which is operated far away from its thermo-equilibrium. Under the current carbon-constraint environment, it has been a promising carbon capture technology in terms of fuel combustion for power generation. Its disadvantage is that it is less mature in terms of technological commercialization.

In this DOE-funded project, accomplishment is made by developing a series of advanced copper-based oxygen carriers, with properties of the higher oxygen-transfer capability, a favorable thermodynamics to generate high purity of CO<sub>2</sub>, the higher reactivity, the attrition-resistance, the thermal stability in red-ox cycles and the achievement of the auto-thermal heat balance. This will be achieved into three phases in three consecutive years. The selected oxygen carriers with final-determined formula were tested in a scaled-up 10kW coal-fueled chemical looping combustion facility. This scaled-up evaluation tests (2-day, 8-hour per day) indicated that, there was no tendency of agglomeration of copper-based oxygen carriers. Only trace-amount of coke or carbon deposits on the copper-based oxygen carriers in the fuel reactor. There was also no evidence to show the sulphidization of oxygen carriers in the system by using the high-sulfur-laden asphalt fuels. In all, the scaled-up test in 10 kW CLC facility demonstrated that the preparation method of copper-based oxygen carrier not only help to maintain its good reactivity, also largely minimize its agglomeration tendency.

# **TABLE OF CONTENTS**

TABLE OF CONTENTS	4
LIST OF FIGURES	5
LIST OF TABLES	7
1. Executive Summary	8
1.1 Overview of the Technology	8
1.2 Goals and Objectives for the Project	10
1.3 Task 1 - Project Management and Planning	11
1.4 Task 2 - Preparation of Oxygen Carriers	12
1.5 Task 3 - Selection of Oxygen Carriers	15
1.6 Task 4 - Evaluation of Oxygen Carriers in a 10 kW Hot-Model CLC Facility .	18
1.7 Conclusions and Issues for Further Study	23
2. Report Body	25
2.1 Background	25
2.2 Preparation of Oxygen Carriers	30
2.3 Evaluation of Prepared Oxygen Carriers in 100W CLC Facility	59
2.3.1 Preparation and Characterization of Selected Coals and Their Ash	59
2.3.2 Lab-scale fluidized bed CLC facility	64
2.3.3 Cyclic Operations of Coal-fired Chemical Looping Combustion (20 cycles) .	67
2.3.4 Characterization of Used Oxygen Carriers from Coal-fired CLC Combustion	n72
2.4 Evaluation of Prepared Oxygen Carrier in 10 kW CLC Facility	76
2.5 Oxygen Carrier Uncoupling.	85
2.6 Conclusion	91
2.7 Acknowledgement	93
3. References	94

# LIST OF FIGURES

Figure 1. Figure 1. Particle size distribution of supporting materials of oxygen carriers	36
Figure 2. SEM images and EDX analysis of supporting material (after treated under 800 $^{\rm o}$	C in
air)	36
Figure 3-1. CA series samples	37
Figure 3-2. CA series after reduction using asphalt	38
Figure 3-3. CA series after 20 cycles of redox in air-H <sub>2</sub> using Chemisorb instrument	38
Figure 4. cycles of redox tests with CCA series samples	39
Figure 5-1. LCA series- Original samples.	40
Figure 5-2. LCA series sample under 50 cycles of redox using H <sub>2</sub> Chemisorb	41
Figure 6-1 Pore size distribution analysis	43
Figure 6-2 Pore size distribution analysis	44
Figure 6-3 Pore size distribution analysis	45
Figure 6-4 Pore size distribution analysis	46
Figure 6-5 Pore size distribution analysis	47
Figure 7-1 XRD analysis CA series sample	48
Figure 7-2. XRD analysis	50
Figure 8. ChemiSorb instrument (air-H <sub>2</sub> cycles)	52
Figure 9. Measurement of CuO loading amount and evaluation on prepared oxygen carrie	rs and
evaluation of redox performance of prepared oxygen carriers using air-H <sub>2</sub>	
ChemiSorb	53
Figure 10: TGA results of copper-based oxygen carrier – totally 864 cycles (H <sub>2</sub> as Fuel)	57
Figure 11. Strength tests of oxygen carrier using attrition test facility and preliminary resu	lts58
Figure 12. Characterization of combustion and gasification reactivity of tested coal	62
Figure 13. Particle size distribution of selected coal samples and oxygen carriers	63
Figure 14-1. Schematic of lab-scale test facility on chemical looping	
combustion	66
Figure 14-2 Picture of lab-scale test facility on chemical looping combustion	66
Figure 15. Profiles of gas concentrations at the exit of fuel reactor.	70
Figure 16. Thermodynamics analysis of interaction of CuO-Cu and sulfur	71
Figure 17. Crystal analysis of fresh and used oxygen carrier samples	73
Figure 18. The phase diagram for CuO and Cu <sub>2</sub> O (P <sub>O2</sub> - T)	73

Figure 19. SEM pictures of performance-improved oxygen carriers (after 20 cycles operation	).74
Figure 20. Analysis of pore surface and pore structure in nanometer level (fresh and used oxy	ygen
carriers)	75
Figure 21. Technical history of development of solid recirculation system in ICSET	Γof
WKU	76
Figure 22-1 1 <sup>st</sup> -8-hour run in 10 kW CLC facility	78
Figure 22-2 2 <sup>nd</sup> -8-hour run (100 % natural gas firing) in 10 kW CLC facility	79
Figure 22-3 3 <sup>rd</sup> -8-hour run (100 % natural gas firing) in 10 kW CLC facility	80
Figure 23-1 SEM pictures of used oxygen carriers firing in for 3 day totally 24-hour (	Fuel
reactor)	81
Figure 23-2 SEM pictures of used oxygen carriers firing in for 3 day totally 24-hour	(Air
reactor)	81
Figure 24: TGA curves for the three copper oxide oxygen carriers under nitro	ogen
flow	.86
Figure 25: XRD analysis of the entrained commercial CuO powder on the filter paper	88
Figure 26-1 Decomposition of copper oxide sample in a quartz reactor	89
Figure 26-2 Commercial CuO and CLCA sample 800 °C through 990 °C	.90
Figure 26-3. SEM image of CLCA	.90
Figure 27. Equilibrium curves of CuO, Cu <sub>2</sub> O and O <sub>2</sub>	.90

# LIST OF TABLES

Γable 1. Initial trials on increasing loading amount of CuO on Al <sub>2</sub> O <sub>3</sub>	52	
Table 2. Properties of coal and ash	61	
Table 3. Summary of test condition and results	69	
Table 4. Copper oxide contents on the collected oxygen carrier samples	83	
Table 5. The carbon and sulfur contents in the used oxygen carriers	84	

# 1. Executive Summary

## 1.1 Overview of the Technology

The project PMP document provides with the guideline, by which all project tasks have been finished. There are three categories of oxygen carrier samples have been prepared as planned. All three categories copper-based oxygen carrier use porous Al<sub>2</sub>O<sub>3</sub> as supporting materials. An extensive evaluation of all three categories of oxygen carrier samples, in the TG and the bench-top fluidized bed reactor, indicated the significant agglomeration of copper on surface of supporting materials with formula of Category 1 and 2 oxygen carriers. This brought up with efforts on Category 3 oxygen carrier sample, which was finally selected as the final formula for its scaling-up. It is made of the porous Al<sub>2</sub>O<sub>3</sub>, impregnated with 20-30% (by weight) of copper oxide. Its performance is enhanced by the raw earth metal (such as lanthanum) and dispersion agent (centric acid). It was initially passed an life-span evaluation test (864 redox cycle) using TG. This finalized Cu-based oxygen carrier presents very good reactivity, less agglomeration tendency and prevention from carbon and sulfur deposits and thermal stability in performance tests in a bench-top fluidized bed reactor.

This is finally followed-up by its tests in a 10 kW chemical looping combustor, fueled by natural gas, or a mixing fuel including natural gas and asphalt. This 10 kW CLC facility is built-up with supporting funds from a Canadian natural gas company. This scaled-up evaluation tests (2-day, 8-hour per day) indicated that, there was no tendency of agglomeration of Category 3 oxygen carrier sample. The evaluation of used oxygen carrier samples, collected after the test, indicated only trace-amount of coke or carbon deposits on the copper-based oxygen carriers in the fuel reactor. This indicated there may be a tendency of carbon deposits under current operational conditions, but the carbon deposits had been largely controlled by the system tuning (system temperatures for achieving higher fuel conversion efficiency). There was also no evidence to show the sulphidization of oxygen carriers in the system by using the high-sulfur-laden asphalt fuels, only the trace-amounts of sulfur on samples in two baghouses,

where temperatures were as low as 150 °C. This matched well with theoretical thermodynamics calculation regarding correspondences of temperatures and sulphidization of copper-based oxygen carriers. In all, the scaled-up test in 10 kW CLC facility demonstrated the acceptable performance of Category 3 copper-based oxygen carrier developed in this project.

The major issue found in this long-term evaluation test in a scaled-up CLC facility was the attrition loss of active ingredient (copper). Unlike those tests in TG, where oxygen carrier was kept in static status for the testing period, high circulation rates of oxygen carrier was maintained during the continuous operations of the 10 kW CLC pilot. Collisions of oxygen carrier particles against themselves and the reactors and cyclones were constant, resulting in the breakage of oxygen carrier particles. Because of our preparation method in this project, the active ingredient of Cu-CuO remained in the surface shells of the oxygen carriers, where attrition occurred as a result of the particle-particle and particle-wall collisions. The outcome was the loss of the active ingredients which were collected in the filter bags and not returned to participate in the recirculation inside the reactors.

During this project, the spaniel structure of CuAl<sub>2</sub>O<sub>4</sub> (the interaction between CuO and Al<sub>2</sub>O<sub>3</sub>), was found the major reason to stable prepared copper-based Category 3 oxygen carrier. On the other hand, it indicated the instability of selected porous Al<sub>2</sub>O<sub>3</sub> supporting materials, which previously thermally-tough under higher temperatures. Combining this insightful finding and the aforementioned finding, regarding loss of the outmost surface copper, some additional work was continued to generate Category 4 copper-based oxygen carrier. In this formula, more thermally-stable TiO<sub>2</sub> was selected as the supporting material, the preparation method is based on the mechanic mixing (MM), wet impregnation (WI), sol-gel method (SG). The purposes of this study is to investigate how the preparation methods affect the dispersion and melting performance of copper on supporting material, TiO<sub>2</sub>. Copper cannot combine with titanium dioxide to produce copper titanate until a very high temperature (over 1000°C). At 1350°C, both copper (through decomposition of CuO) and copper titanate (through interaction between CuO and TiO<sub>2</sub>) appeared out of original phases of CuO and TiO<sub>2</sub>. The SG method prepared oxygen

carrier, compared to other two methods (MM method and WI method), could let CuO well dispersed on the supporting material TiO<sub>2</sub>. The prepared oxygen carriers based on the SG method presented the least variance and standard deviation, which are 2% and 14%, respectively. This was contrast to 3% and 17% in variance and standard deviation for samples based on WI method, and even larger to 25% and 50 % for samples based on MM method. Therefore, the SG method provided an opportunity of better dispersion of Cu on TiO<sub>2</sub> under conditions of same Cu loading.

Some other practices, happened in this project include search the inexpensive supporting materials and copper source, such as copper minerals to bring down costs of oxygen carrier. This practice was not continued after the initial trials, because 1) inexpensive clay supporting material generally contains calcium (CaO), which could traps sulfur in the fuel reactor and later on release in the offgas of the air reactor in a dilute concentration. This may cause burdens of sulfur emission controls. 2) Copper mineral was initially identified to be less rich in copper content, thus infeasible to be oxygen carrier with higher oxygen loading capability.

Regarding potentials of reactivity enhancement through the chemical looping uncoupling when copper is used, our tests presented the  $Al_2O_3$  support significantly impacts the oxygen releasing performance and thermal stability of the CuO on  $Al_2O_3$  oxygen carrier, comparing with the commercial CuO powder. The kinetics of the  $O_2$  release from CuO decomposing to copper (I) oxide ( $Cu_2O$ ) was slow and temperature-dependent. However, there was no serious agglomeration of CuO on  $Al_2O_3$  oxygen carriers. This contrasted the severe agglomeration of commercial CuO powder. The quick formation of a new crystal phase ( $CuAl_2O_4$ ) cross-linking CuO and  $\gamma$ - $Al_2O_3$  may be the major reason contributing to both the stability of copper-based oxygen carrier under severe uncoupling condition (close to melting point of copper), and slow kinetics of  $O_2$  release. It was also found the reactor material was highly active, such as iron in the regular stainless steel, and likely consumed the released oxygen. This could be largely minimized when the reactor was made of quartz material.

#### 1.2 Goals and Objectives for the Project

Goals. The goal of the project is to develop a series of advanced oxygen carriers for CLC looping combustion. The development of the advanced oxygen carriers will focus on improving overall physical and chemical characteristics and test carriers in an actual CLC facility. Project goals include: 1) Developing attrition-resistant and thermally stable oxygen carriers to achieve an auto-thermal heat balance of the processes for generating high purity CO<sub>2</sub> with favorable kinetics; 2) Evaluating the impacts of scale-up methods and application of inexpensive raw materials (copper-based minerals and widely-available inexpensive clays) for preparation of oxygen carriers on reaction performance in testing within hot-model conditions; 3) Preparing multi-metal or free-oxygen-releasing oxygen carriers and exploring their optimal formula and reaction mechanisms; 4) Evaluating the adaptability of prepared oxygen carriers to diversified fuels in the hot-model tests and investigating methods for eliminating carbon deposits on oxygen carriers.

**Objectives:** This project is accomplished by developing a series of advanced oxygen carriers, with properties of the higher oxygen-transfer capability, a favorable thermodynamics to generate high purity of CO<sub>2</sub>, the higher reactivity, the attrition-resistance, the thermal stability in red-ox cycles and the achievement of the auto-thermal heat balance. The developed oxygen carrier will be integrated into operations of a scaled-up chemical looping combustion process to generate pure CO<sub>2</sub>. This will be achieved into three-stage in three consecutive years. In Stage I, basic formula of oxygen carriers will be determined; in Stage II, interferences of prepared oxygen carriers under high-sulfur-chlorine will be eliminated; in Stage III, oxygen carriers with final-determined formula will be subject to be tested in a 10kW chemical looping combustion facility.

#### 1.3 Task 1 - Project Management and Planning

#### A. Summary of Project Management Activities and Meeting of ARRA Requirements

The Sponsored Programs of WKU is the compliance management for the entire campus. They are responsible for both the fiscal compliance, in addition to the coordination and implementation of pre and post-award documentation. Dr. Wei-Ping Pan is the Principal

Investigator of the project, and is responsible for the carrying out of the objectives outlined in this proposal. Dr. Yan Cao, serve as the Co-Principal Investigator, who is responsible for directing the team in carrying out the objectives outlined. Terrill Martin acts as the facility fiscal manager, and is responsible for the financial reports are done and accurate, procure materials and supplies for the project, and ensure that expenditures are within the guidelines established. Graduate students Mr. Yin Wen, Chia-Wei Lin, Yaowen Cui, and many other student interns were being trained during this program. Several technicians, Marten Cohron, William Ondorff, Kevin Ducket were assisting both the PI and Co-PI in the actual carrying out of the scaled-up 10 kW tests.

#### 1.4 Task 2 - Preparation of Oxygen Carriers

A. Goal and Objectives of the Task

Initially, previous experience on the preparation of oxygen carriers will be reviewed and passed onto new team within this project. Based on previous work, three guidelines on preparation of oxygen carriers will be setup and followed during preparation. At this initial stage of the project, management of personnel, method procedures and sample naming system will be setup. Prevention of risks of material development will be realized by applying a minimum amount of additive for stabilization of quality of prepared oxygen carriers. In order to optimize development process, we will have two teams (Dr. Pan with one student and Dr. Cao with another student), and each team will work on three categories of oxygen carriers independently, but will frequently share success/failure experiences during material development.

There are three subtasks in the Task 2. **Subtask 2.1** (Development of Category 1 Oxygen Carriers) addresses that, inexpensive procedures that utilize inexpensive traditional copper-based compounds to synthesize targeted non-traditional copper-based compounds will be investigated; **Subtask 2.2** (Development of Category 2 oxygen carriers) addresses that, a systematic test matrix will be conducted to search the best performance on the durability of oxygen carriers which will be based on the test results using ASTM standard attrition procedure (ASTM

D5757-95). The dry or wet impregnation method to load the oxygen carriers on the different supporting materials will also be included in this subtask. Our goal on the durability and attrition-resistance of prepared oxygen carriers is to maintain the chemical and physical properties of the oxygen carriers after more than 50 cycles test runs. **Subtask 2.3** (Development of Category 3 oxygen carriers) addresses, **i**nvestigate mechanisms on observed contamination impacts from copper-based compounds on formation of Si and Al porous structures to find an optimal procedure to prevent this impact on pore-development and to optimize preparation procedures.

#### B. Apparatus and Testing Methods

**TPR-TPO cyclic Test Facilities.** The copper loading amount and the durability of prepared oxygen carriers were initially evaluated under TPR(10%H<sub>2</sub>)-TPO(air) (Temperature Programmed Reduction and Oxidation) cycles in a Micrometrics ChemiSorb 2720 instrument. 25mL/min of 10% hydrogen in argon was introduced into ChemiSorb system to reduce the prepared oxygen carriers under programmed temperature from room temperatures to 800 °C at a temperature ramp rate of 20 °C/min. This was followed by dropping the temperatures to room temperature with argon. Then air was introduced into the instrument for oxidation at the similar temperature ramp at 20 °C/min. An alternative method was to maintain a constant temperature of 800 °C between reduction and oxidation cycles. The test procedure of Scheme 1 was applied to samples Category 1 and 2 samples, and both Scheme 1 and Scheme 2 were applied to Category 3 sample. During the redox cycle, oxygen carriers were fully reduced and fully oxidized. Both procedures were repeated until the desired number of Redox cycles of prepared oxygen carriers was reached. The calibration curve of hydrogen intensity as a function of CuO concentration was established using different amounts of pure CuO in the system and also the calibration curve of hydrogen amount was setup to verify the hydrogen consumption. Thus the loading amount of CuO in the supporting materials could be determined using TPR tests.

**Thermal Thermogravimetric (TG)**. A total of 864-cycle redox tests of CLCA sample has been conducted using thermogravimetry (TG) under isothermal condition at 800 °C. Each cycle

consists of five minutes of reduction time with 10% hydrogen in nitrogen, followed by nitrogen purging for 10 minutes, and then oxidation in air for 5 minutes. The multiple TG measurement was obtained using a TA Instruments 2950 TG. The initial sample weight was 20 mg. A platinum pan was used as holder in TG. The time periods for reduction and oxidation cycles were setting to enough long, to allow complete reactions of each cycle.

#### C. Results and Conclusions

In Phase I, successful preparation of CuO-based oxygen carriers using commercially available supporting material (Al<sub>2</sub>O<sub>3</sub>). The prepared oxygen carriers have good performance in redox tests in a bench scale chemical looping combustion facility. These good performances mainly include higher reaction kinetics than Ni-based and Fe-based oxygen carriers under similar operational conditions, acceptable attrition resistance, durability in several cyclic redox tests, and a good resistance to agglomeration; the selected copper-based oxygen carrier has finally been passed 854 redox cycles in TGA, and only minimal degradation was found during this screening tests. The selected sample (labeled as CLCA) was ready for evaluations of interferences with coal-flue-gases and long-term stability in 2 scaled-up facilities, including 100 W and 10 kW CLC facilities.

In order to improve the process kinetics, a concept called chemical looping combustion uncoupling has been put forward. In this uncoupling process, specific metal oxides are selected to directly release free oxygen for the combustion of fuels while the metal oxide is reduced to a lower oxidation state, instead of metal. The free oxygen oxidizes the fuel similar to the conventional oxy-fuel combustion. The major oxygen releasing metal oxides are copper oxide (CuO) and manganese oxide (Mn<sub>2</sub>O<sub>3</sub>). In this study, copper (II) oxide (CuO) on Al<sub>2</sub>O<sub>3</sub> support oxygen carrier, was investigated in view of its oxygen releasing properties and thermal stability. Results indicated the Al<sub>2</sub>O<sub>3</sub> support significantly impacts the oxygen releasing performance and thermal stability of the CuO on Al<sub>2</sub>O<sub>3</sub> oxygen carrier, comparing with the commercial CuO powder. The kinetics of the O<sub>2</sub> release from CuO decomposing to copper (I) oxide (Cu<sub>2</sub>O) was slow and temperature-dependent. However, there was no serious agglomeration of CuO on Al<sub>2</sub>O<sub>3</sub>

oxygen carriers. This contrasted the severe agglomeration of commercial CuO powder. The quick formation of a new crystal phase (CuAl<sub>2</sub>O<sub>4</sub>) cross-linking CuO and  $\gamma$ -Al<sub>2</sub>O<sub>3</sub> may be the major reason contributing to both the stability of copper-based oxygen carrier under severe uncoupling condition (close to melting point of copper), and slow kinetics of O<sub>2</sub> release. It was also found the reactor material was highly active, such as iron in the regular stainless steel, and likely consumed the released oxygen. This could be largely minimized when the reactor was made of quartz material.

864-cycle reduction (5 minutes) and oxidization (5minutes) of the Category 1 copper-based oxygen carrier sample (CLCA) has been accomplished using TG under 800 °C. No major degradation of this oxygen carrier sample based on the first formula was found as shown in Figure 1, in view of process kinetics and oxygen transfer capacity throughout the 864-cycle. 100 % of the conversion efficiency of this first sample could be achieved within 1 minute to 2 minutes throughout the 864-cycle, presenting the perfect reaction kinetics and stability of Category 1 oxygen carrier sample for both reduction reaction using 10 % hydrogen and the oxidization reaction using air. The available oxygen capacity of Category 1 oxygen carrier sample, under the preferable reaction kinetics, was about 18 % -20 %. The formula and preparation procedure have been presented in the previous quarterly report. So far, the evaluation tests on the life-span of the Category 1 oxygen carrier have been accomplished. Investigation of sample residues, after the 864 cycles of reduction and oxidization reactions using this last formula, revealed stability of prepared copper-based oxygen carrier. Three basic analytical tools were used to characterize sample residue to investigate the transformation of crystal structure and material surface, including X-ray Diffraction (XRD), Scanning electron Microscope (SEM), BET and pore structure.

#### 1.5 Task 3 - Selection of Oxygen Carriers

A. Goal and Objectives of the Task

The improvement of chemical formula and preparation procedures of selected categories of

oxygen carriers will be conducted in 2011. The improvement includes kinetics, capacity, and attrition resistance. Good kinetics of oxygen carriers will decrease re-circulation rates inside the loop cycle between the air and fuel reactors, and thus help to decrease the attrition potential and material loss and emissions of trace amounts of metals into the environment. Once sufficient kinetics could be achieved, the amount of active agents on the substrate selected needs to be maximized and attrition resistance needs to be significantly improved. An innovative concept will be explored on coating a hard gas-penetrable layer outside the oxygen carriers. At the end of Task 3, the preparation of oxygen carriers for 10 kW facility tests based on the finalized formula of oxygen carrier shall be started. This includes finalization of the preparation procedure for scaled-up production of oxygen carriers, production of a large amount of oxygen carrier to satisfy several runs at 4-8 hours per run in the aforementioned 10 kW hot-model chemical looping facility.

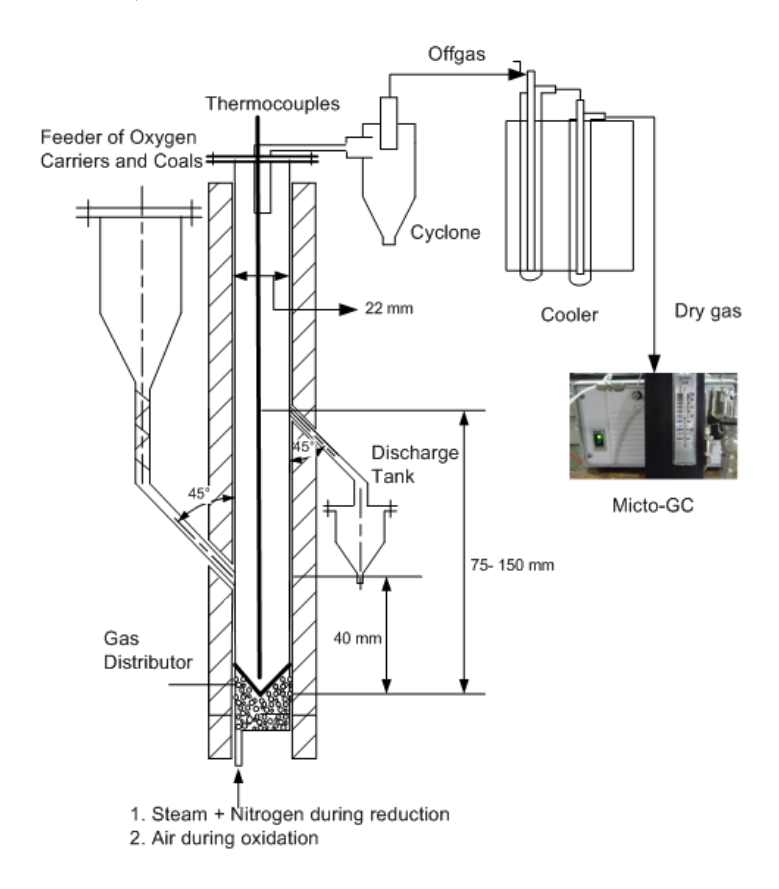
#### B. Apparatus and Testing Methods

The below figure shows the scaled-up facility for preparation of oxygen carriers for firings of the 10 kW CLC facility based on "dry" impregnation method. The initial preparation made up 55 Kg, which was followed-up by the second preparation at amount of about 45 Kg after half year operation of the 10kW CLC facility.





The 100 W fluidized bed reactor was setup for further evaluation of prepared oxygen carrier in real applied conditions, see below.



#### C. Results and Conclusions

Successful setup of a lab-scale 100 W fluidized bed chemical-looping facility to achieve prompt and efficient evaluations of prepared oxygen carriers under direct and continuous coal-oxygen carrier-feeding conditions. Feeding rates of coals and oxygen carriers, reactor temperatures, and solid residence times of oxygen carriers could be flexibly handled in this facility, which greatly help to quickly screen out optimal chemical formula and evaluate reaction kinetics and lifespan of prepared oxygen carriers. The CLC of solid fuel is more comparable to the gasification process of solid fuel. Like gasification of solid fuel, CLC of solid fuel yields less reactive char residue, which needs more severe operational conditions to fully convert it. This causes CLC of solid fuel to face both technical and economic challenges. Based on the kinetics

of combustion and gasification of solid fuels, partial coal gasification and combustion using the chemical looping technology and partial residue char combustion in existing boilers can solve this issue and resolve these challenges within one process cycle. Our studies in the lab-scale CLC facility confirmed that various solid fuels of differing reactivity will be adaptable to achieve the varied carbon conversion efficiencies in a range between 50-100 % under optimal utilization temperatures of CuO at 900-950 °C. Gas concentration profiles at the fuel-reactor exit using Kentucky coal as fuel presents 100 % of CO<sub>2</sub> on an SO<sub>2</sub> free basis (assuming SO<sub>2</sub> is only air pollutants). Sulfur dioxide will be removed prior to sequestrating CO<sub>2</sub> during the initial redox cycles. There was no H<sub>2</sub>, CO or CH<sub>4</sub> found at the fuel exit. A slight degradation of prepared oxygen carriers was found as an indication of the decrease of H<sub>2</sub> in offgas when the cyclic operation approached 20 cycles. Studies also indicated that at 900-950 °C, SO<sub>2</sub> reacted with copper under operational temperatures over 900 °C. This test successfully demonstrated the feasibility of obtaining pure CO<sub>2</sub> for sequestration in the proposed process, and the importance of maintaining temperatures in the fuel reactor.

#### 1.6 Task 4 - Evaluation of Oxygen Carriers in a 10 kW Hot-Model CLC Facility

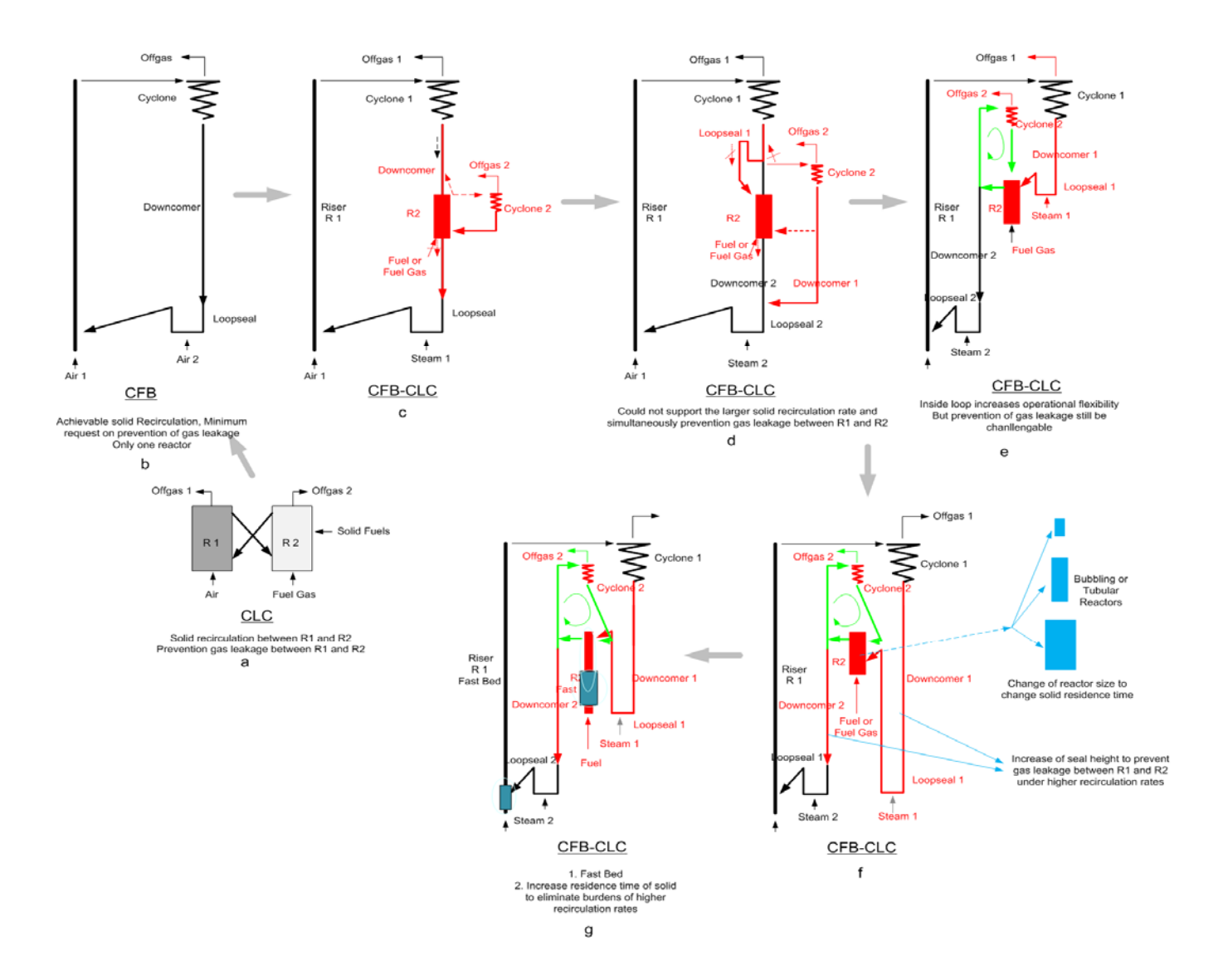
#### A. Goal and Objectives of the Task

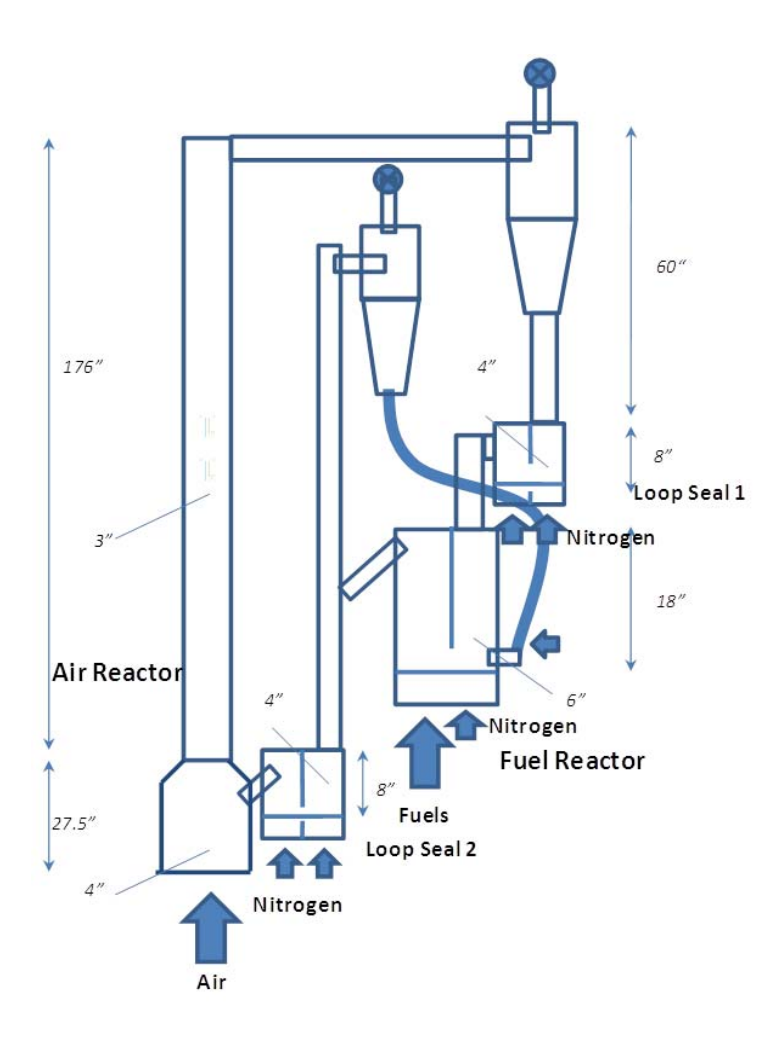
Evaluation of Oxygen Carriers in a 10 kW Hot-Model CLC Facility. The optimized oxygen carriers developed in Task 3 will be tested in the 10 kW hot-model CLC facility to obtain critical design parameters for future demonstration tests. The test period will be sufficient (4-8 hours daily for over two weeks) to evaluate oxygen carrier performance and control strategies of chemical looping facility, as well as to train students to grasp the mechanism and procedure to handle the hot-model test facility, which will greatly improve their practical skills.

#### B. Apparatus and Testing Methods

A flexible cold chemical looping facility to achieve the solid recirculation between air and fuel reactors, based on a concept of circulating fluidized bed with loop seals, has been successfully setup and tested. After extensive tests following several major modifications as

indicated in Figure below.





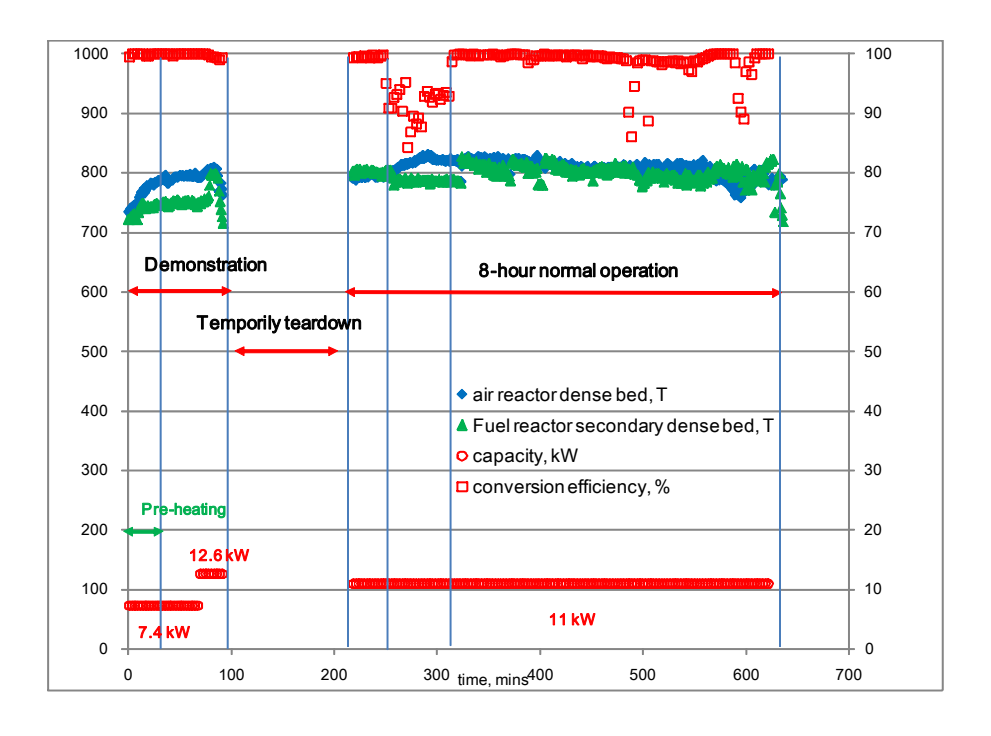
The most updated setup of the cold model facility could be operated under higher solid recirculation rates, and simultaneously prevent gas leakage between air and fuel reactors. This setup could also be operated modes to adapt to different change residence times of oxygen carriers as a function of their kinetics. Finally, the essential insights gained from the cold-model facility, was transferred into the design of the 10 kW hot-model facility.

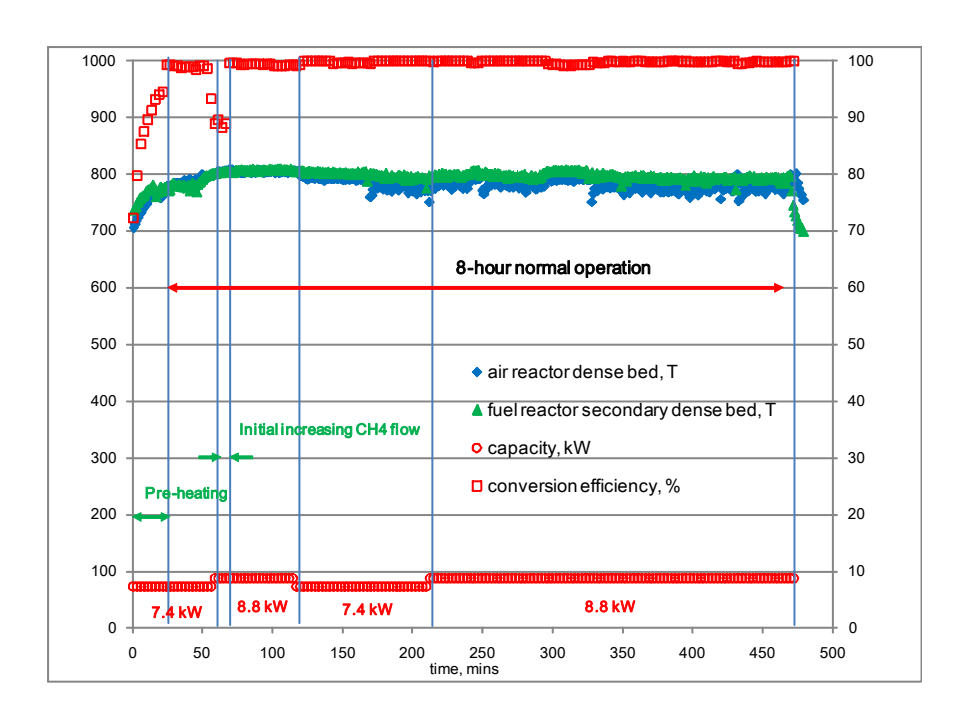
#### C. Results and Conclusions

A necessary preparation for the 10 kW hot-model CLC tests has been done. This first step toward the firing of the 10 kW CLC focuses on studying of the flow dynamics of solid re-circulation without gas leakage between the air and fuel reactors in a 10 kW equivalent cold-model CLC pilot. On the other hand, the preparation of oxygen carrier with acceptable

quality used in the 10 kW CLC pilot is also important. These two factors have been well investigated with outcomes of mastering controls of solid re-circulation, the prevention of gas leakage and the finalized formula of oxygen carrier. The initial 50 Kg of copper-based oxygen carriers was prepared using a scaled-up oxygen carrier preparation pilot; later on the second batch of oxygen carrier in 30 Kg was prepared. The inventory of the 10 kW CLC pilot is generally varied between 12-22 Kg and re-circulation rates ranged between 15-50 g per second. Asphalt, as substitute for bitumen, was used as the targeted fuel, with assistance of natural gas and other mixing gas such as CO<sub>2</sub>, H<sub>2</sub>, CH<sub>4</sub> and C<sub>2</sub> hydrocarbon because of the insufficient capacity of current asphalt injection pilot. The accumulation time for the operation of this hot-model pilot was about 500 hours, generally 4 hours per day (not including the pre-heating of the system) during the normal conditional tests. Following a successful on-site demonstration test of the 10 kW CLC pilot for 2-hour, the operation of this pilot was extended into three 8-hour in 3 consecutive days (totally 24 hours) with achieving steady state runs at 8-11 kW thermal equivalent. During this long-term evaluation runs, a mixing gas (about 15% of 10 kW capacity contributed by the asphalt injection, the rest of 10 kW capacity by natural gas) was applied.

The major results have been shown in two Figures below.





Major achievement in this part of work demonstrated the feasibility of the technical path using natural gas and/or asphalt, which are light and heavy hydrocarbons, as fuels for firing the CLC up to 10 kW capacity. There was absolutely no gas leakage between the air and fuel reactors, which was independent of operation conditions. During the normal operation period, less intensive manual handling of the system was necessary except for the initial period to establish the optimized solid-recirculation rate. As an important component of this study, the evaluation of oxygen carrier in this 10 kW CLC pilot seemed satisfied. After the initial a few hours of quick loss of some of oxygen transfer capacity, the prepared oxygen carrier performed stably for a long term. The evaluation of used oxygen carrier samples, collected after tests, indicated that only trace-amount of coke or carbon deposit on the copper-based oxygen carriers in the fuel Reactor, indicting the tendency of carbon deposits under current operational conditions, but has been maximized controlled by system tuning. There was also no evidence to show the sulphidization of oxygen carriers in the system by using the high-sulfur-laden asphalt fuels. There were trace-amounts of sulfur on samples at two baghouses, where temperatures were

as low as 150 °C.

#### 1.7 Conclusions and Issues for Further Study

Besides accomplishment achieving the successful firing the 10 kW CLC pilot, there were some critical lessons learned during the building, commission and firing of the 10 kW CLC pilot. Heating elements were one of the major operation issues, which caused most of the project delays. This issue frequently occurred throughout the project period, but was finally solved by successful manufacturing of the self-made heating parts and the self-made cooling-type temperature control system. Currently the applied heating elements could maintain system temperatures to well above 750 °C, which is sufficient for the ignition of the Redox reactions in the CLC pilot quick enough for the following-up temperature-elevation using fuel combustion. The good heating elements also support the CLC operating over a long-period, which are necessary conditions for our focused works on mastering the system. The second core issue of the current stage regarding to the oxygen carrier preparation is the tendency of loss of oxygen transfer capability because of the attrition during the re-circulation of oxygen carriers. This was evidenced by the following-up analysis in TG on decreasing copper content on the collected oxygen carrier sample from the pilot during the system maintenance, as well as evidence on increasing the copper content of collected fine samples in the baghouses of both the air reactor and the fuel reactor. However, the good thing was that the total mass of fine particles was in a minimum amount, indicating the attrition rate was less than 0.001 wt%/hour; and the bad thing was that copper ingredient was preferentially occurred outside surface of prepared oxygen carrier, where attrition was easily attack.

As a best estimate, aforementioned issue could be relatively easy to be solved under a further scaled-up CLC pilot. The scaled-up pilot may easily overcome the heat loss of the pilot because the heat loss is inversely proportional to the scale of the pilot by a factor of ratio of system sizes. Because of the copper-based oxygen carrier is used, the exothermic reactions could be achieved in both the air reactor and the fuel reactor. This may well balance the controlling of both the air reactor and the fuel reactor. Similarly, the issue regarding bitumen atomization could

be solved when the system is scaled-up. The current major engineering concept achieving the CLC is the application of the circulating fluidized bed system. This idea would be fully supported by our currently-available 0.6 MW circulating fluidized bed in the combustion tower, which is expected to push the CLC pilot operation to approximately 1 MW based on a simply estimate. If this could be achieved, this 1 MW CLC pilot could be unique in the world because of the current biggest scale of CLC pilot is around 100 kW.

# 1. Report Body

# 2.1 Background

The current state-of-art technological options to combust fossil fuels (especially for coals), simultaneously to capture the emitted carbon, include the post-combustion, the pre-combustion, and the oxy-combustion processes. The post-combustion options refer to the carbon-capturing technologies that remove the diluted CO<sub>2</sub> from the flue gas atmosphere. There are significant energy penalties incurred in these process options, which significantly increase costs and utility burden in order to abate the carbon emission. Its incremental cost would be 80% over the combustion without carbon capture based on DOE estimates (90% of carbon capture). To control the cost increment, pre-combustion technology options have been developed, which are based on the coal gasification process. In this setup, a decreased volume of the syngas and an increased CO<sub>2</sub> concentration (compared to those in the post-combustion technologies) will expect to significantly decrease the cost increment for the carbon capture based on the classic reaction kinetics theory, although the coal gasification is inherent costly. Major cost increment in the coal gasification process attributes to expensive air separation stage for producing pure oxygen as well as the complexity of the syngas cleanup stage. According to an NETL systems analysis, the air separation unit (ASU) is responsible for about 65% of the increase in the cost of electricity (COE) for 1st generation oxy-combustion systems. There are two categories of oxy-combustion process, including the oxy-combustion and chemical looping combustion (CLC). The oxy-combustion currently is in its pre-mature development stage and negatively includes the expensive ASU, and some other technical issues, such as the flue gas purification and the flue have recirculation.

The CLC could totally negate the necessity of pure oxygen by using oxygen carriers. It splits the single coal combustion reaction into two linked reactions using oxygen carriers. The two linked reactions are the oxidation of oxygen carriers in the air reactor using air, and the reduction

25

of oxygen carriers in the fuel reactor using fuels (i.e. coal). Generally metal/metal oxides are used as oxygen carriers and operated in a cyclic mode. Chemical looping combustion significantly improves the energy conversion efficiency, in terms of the electricity generation, because it improves the reversibility of the fuel combustion process through two linked parallel processes, compared to the conventional combustion process, which is operated far away from its thermo-equilibrium.<sup>2-5</sup> Therefore, the nature of CLC is the significant improvement of the combustion conversion efficiency over the conventional direct air combustion. Another consequence of CLC is inherent generation of purified carbon dioxide (CO<sub>2</sub>), which is not mixed with nitrogen in air. Under the current carbon-constraint environment, it has been a promising carbon capture technology in terms of fuel combustion for power generation. Its disadvantage is that it is less mature in terms of technological commercialization. Thus, the development of chemical looping combustion (and/or gasification) provides opportunities for both carbon capture and efficiency improvement.

Continuous CLC units have been demonstrated in laboratory tests on 300 W to 140 kW units with natural gas or syngas as fuel.<sup>6-9</sup> In contrast to the use of CLC with gaseous fuels, recent focus has been on the development of CLC using solid fuels. <sup>10-29</sup> Only few publication have been reported regarding to liquid-fuel-CLC<sup>30-31</sup>. The concept of CLC technology for solid fuels in two interconnected fluidized beds was patented in the 1950s.<sup>23</sup> Dennis and Scott proposed in-situ gasification and chemical looping for solid fuels in one fluidized bed.<sup>14,18</sup> Cao and Pan proposed the CLC of solid fuels in two interconnected fluidized beds.<sup>24-25</sup> This technical approach has been proposed and demonstrated in laboratory tests and a continuous 10 kW (equivalent or above) thermal CLC reactor with interconnected fluidized beds in Chalmers University of Technology<sup>16,19,26,32</sup>, Vienna University of Technology<sup>34</sup>, Southeast University<sup>28-29,33</sup>, The Ohio State University<sup>35</sup>, and Instituto de Carboquimica (CSIC)<sup>36-37</sup>. These successful demonstrations show that CLC of solid fuels is promising but challenging.

In this DOE-funded project, accomplishment is made by developing a series of advanced oxygen carriers, with properties of the higher oxygen-transfer capability, a favorable

thermodynamics to generate high purity of CO<sub>2</sub>, the higher reactivity, the attrition-resistance, the thermal stability in red-ox cycles and the achievement of the auto-thermal heat balance. The developed oxygen carrier will be integrated into operations of a novel coal-fueled chemical looping combustion process to generate pure CO<sub>2</sub>, which is ready for sequestration. This will be achieved into three phases in three consecutive years. In Phase I, the optimized formula of oxygen carriers will be determined; in phase II, interferences of prepared oxygen carriers under high-sulfur-chlorine will be eliminated; in Phase III, oxygen carriers with final-determined formula will be subject to be tested in a 10kW coal-fueled chemical looping combustion facility.

All aspects regarding to develop high quality oxygen carriers are addressed as following, which will be subject to intensive investigation within time frame of this project:

- Attrition-resisting and thermally stable oxygen carriers will be developed to achieve auto-thermal heat balance of the processes, generation of a high purity CO<sub>2</sub> and favorable kinetics. The measureable goals are that the prepared oxygen carriers should have favorable kinetics (100% conversion in minutes), suitable for application in fast fluidized beds under high attrition environment and thermal-stable under elevated temperatures (around 800 °C). There should be no obvious degradation and agglomeration tendency found in looping operations (for example, 50 red-ox cycles);
- Impacts of scale-up methods and application of inexpensive raw materials (copper-based minerals and widely-available inexpensive clays) for preparation of oxygen carriers on reaction performance in testing within a hot-model conditions will be evaluated. The prepared oxygen carriers should be thermal-stable-and-robust.
- Multi-metal or free-oxygen-releasing oxygen carriers will be prepared and their optimal formula and reaction mechanisms will be explored.
- Adaptability of prepared oxygen carriers to diversified coal types in the hot-model tests will be evaluated. Methods for tolerances of prepared oxygen carriers to chlorine and sulfur from coals will be developed. Methods for elimination of carbon deposits on oxygen carrier will be investigated.

Major tasks will be covered in this project include:

■ Preparation of Oxygen Carriers: Initially, previous experience on the preparation of oxygen carriers will be reviewed and passed onto new team within this project. Based on previous work, three guidelines on preparation of oxygen carriers will be setup and followed during preparation. At this initial stage of the project, management of personnel, method procedures and sample naming system will be setup. Prevention of risks of material development will be realized by applying a minimum amount of additive for stabilization of quality of prepared oxygen carriers. In order to optimize development process, we will have two teams (Dr. Pan with one student and Dr. Cao with another student), and each team will work on three categories of oxygen carriers independently, but will frequently share success/failure experiences during material development.

<u>Development of Category 1 Oxygen Carriers:</u> Inexpensive procedures that utilize inexpensive traditional copper-based compounds to synthesize targeted non-traditional copper-based compounds will be investigated.

Development of Category 2 oxygen carriers: A systematic test matrix will be conducted to search the best performance on the durability of oxygen carriers which will be based on the test results using ASTM standard attrition procedure (ASTM D5757-95). The dry or wet impregnation method to load the oxygen carriers on the different supporting materials will also be included in this subtask. Our goal on the durability and attrition-resistance of prepared oxygen carriers is to maintain the chemical and physical properties of the oxygen carriers after more than 50 cycles test runs.

<u>Development of Category 3 oxygen carriers:</u> Investigate mechanisms on observed contamination impacts from copper-based compounds on formation of Si and Al porous structures to find an optimal procedure to prevent this impact on pore-development and to optimize preparation procedures.

■ Selection of Oxygen Carriers. The improvement of chemical formula and preparation procedures of selected categories of oxygen carriers will be conducted in 2011. The improvement

includes kinetics, capacity, and attrition resistance. Good kinetics of oxygen carriers will decrease re-circulation rates inside the loop cycle between the air and fuel reactors, and thus help to decrease the attrition potential and material loss and emissions of trace amounts of metals into the environment. Once sufficient kinetics could be achieved, the amount of active agents on the substrate selected needs to be maximized and attrition resistance needs to be significantly improved. An innovative concept will be explored on coating a hard gas-penetrable layer outside the oxygen carriers. At the end of Task 3, the preparation of oxygen carriers for 10 kW facility tests based on the finalized formula of oxygen carrier shall be started. This includes finalization of the preparation procedure for scaled-up production of oxygen carriers, production of a large amount of oxygen carrier to satisfy several runs at 4-8 hours per run in the aforementioned 10 kW hot-model chemical looping facility.

■ Evaluation of Oxygen Carriers in a 10 kW Hot-Model CLC Facility. The optimized oxygen carriers developed in Task 3 will be tested in the 10 kW hot-model CLC facility to obtain critical design parameters for future demonstration tests. The test period will be sufficient (4-8 hours daily for over two weeks) to evaluate oxygen carrier performance and control strategies of chemical looping facility, as well as to train students to grasp the mechanism and procedure to handle the hot-model test facility, which will greatly improve their practical skills.

# 2.2 Preparation of Oxygen Carriers

To stabilize high temperature performance of oxygen carriers and to maintain the balance between mass transfer limitation and maximization of the loading of active constituents (CuO-Cu), a commercially available supporting material (Al<sub>2</sub>O<sub>3</sub>) was initially used in the preparation of oxygen carriers. The size distribution of this supporting material is shown in Figure 1. The majority of particle size is in the range between 175µm and 300µm, averaged at 250µm. This size of particle with a narrow size distribution makes the selected supporting material an excellent candidate for preparation of oxygen carriers being operated in fluidization modes. Its purity is high, as indicated in Figure 2 using SEM-EDX analysis.

It was found that less than 5 wt% of CuO was loaded on the supporting material (Al<sub>2</sub>O<sub>3</sub>) using the traditional "wet" impregnation method. After several trials, a "dry" impregnation method was developed with a dry method. The major point on difference between "wet" and "dry" methods is removal of moisture occupied inside pore structure of supporting materials prior to doping procedures. The loading amount of CuO was increased from about 5 wt% to over 20 wt%. The "dry" impregnation method is listed below:

- 1) the supporting material was dried in an oven under 120°C overnight,
- 2) droplets of prepared saturated Cu(NO<sub>3</sub>)<sub>2</sub> were applied on this dried supporting material, until it was fully wetted,
- 3) a few droplet of ethanol was continuously applied to the prepared wet oxygen carriers and then the prepared sample was dried in oven under 120°C again for another 2 hours,
- 4) the dried sample was subject to the procedure 3) again,
- 5) Procedure 1) through 4) will be repeated by two times, and finally
- 5) Samples were calcined in the oven under 500°C for 5 hours.

Initially, more than 50 oxygen carrier samples were prepared by adding different kinds of additives, based on aforementioned procedures. Three major types of samples will be extensively discussed in this report, which different significantly in their physical and chemical properties

and kinetics performance.

Sample 1 is labeled as CA, which was prepared solely based on the aforementioned standard procedure without using any additives. Sample 2 is labeled as CCA, in which a dispersion reagent (citric acid) was applied based of the standard procedures. Sample 3 is labeled as LCA, in which both dispersion reagent and strength-enhanced reagent (Lanthanum-based chemicals) were applied. As indicated in a series of figures on images of prepared oxygen carrier samples (Figure 3 for CS series samples, Figure 4 for CCA series samples, and Figure 5 for LCA series samples), active constituent (CuO) was evenly distributed on the surface of supporting materials and which penetrated a few micrometer into the supporting materials. Thus, the inside of supporting material has been left unoccupied by CuO. Doping of active constituents outside surface of supporting material would promote good redox kinetics.

After redox tests under different conditions using fuel gases with different compositions in reduction step (commonly 800°C), all used CA series oxygen carrier samples showed a major phase transformation. A serious melting or agglomeration of CuO-Cu was identified, which appeared as compared to fine crystal of CuO-Cu on the surface of the original CA samples. A hard crest of CuO-Cu has formed on the surface of supporting materials, which demonstrated significant melting or agglomeration of Cu after cyclic redox tests. For CCA samples, the application of dispersion reagents has achieved the improvement of even distribution of CuO-Cu on the surface. It did not significantly prevent the the melting or agglomeration of CuO-Cu. However, this was not the case in the performance of LCA samples. As indicated in Figure 5-1 and 5-2, a comparison of original and tested LCA samples has demonstrated that the melting or agglomeration was minimized on the surface of LCA samples after 50 cycles of redox tests at 800°C. Here are some thoughts on what we investigated: 1) it was expected that tested oxygen carriers should experience some over-heat inside reactor. That means a controlled test temperature at 800°C may be just "skin" temperature of tested oxygen carriers, and temperatures inside oxygen carriers could be somehow higher than 800°C because of propensities of exothermic reduction of CuO. 2) Despite significant melting and agglomeration of copper on the

surfaces of CA and, CCA, and slight melting and agglomeration on LCA samples, it did not cause the loss of fluidization of all prepared oxygen carriers in the bench scale fluidized bed reactor under 800°C. Thus, the preferred operational temperature, would be 800°C, for the operational temperatures of CLC system based on available Cu-based oxygen carriers, and also considering the other factors (such as remaining sulfur in gas phase).

Besides SEM images, another analysis method was applied to identify the stabilization of CuO-Cu on the surface of supporting material. Variations of pore size distribution of original and used oxygen carriers were presented in Figures 6-1 to 6-5. There was no major change of the pore size distribution between original supporting material and its treated samples under higher temperatures, ranging from  $800^{\circ}$ C to  $1150^{\circ}$ C. However, the increase of pore volume of the original sample after being treated under  $1150^{\circ}$ C was unexpected.  $1150^{\circ}$ C is likely a phase transformation threshold temperature for the selected  $Al_2O_3$  (originally  $\alpha$ - $Al_2O_3$ , then changed to  $\gamma$ - $Al_2O_3$  after a treatment treated under  $1150^{\circ}$ C). Generally speaking, the pore structure of  $\gamma$ - $Al_2O_3$  more could be crushed when it was treated under such high temperatures. Thus, a further study will be conducted to take advantages of these "open" pores of the original supporting material treated under  $1150^{\circ}$ C prior to loading CuO into the supporting materials. This new process will be taken into consideration in future preparation of oxygen carriers.

Figure 6-2 presents variation of pore size distribution after original supporting material was loaded with CuO. Loaded CuO could occupy pores of supporting material between 3 and 15 nm. At the same time, it could also generate much larger pores size (greater than 15 nm). The similar case was found for the original supporting material treated under 800°C, but it may be also due to the integration of smaller pores (between 3-15 nm). As expected, tested CA sample would lose smaller pores below 15 nm significantly under higher temperatures and 10 redox cycles, which has been verified and presented in Figure 6-3. Similar observations were found in Figure 6-4 for CCA and LCA samples. It is noticed that there were still significant loss of smaller pores, from 3 to 12 nm for tested LCA sample. So far, we are not sure if this corresponded to occurrence of melting or agglomeration of CuO-Cu under micro-scale dimension.

Another evidence of phase transformation of oxygen carrier samples was from analysis results using XRD results, as indicated in Figure 7-1 for tested CA sample, and Figure 7-2 for original and used LCA sample. For both case, there were clear evidences of the formation of integrated crystal phase between CuO and Al<sub>2</sub>O<sub>3</sub>, i.e., CuAl<sub>2</sub>O<sub>4</sub> spinel. This was a new solid phase formed in the cyclic redox tests under higher temperature (800°C or above). The CuAl<sub>2</sub>O<sub>4</sub> spinel was not found in the original sample (only CuO and Al<sub>2</sub>O<sub>3</sub> are presented), as indicated in Figure 7-2. However, loaded CuO-Cu did not fully reacted with Al<sub>2</sub>O<sub>3</sub> and subsequently converted into CuAl<sub>2</sub>O<sub>4</sub>, because of either crystal phase of CuO or Cu could still be found in used samples. The reason for the formation of CuAl<sub>2</sub>O<sub>4</sub> spinel on both oxygen carriers (CA-unmodified samples, LCA-intensive modified samples) is not clear at this point. It may be due to the shift of pore size distribution. It may also be the products of the degradation during the cyclic redox reactions. However, this new phase between CuO-Cu and Al<sub>2</sub>O<sub>3</sub> deserved to be further studied. If this new phase could be stable under higher temperatures (compared to definitely unstable tendency of CuO-Cu under similar temperatures), this may give us an opportunities to enhance its formation in order to obtain the thermal-stable Cu-based oxygen carriers. On the other hand, the partial loss of original redox kinetics would likely occurred after the formation of this new solid phase. Further study should be undertaken to investigate the balance between thermal-stability and redox kinetics of prepared oxygen carriers.

In this study, two evaluation methods of redox kinetics of prepared oxygen carriers were applied, including TPR(H<sub>2</sub>)-TPO(air) (TPR-Temperature Programmed Reduction; TPO-Temperature Programmed Oxidation) cycles in Micrometric ChemiSorb 2720 Instrument (it is shown in Figure 8) and tests in a bench scale fluidized bed CLC facility using different setups of fuel supplies. 100ml/min of 10% hydrogen in nitrogen was introduced into chemisorbs system to reduce the CuO back to Cu under programmed temperature. The calibration curve of hydrogen intensity as function of CuO concentration was established using different amount of pure CuO in the system. Thus, the amount of CuO in the supporting materials also could be determined using TPR tests. The peak maximum of hydrogen intensity curve for pure CuO was

occurred at 325°C (Figure 9). The peak maximum temperature shifted to much lower temperature between 210°C and 260°C with an overlapping curve instead of one sharp peak for the pure CuO of 325 °C. The peak maximum for CuO with supporting materials occurred at lower temperature ranges, demonstrated finely-dispersed copper presenting high redox kinetics. Two reduction peaks indicated that the reduction of CuO on the supporting material occurred at two different stages. Further investigation uncovered two stages of reduction of prepared oxygen carriers using H<sub>2</sub> in TPR tests, including one reaction peak under temperature around 210°C and the second around 260°C (mechanisms behind discrete two peaks will be further investigated). With the increase of TPR-TPO cycles, the area of the second peak increased and gradually became dominant process. This may correspond to the formation of CuAl<sub>2</sub>O<sub>4</sub>. The gradual shift of peak area between the first peak and the second peak, may imply the acceleration of transformation from CuO-Cu to CuAl<sub>2</sub>O<sub>4</sub>. Clearly, this transformation would not be reversible. After many redox cycles, CuO-Cu phase could be totally converted to CuAl<sub>2</sub>O<sub>4</sub>. A careful investigation of TPR-TPO results is on-going, in order to extract the degrade rates of prepared oxygen carriers. It is noticed that whatever occurred in actual TPR-TPO curves during phase transformation, the calculated loaded amount of CuO-Cu by integration of peak areas was almost constant under different cycles. This may indicated that all loaded CuO-Cu on prepared oxygen carriers was fully accessible. Reversibility of reduction and oxidization cycles of CuO-Cu was achievable even the CuO occurred as CuAl<sub>2</sub>O<sub>4</sub>. The reaction shifted (from 210<sup>o</sup>C to 260<sup>o</sup>C) from CuO-Cu to CuAl<sub>2</sub>O<sub>3</sub>-CuAl<sub>2</sub>O<sub>4</sub> may be a clear evidence of reactivity loss. The phase transformation of prepared oxygen carriers will be further investigated.

Copper-based oxygen carriers have high reactivity resulting in high purity CO<sub>2</sub> generation, but face the challenges of low copper melting point and potential thermal sintering under high-temperature cyclic operation. A temperature-programmed reduction and oxidation (TPR-TPO) technique (Redox) and Thermalgravimetic (TG) was used to simulate of the cyclic operation of copper-based oxygen carriers in the CLC process. Thermally stable copper-based oxygen carriers have been successfully prepared using commercially-available Al<sub>2</sub>O<sub>3</sub> as the

supporting material and selected additives. A substantial resistance to agglomeration and durability in over 864 cyclic Redox TG tests under high temperature conditions (oxidation at 800 °C and reduction at 800 °C) has been confirmed. Figure 10. presented that only a minimal loss of oxygen capacity (less than 5%) of the prepared oxygen carriers was found aftre 864 redox cycles. Multiple material characterization methods were applied to the fresh and used oxygen carriers, including the determination of pore structure and surface area by Brunauer-Emmett-Telle (BET), crystal structure by X-ray diffraction (XRD) and surface phase diagram analysis by scanning electron microscopy and energy-dispersive X-ray spectroscopy (SEM-EDX). SEM-EDX results confirmed there were no significantly agglomeration of prepared copper based oxygen carriers under higher temperatures. XRD analysis confirmed a new phase between CuO and Al<sub>2</sub>O<sub>3</sub>, which is CuAl<sub>2</sub>O<sub>4</sub> spinel, has been formed during cyclic operation of prepared oxygen carriers.

The last evaluation tests on prepared oxygen carriers were to test their attrition resistance performance based on ASTM D5757-95 method in a fluidized bed setup. The detailed setup and description on procedures of those tests were shown in Figure 11. Results of this attrition tests was calculated based on percentage of weight loss of tested samples after they were subjected to 5 hours of attrition tests. Test results indicated that attrition loss of original supporting material was between 3.36% to 4.94% by weight. After CuO was loaded onto supporting material, the attrition rates dropped to a range between 1.79% to 2.43%. For LCA samples, both original LCA sample and used LCA sample were tested, and there was a significant change samples before and after tests. The weight loss of the original LCA sample varied between 1.13% to 2.38 %; but dropped significantly after sample was subject to redox tests to a larger range between 0.0052 wt% and 0.51 wt%. This would be largely attributed to redox test conditions of used samples. It seemed the strength of attrition-resistance of used samples has been improved in wide ranges. Further studies will be continuously conducted to find reasons for this. Preliminary assumption would be the occurrence of some phase transformation as samples were treated in high temperature environment.

Figure 1. Particle size distribution of supporting materials of oxygen carriers

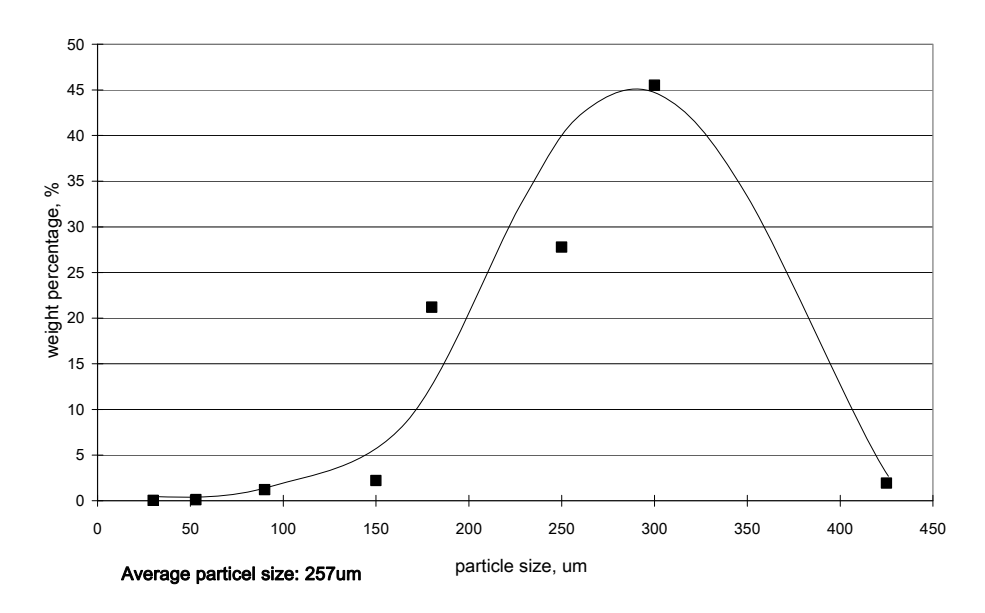
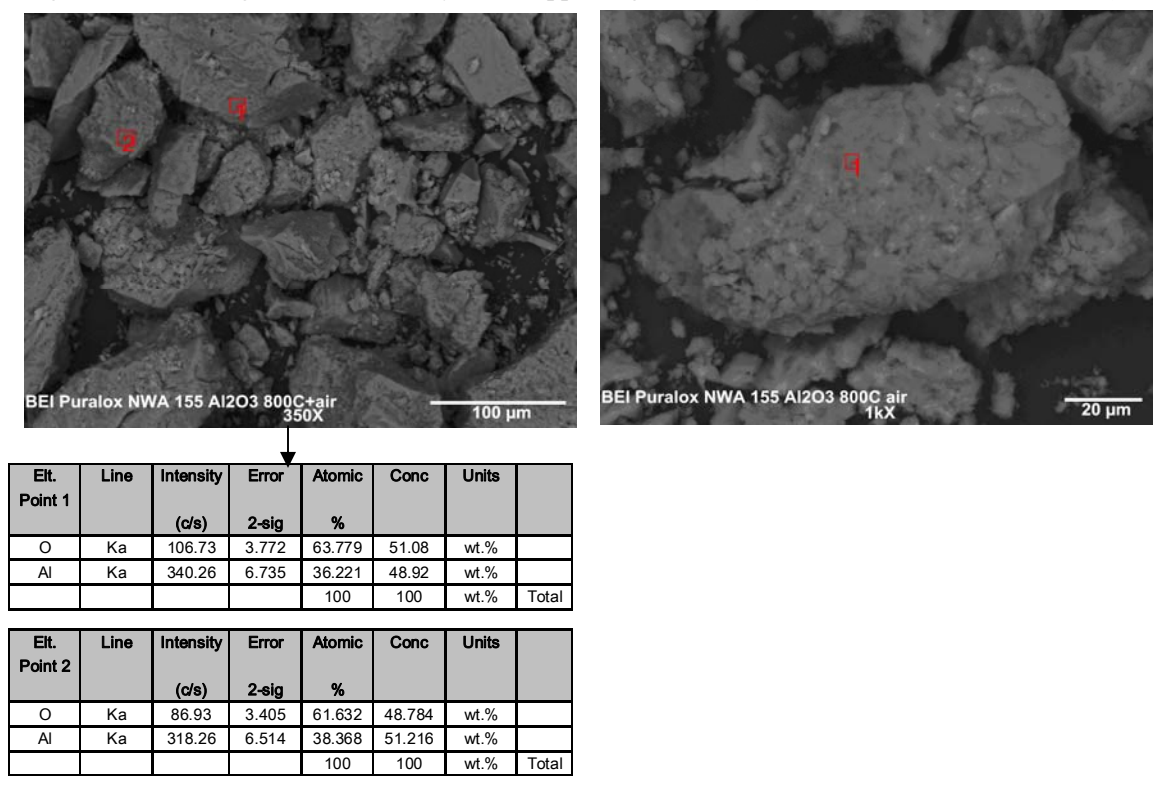
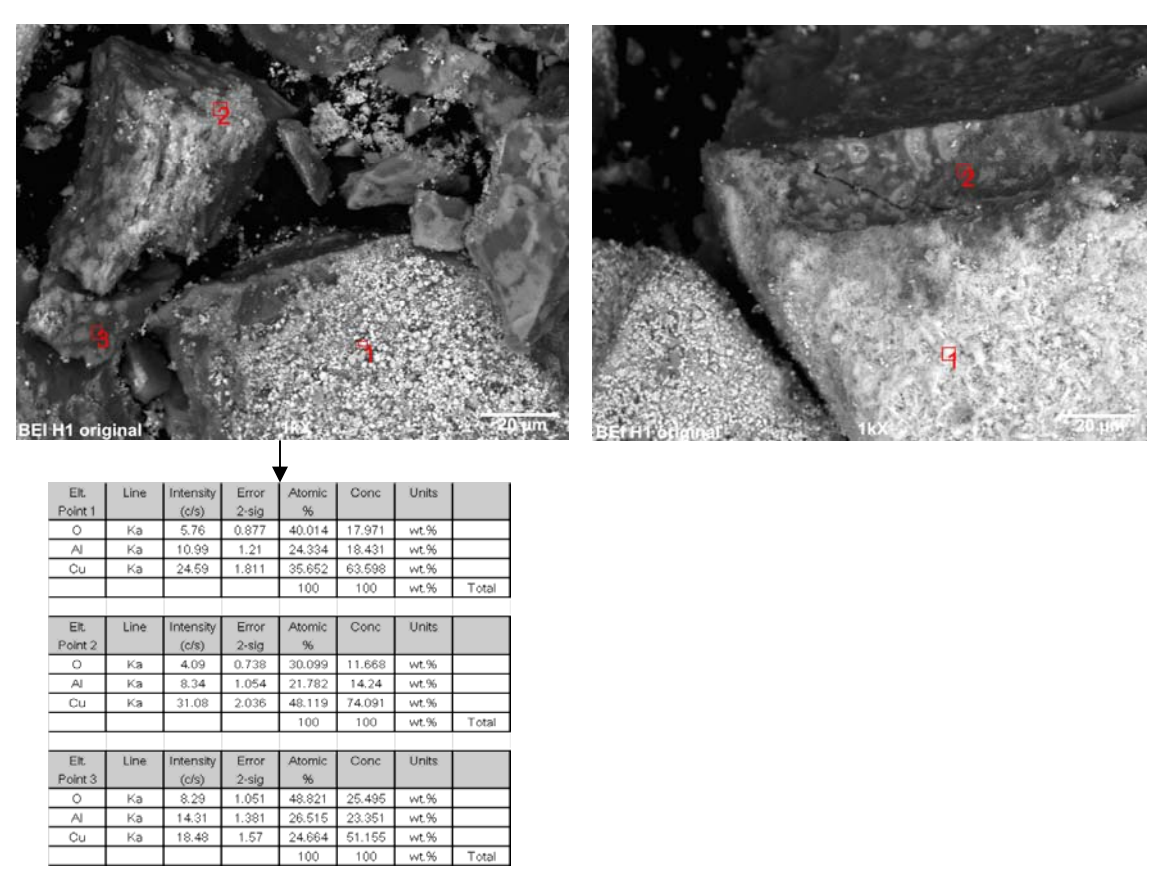


Figure 2. SEM images and EDX analysis of supporting material (after treated under 800 °C in air)



kV 20.0, Takeoff Angle 27.0°, Elapsed Livetime 30.0

Figure 3-1. CA series samples Original sample



After 3 cycles in mixed fuel gas conditions (air-50%H<sub>2</sub>/20%CO/30%CH<sub>4</sub>)

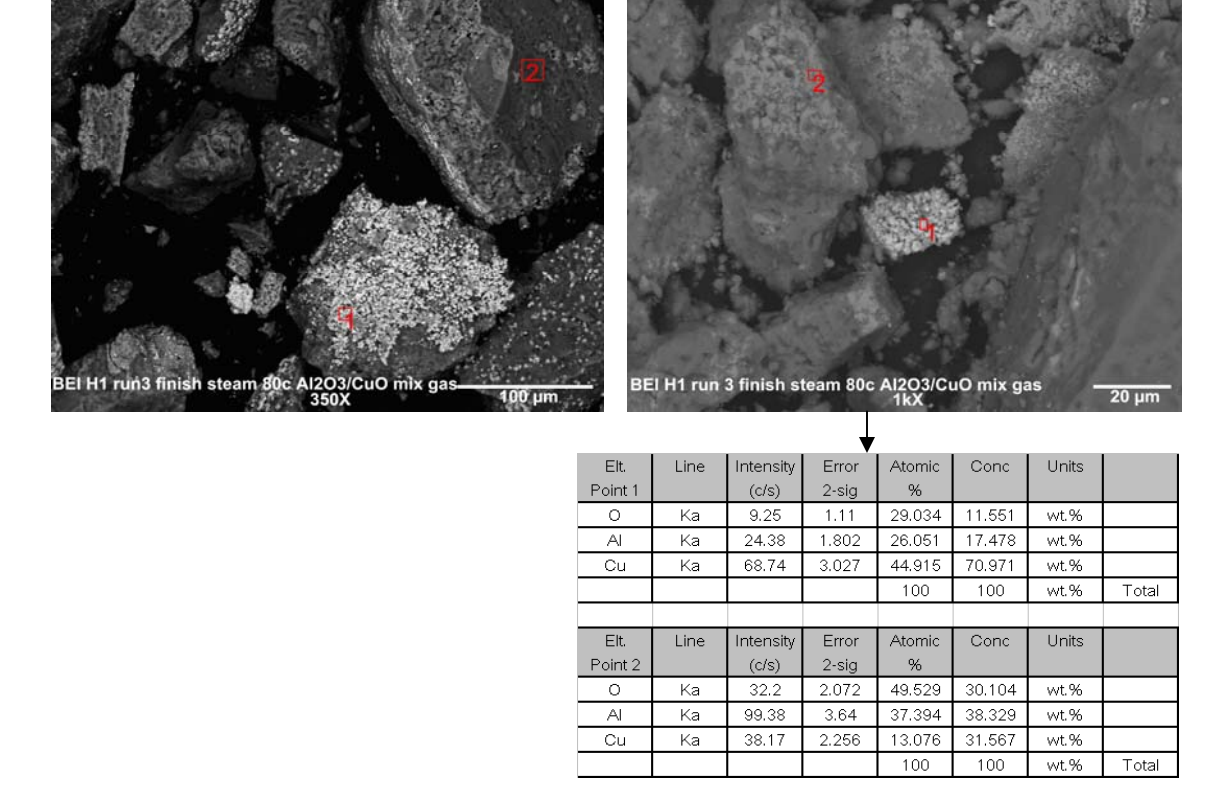


Figure 3-2. CA series after reduction using asphalt

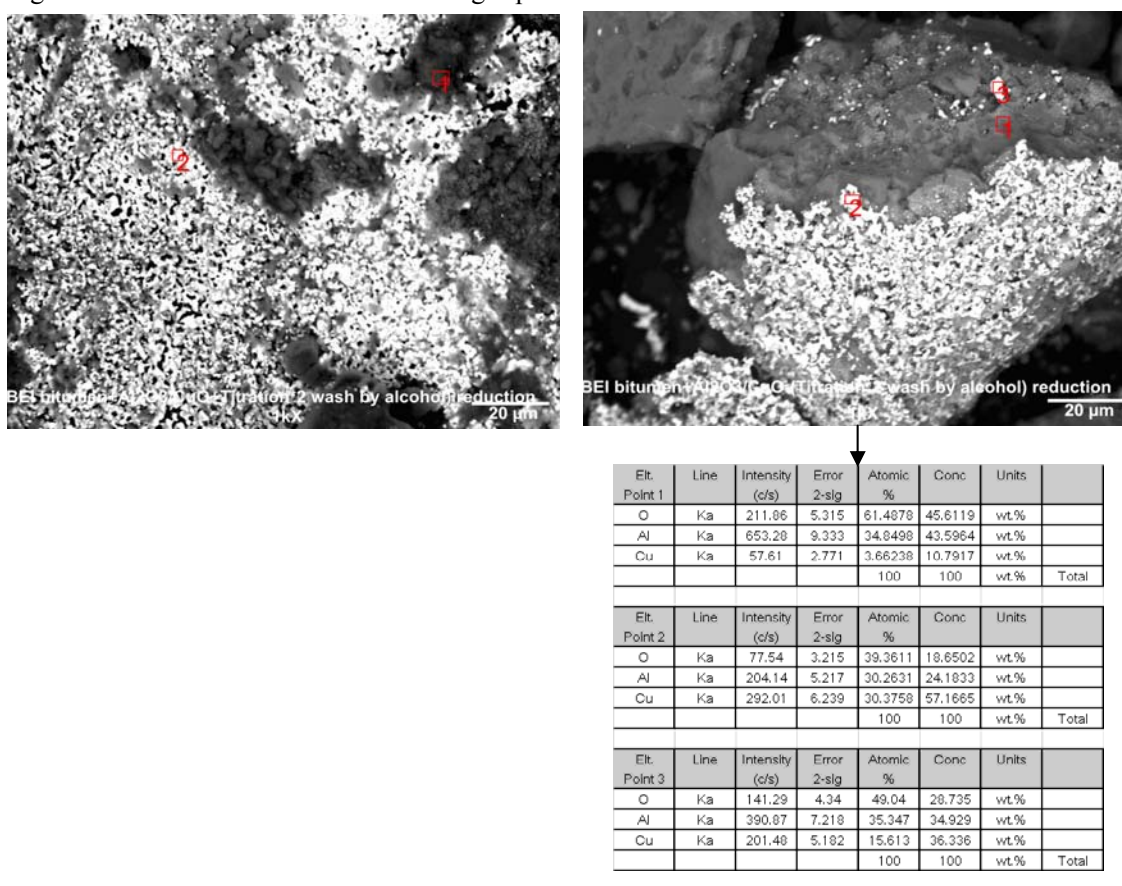
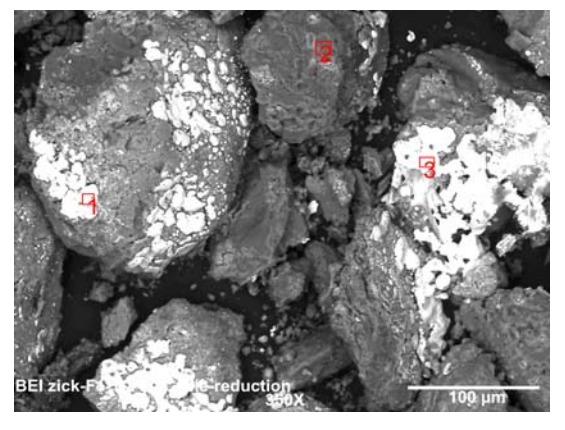
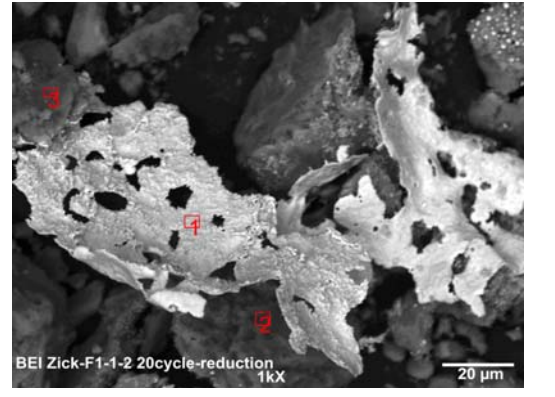


Figure 3-3. CA series after 20 cycles of redox in air-H<sub>2</sub> using Chemisorp instrument





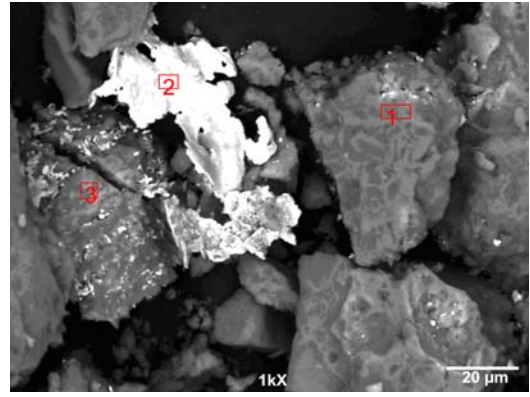


Figure 4. cycles of redox tests with CCA series samples

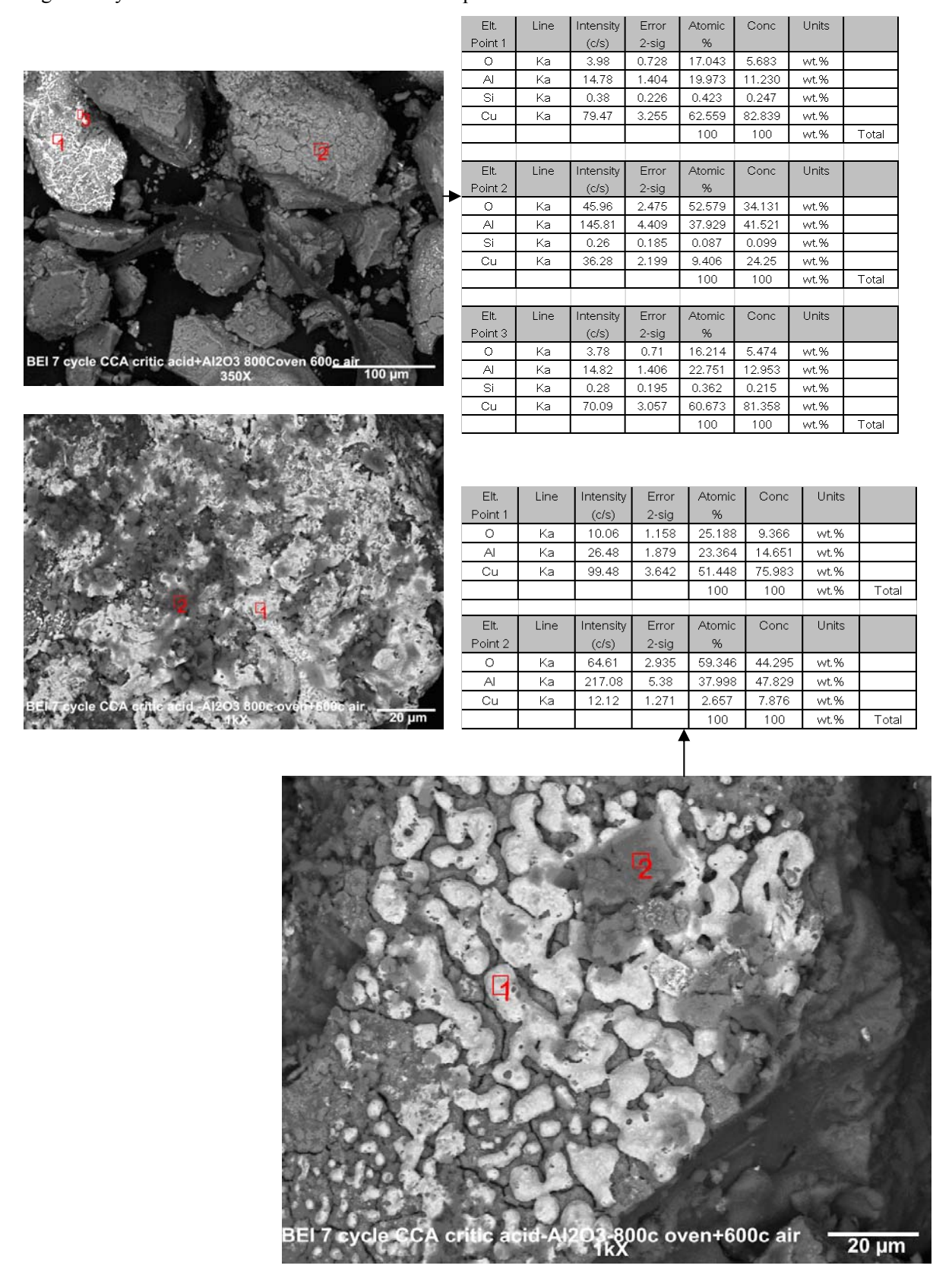


Figure 5-1. LCA series- Original samples

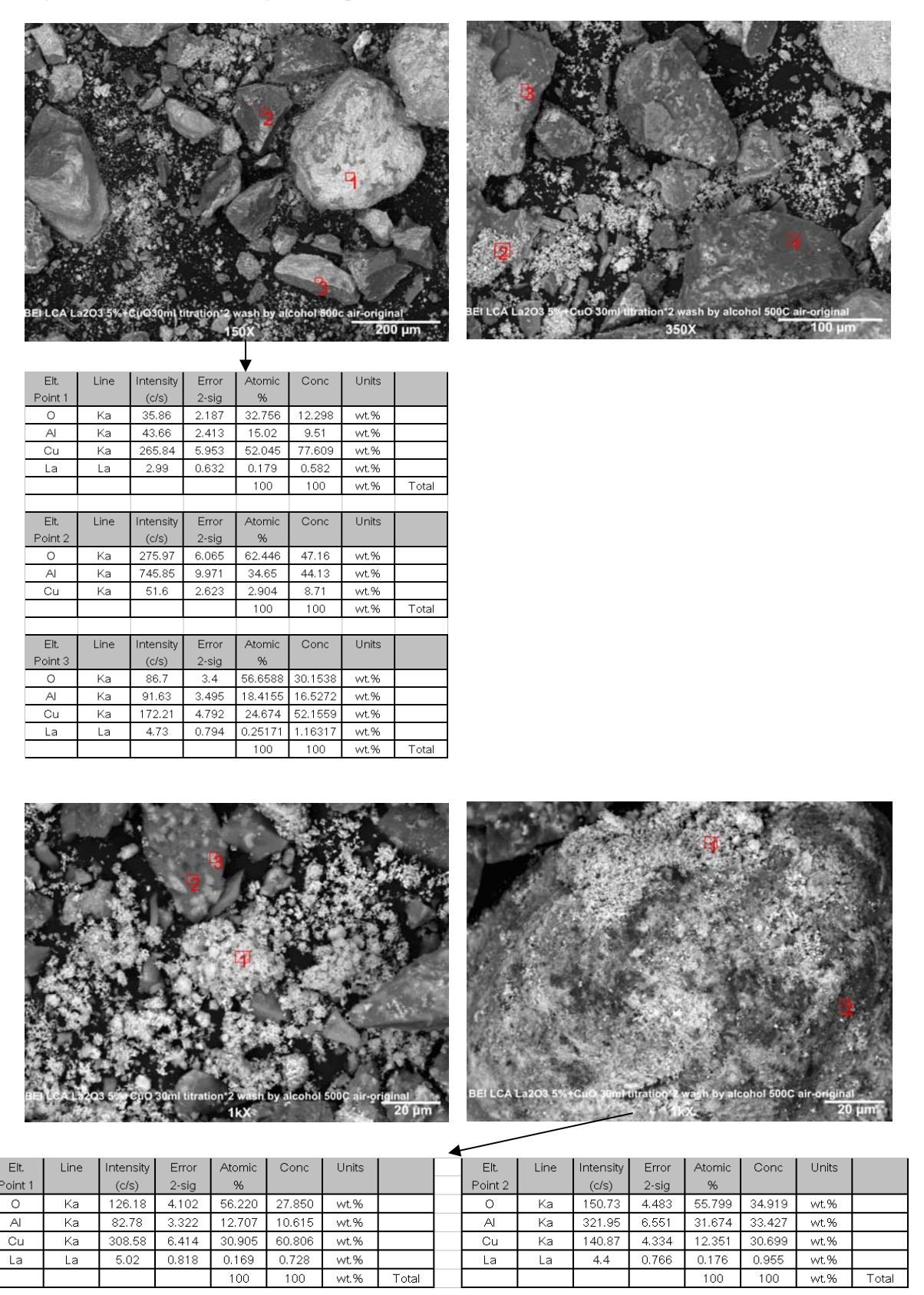


Figure 5-2. LCA series sample under 50 cycles of redox using H<sub>2</sub> Chemisorp Units (c/s) 2-sig Ka 164.12 4.677 29.253 22.916 wt.% 5.629 57.392 wt.% Cu Ka 237.72 31.105 1.441 0.98 La La 0.358 wt.% 100 100 wt.% Elt. Intensity Units Point 2 (c/s) 178.49 4.878 62.750 45.240 wt.% Cu Ka 75.33 3.169 wt.% 6.44 0.226 1.418 wt.% 100 100 wt.% Flt. Conc Units Point 3 (c/s) 40.4 32,404 wt.% Ka 80.26 17.083 11.002 wt.% wt.% BEI 50 cycle LCA La2O3 5%+CuO 30 1kX Units Conc Units Error Error Point 1 Point 3 (c/s) (c/s) 2-sig 2-sig 12.731 Ka 42.38 2.377 31.929 wt.% 260.78 66.873 51.727 wt.% 5.896 108.51 3.803 15,335 wt.% 745.75 40.059 wt.% 332.18 6.654 45.129 71.469 wt.% Cu Ка 43.38 2.404 2.200 6.761 wt.% 0.134 3.01 0.634 0.467 7.57 0.217 1.452 La La wt.% La wt.% 100 100 wt.% 100 wt.% Elt. Units Line Intensity Error Atomic Conc Point 2

0

Cu

La

Ka

Ka

La

50.1

227.5

4.6

2.584

5.507

0.783

39.692

29.455

0.227

18.875

55.629

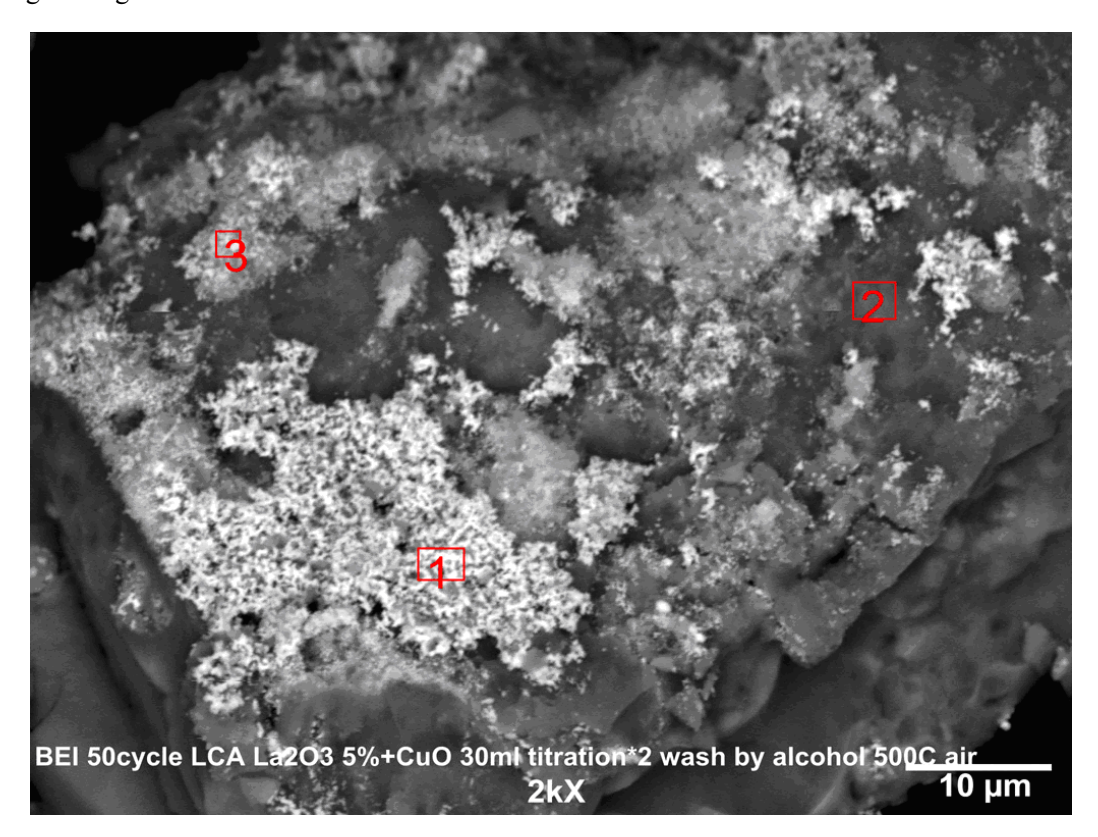
0.937

wt.%

wt.%

wt.%

# Enlarged image



Elt. Point 1	Line	Intensity (c/s)	Error 2-sig	Atomic %	Conc	Units	
0	Ka	41.11	2.341	31.038	12.429	wt.%	
Al	Ka	111.98	3.864	24.684	16.668	wt.%	
Cu	Ka	311.12	6.44	44.026	70.023	wt.%	
La	La	5.27	0.838	0.252	0.879	wt.%	
				100	100	wt.%	Total
Elt. Point 2	Line	Intensity (c/s)	Error 2-sig	Atomic %	Conc	Units	
0	Ka	140.9	4.334	60.910	44.147	wt.%	
Al	Ka	514.91	8.285	34.896	42.653	wt.%	
Cu	Ka	48.1	2.532	3.864	11.122	wt.%	
La	La	7.54	1.003	0.330	2.080	wt.%	
				100	100	wt.%	Total
Elt.	Line	Intensity	Error	Atomic	Conc	Units	
Point 3		(c/s)	2-sig	%			
0	Ka	101.94	3.687	51.990	29.023	wt.%	
Al	Ka	253.23	5.811	28.606	26.931	wt.%	
Cu	Ka	202.29	5.193	19.012	42.154	wt.%	
La	La	9.87	1.147	0.391	1.892	wt.%	
				100	100	wt.%	Total

Figure 6-1 Pore size distribution analysis

(Red - original Al<sub>2</sub>O<sub>3</sub> supporting material, Green – Al<sub>2</sub>O<sub>3</sub> after treated under 800 °C, Blue - Al<sub>2</sub>O<sub>3</sub> after treated under 1150 °C)

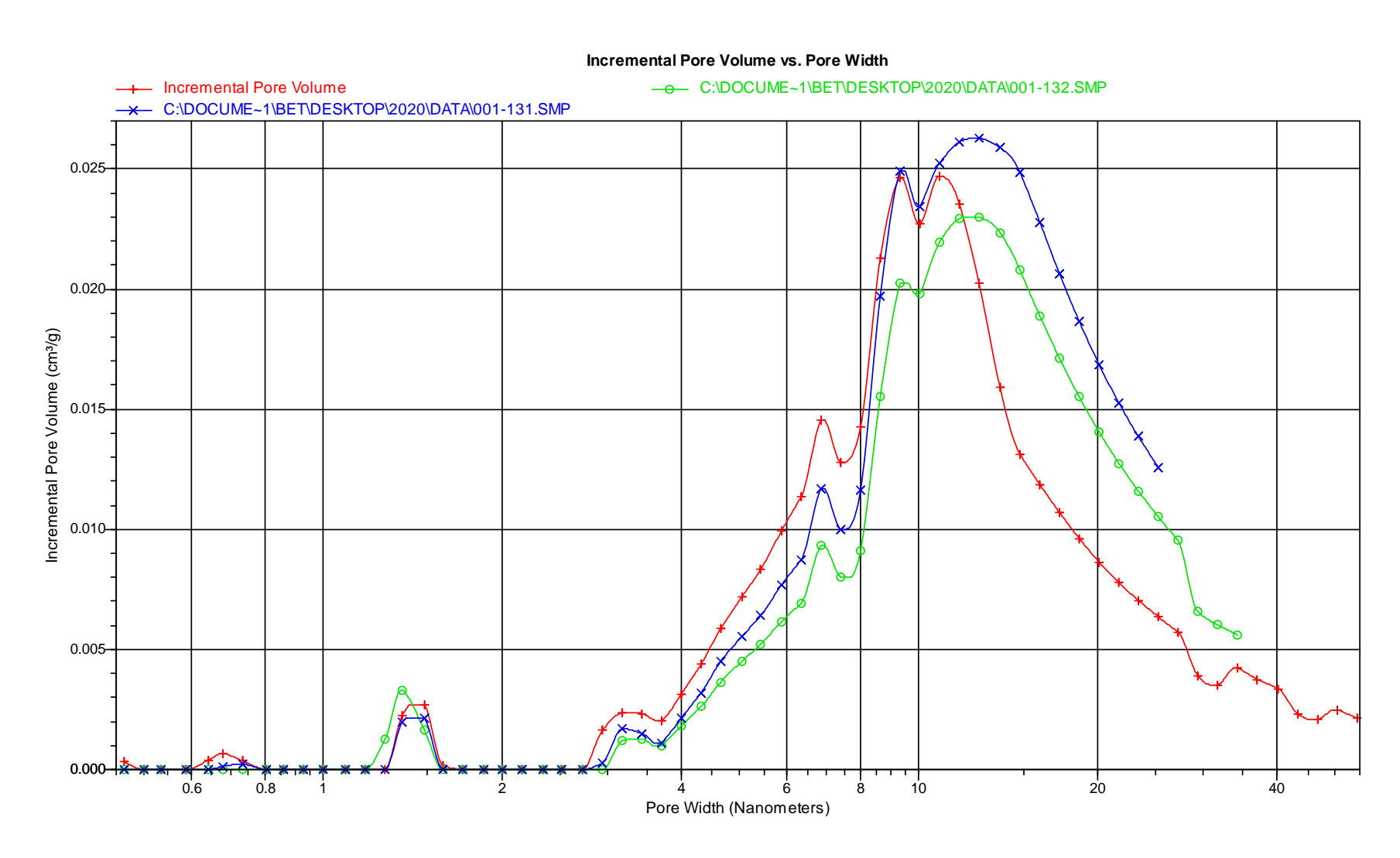


Figure 6-2 Pore size distribution analysis (Red - original  $Al_2O_3$  supporting material, Green –  $Al_2O_3$  after treated under 800 C, Blue – CCA series original sample (loaded with CuO))

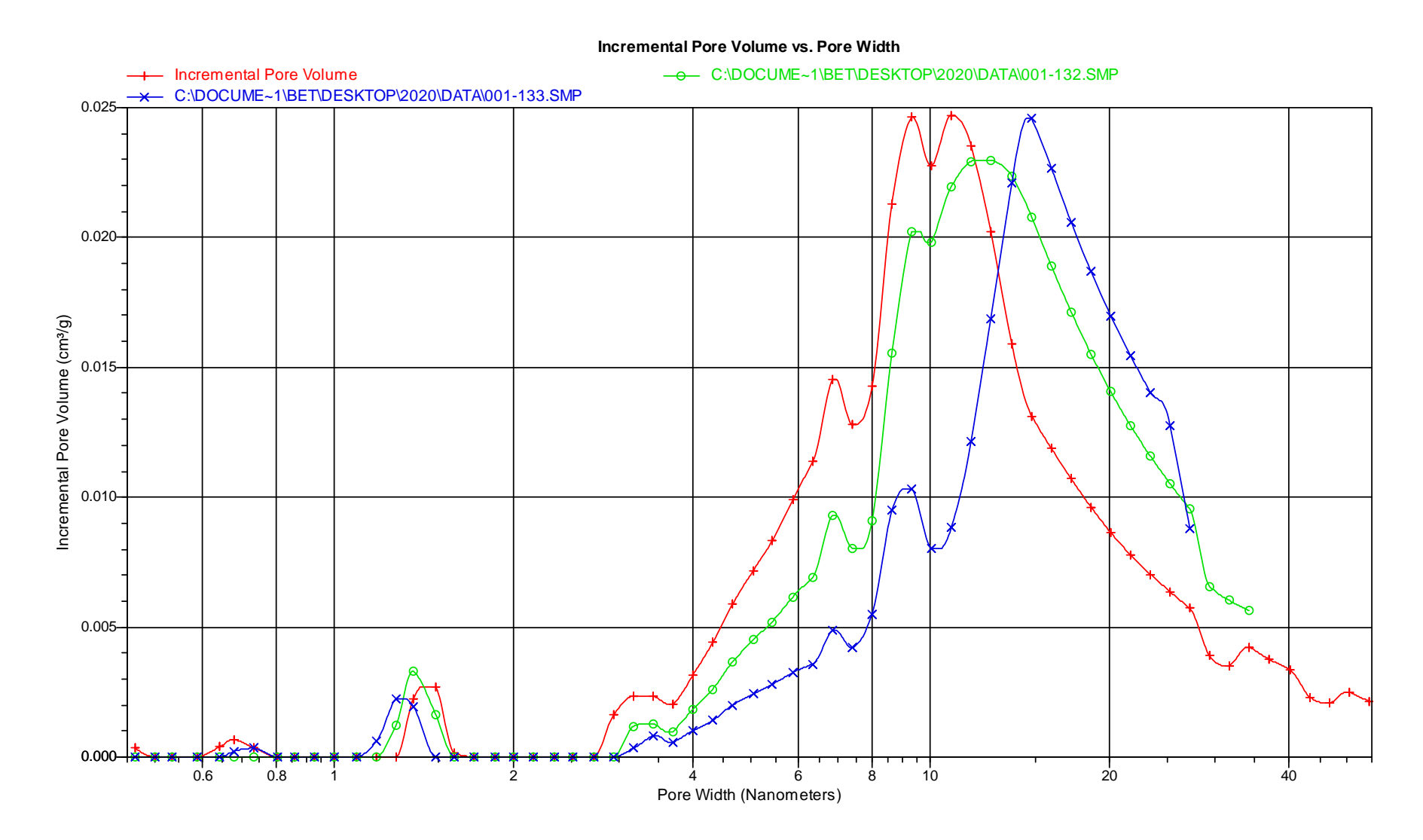


Figure 6-3 Pore size distribution analysis

(Light or dark red - (wash or not after doping) CA series original sample (loaded with CuO)); Green -CA series after 7 cycles of redox, Blue - CA series after 6 cycles of redox

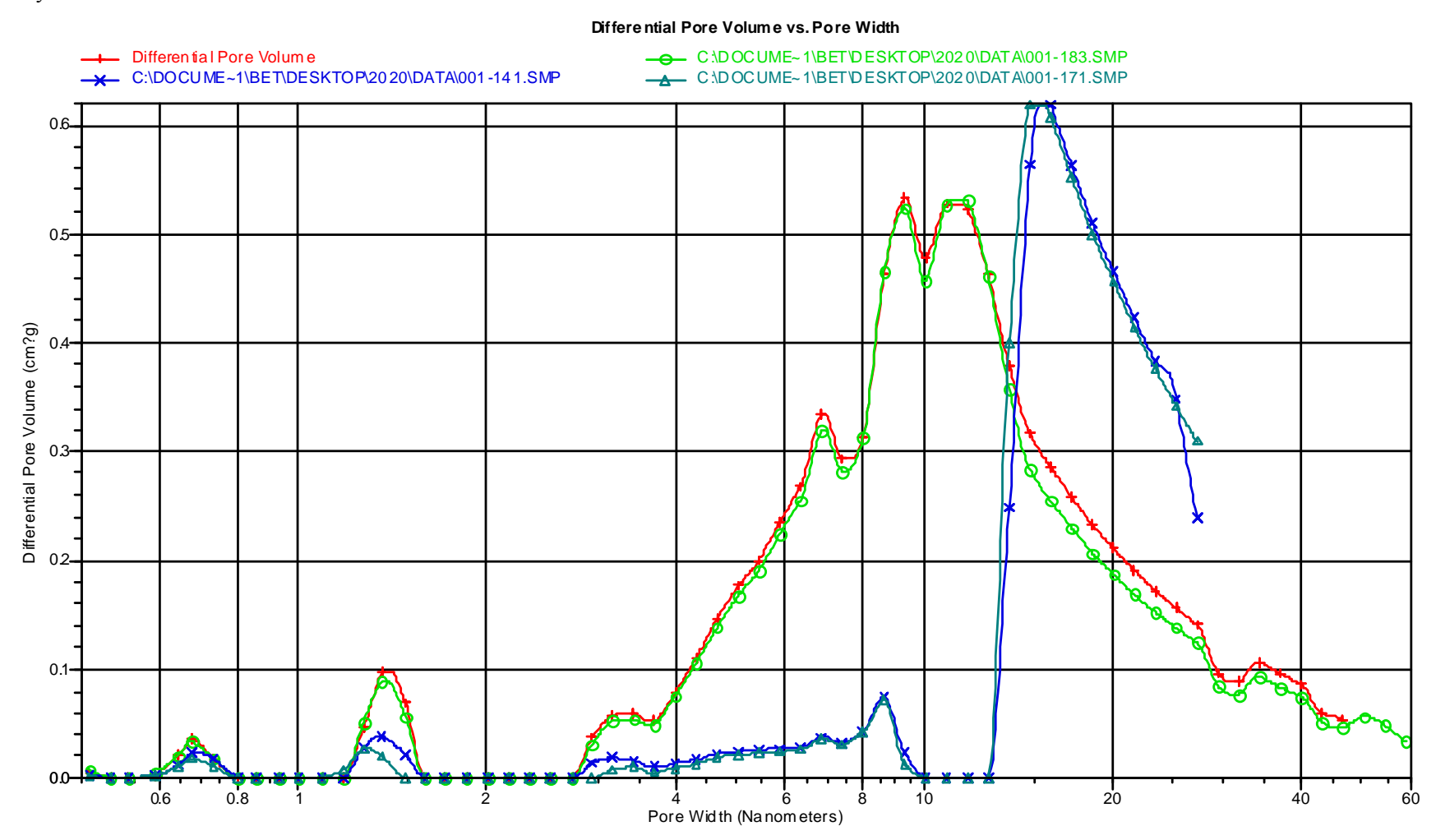


Figure 6-4 Pore size distribution analysis (Red - CCA series original sample (loaded with CuO) Green - CCA series after over 10 cycles of redox under mixed fuel gases)

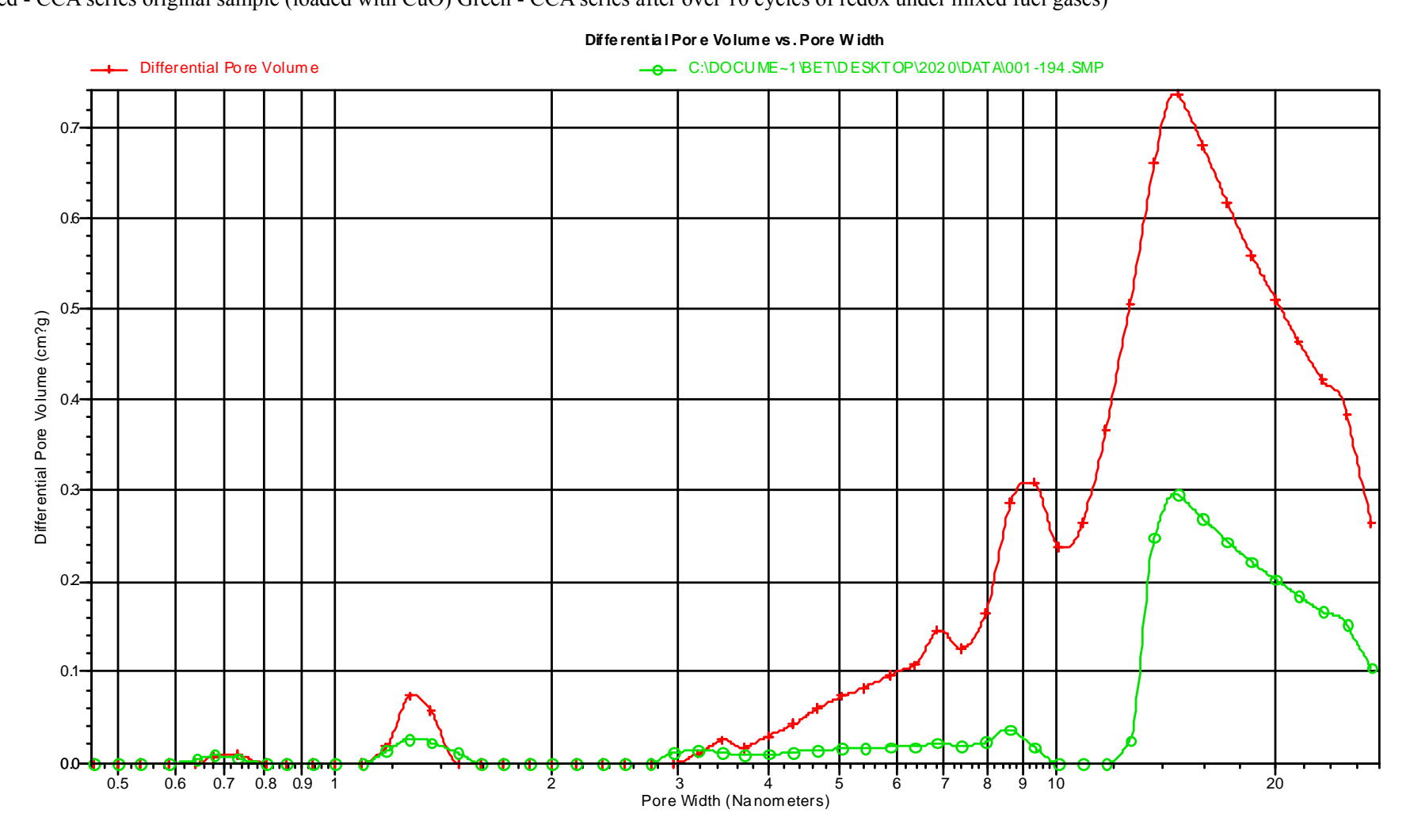
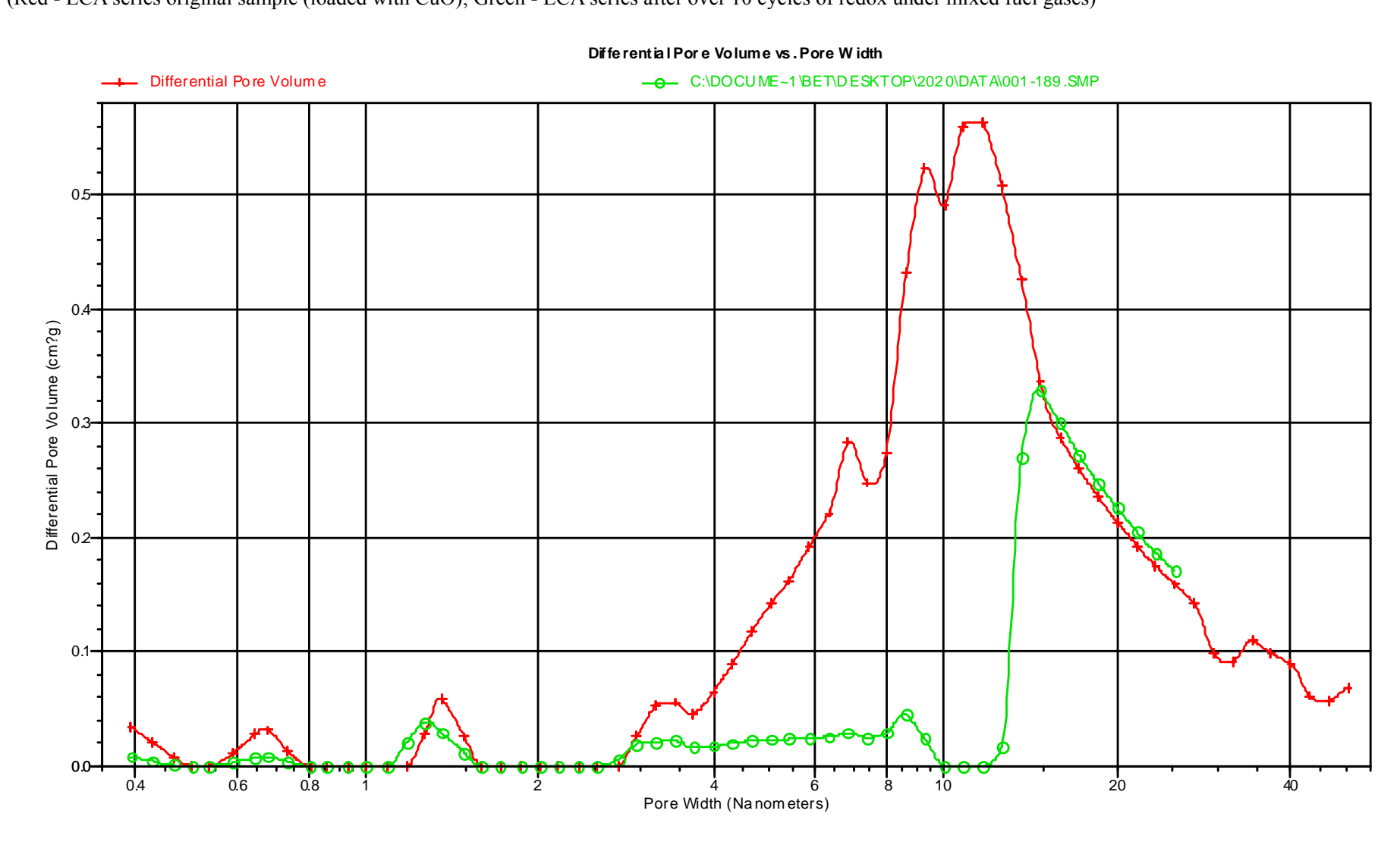
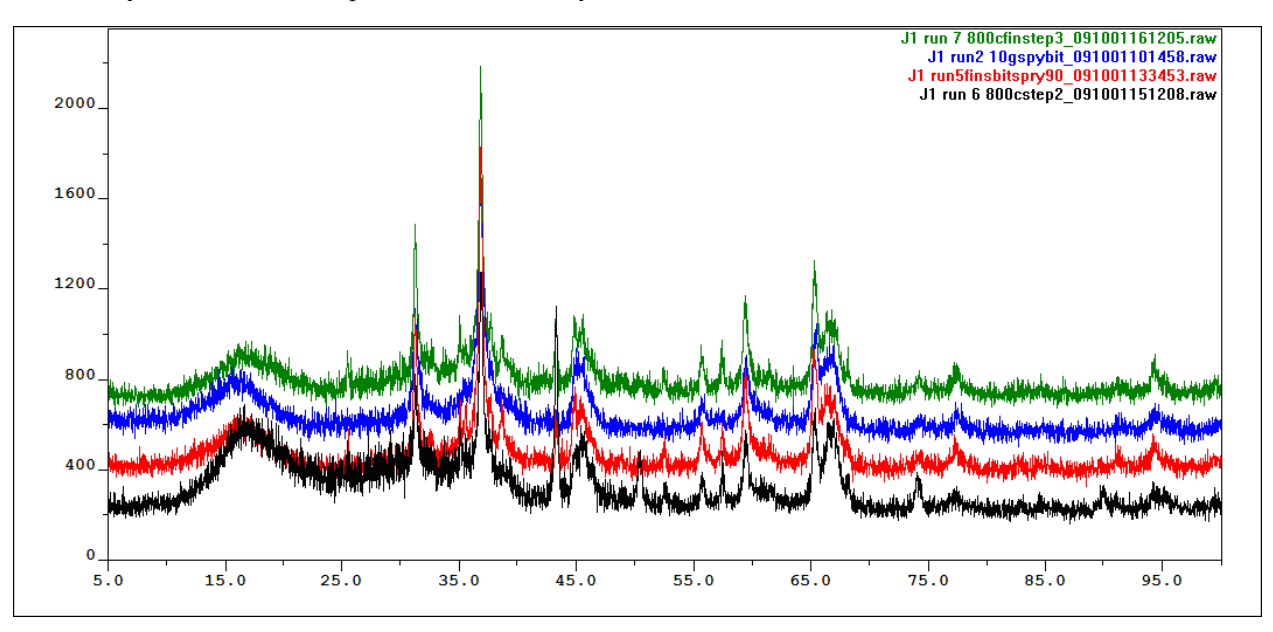


Figure 6-5 Pore size distribution analysis (Red - LCA series original sample (loaded with CuO); Green - LCA series after over 10 cycles of redox under mixed fuel gases)



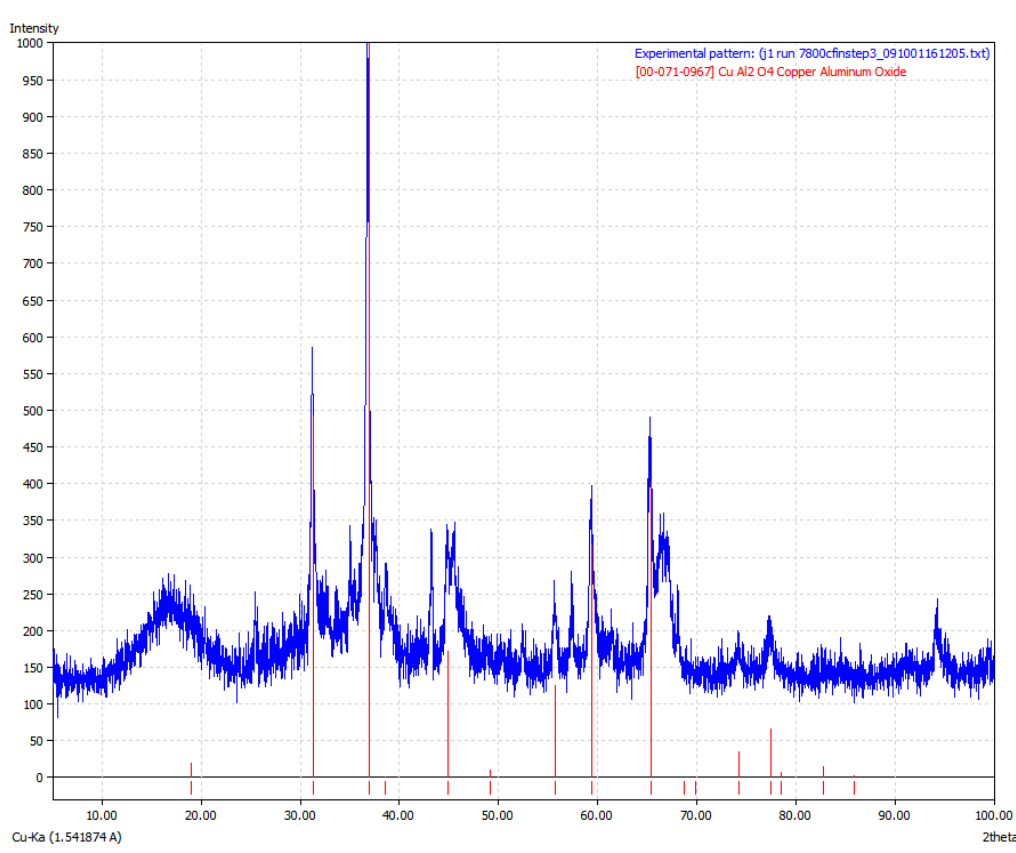
#### 7-1 XRD analysis CA series sample

Overlay of four tested samples from different cycle numbers of redox tests

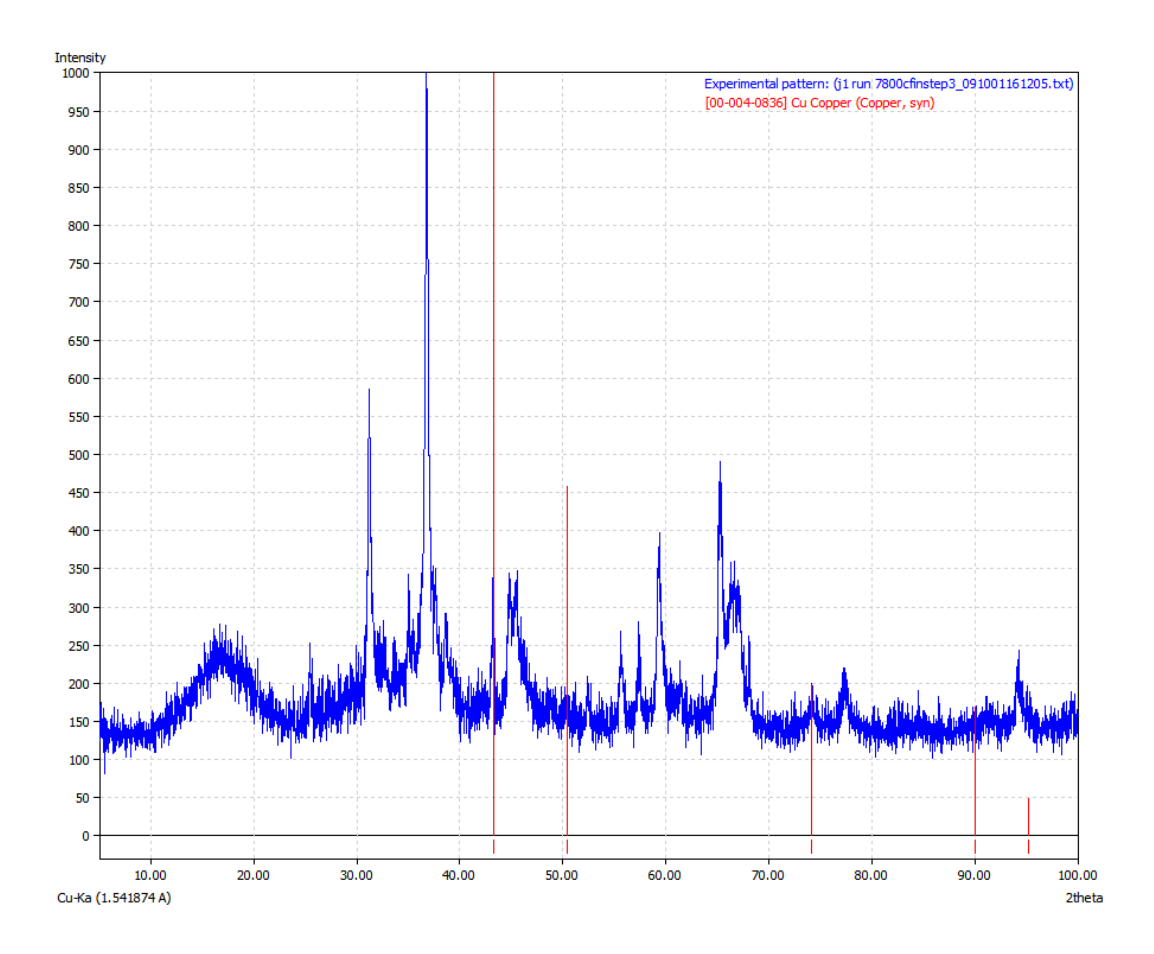


CA series sample after 7 cycles of redox tests – including CuAl<sub>2</sub>O<sub>4</sub>, Al<sub>2</sub>O<sub>3</sub> and Cu.

#### Evidence of CuAl<sub>2</sub>O<sub>4</sub>



#### Evidence of Cu



#### Evidence of CuO

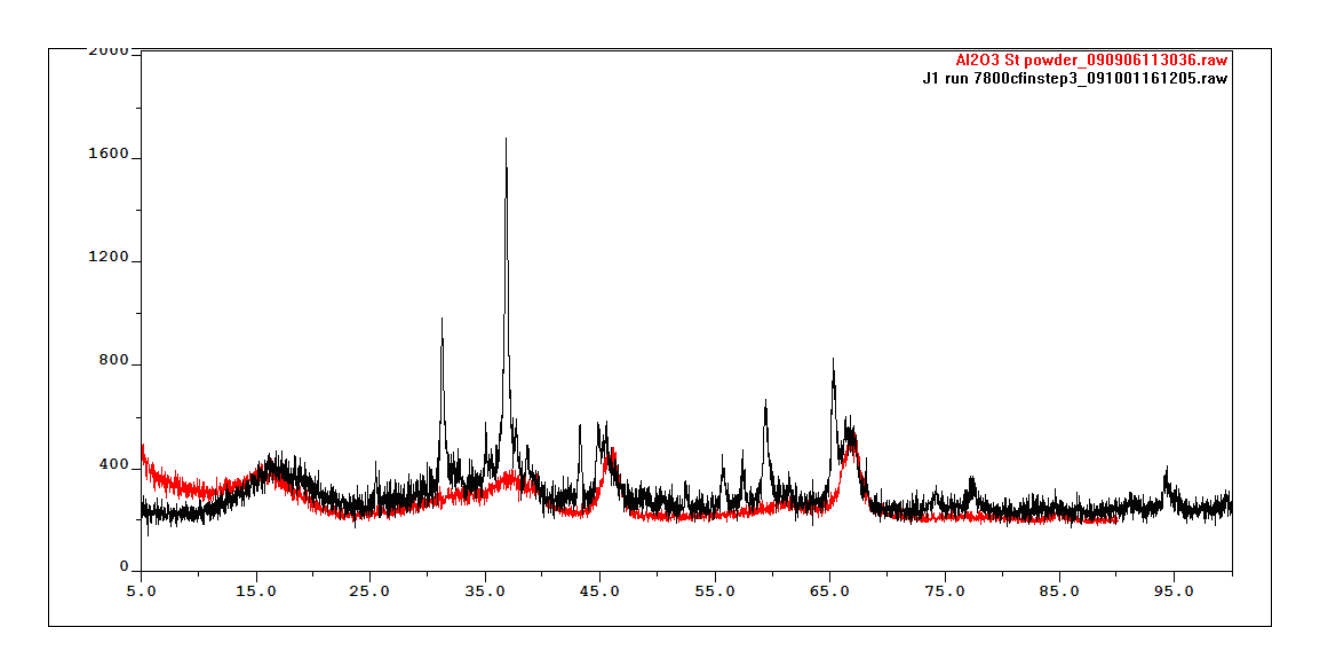
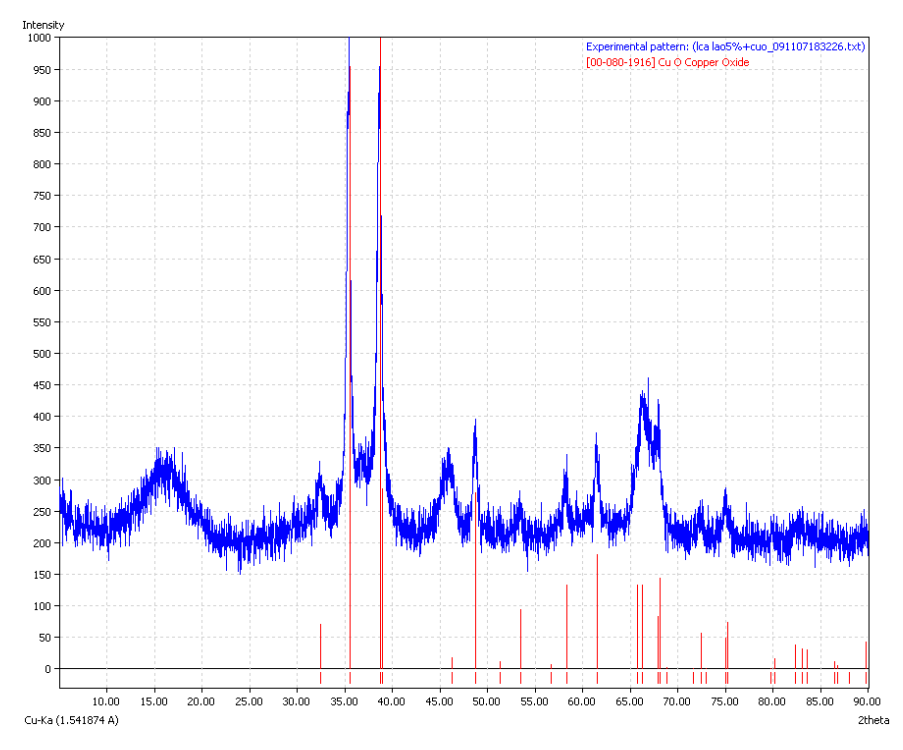


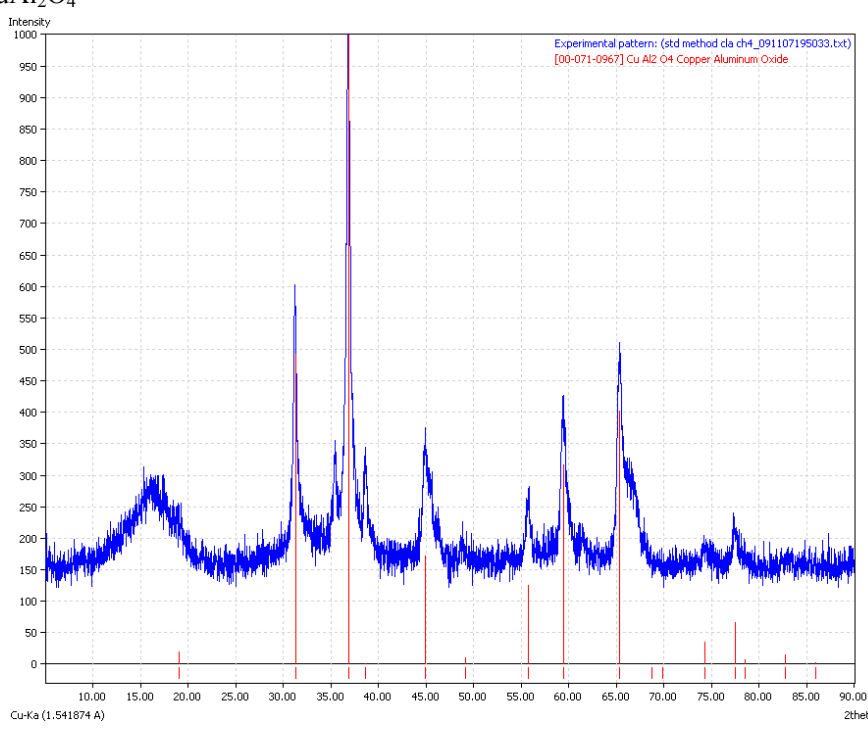
Figure 7-2. XRD analysis

Original CLCA sample – Only including peaks of  $Al_2O_3$  and CuO

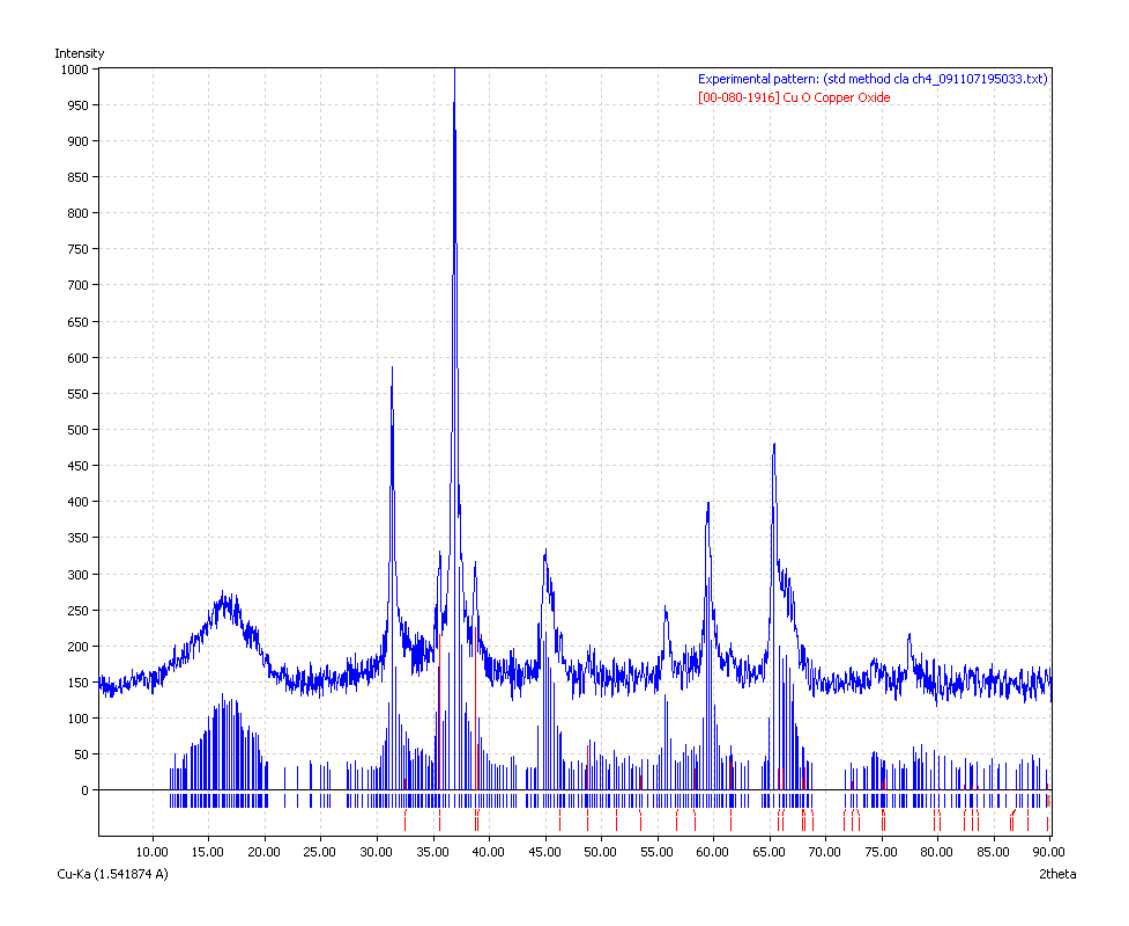


CLCA sample after over 10 cycles of redox tests – including CuAl<sub>2</sub>O<sub>4</sub> besides CuO and Al<sub>2</sub>O<sub>3</sub>

## Peaks of CuAl<sub>2</sub>O<sub>4</sub>



#### Peaks of CuO



## Peaks of Al<sub>2</sub>O<sub>3</sub>

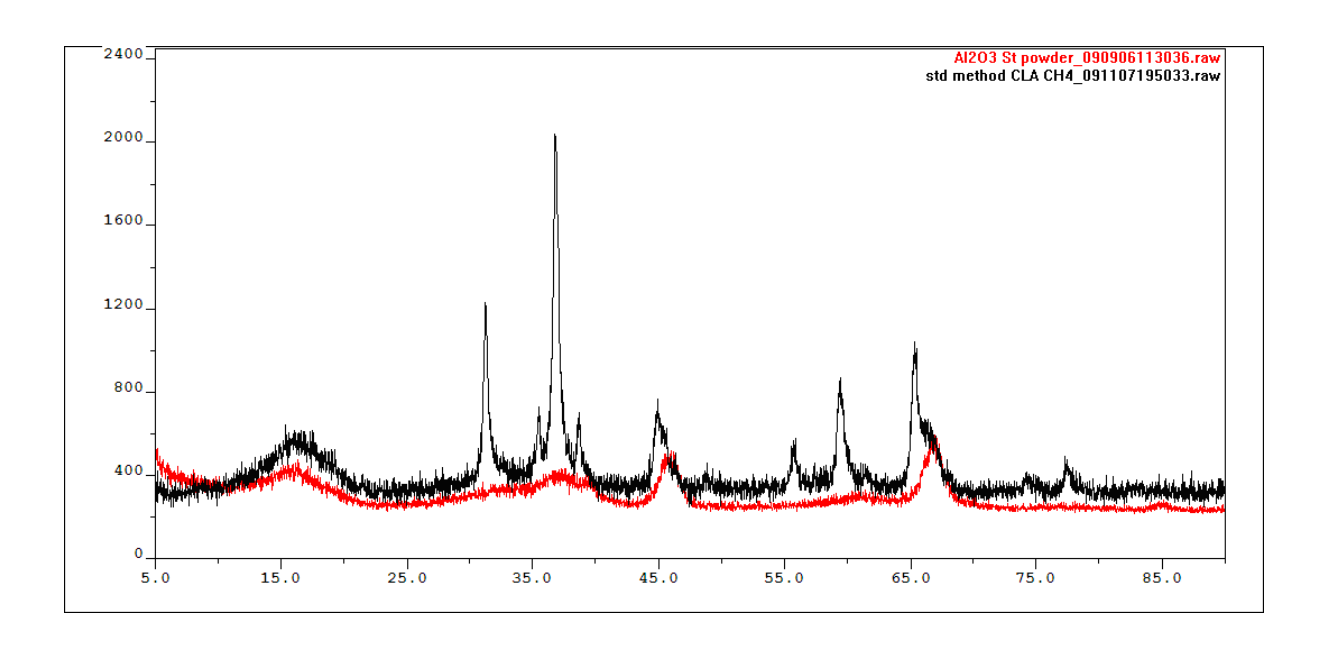


Figure 8. ChemiSorb instrument (air-H<sub>2</sub> cycles)

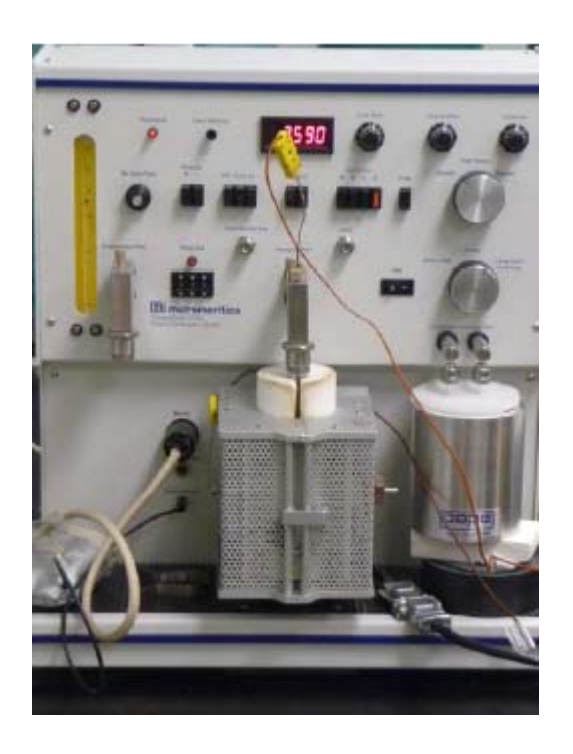


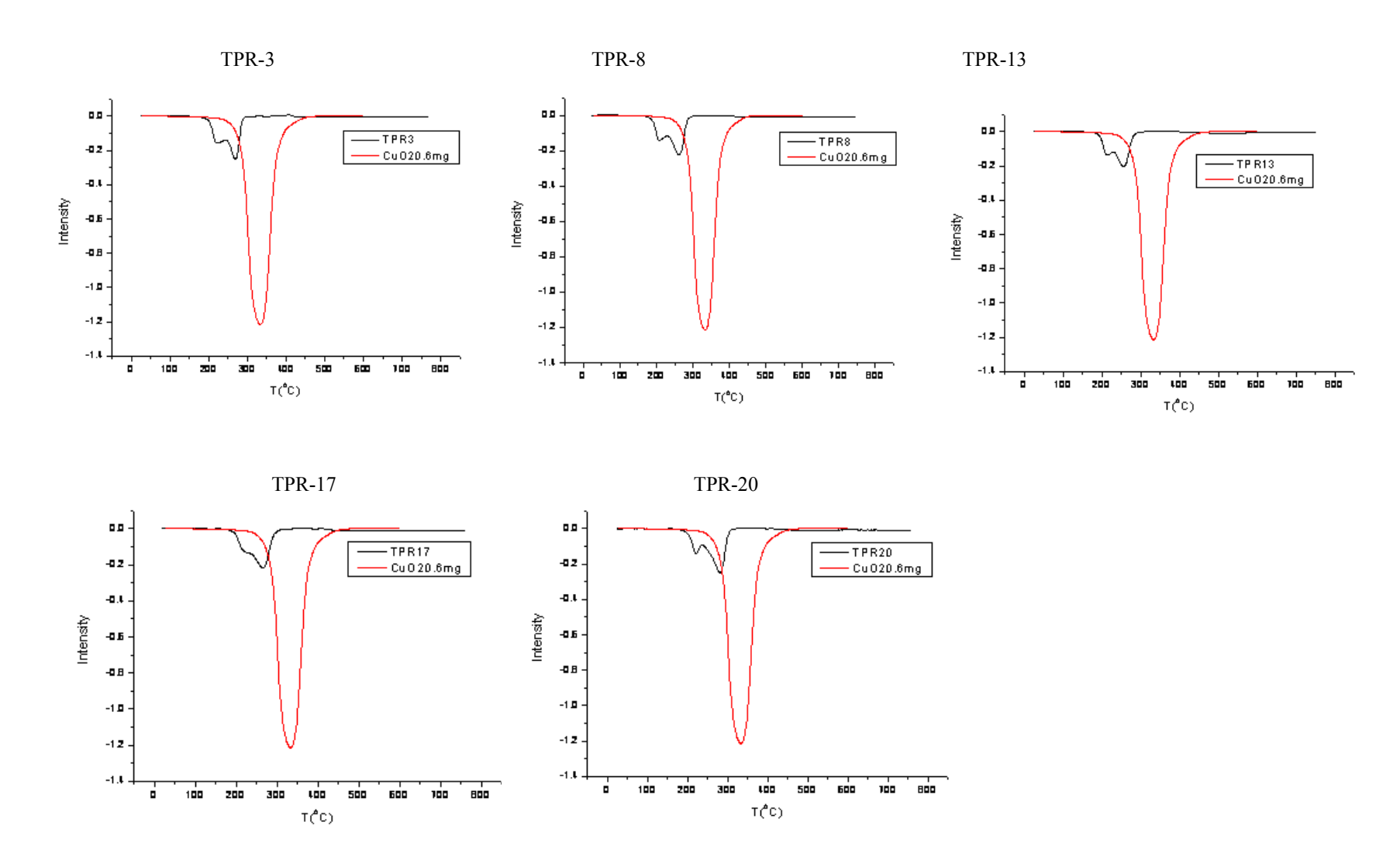
Table 1. Initial trials on increasing loading amount of CuO on Al<sub>2</sub>O<sub>3</sub>

Sample ID	Area	Percent of CuO
PureCuO	57.7	100%
Cao-1 no rinse -TPR	16.4	28.4%
Cao-1 no rinse-TPR-TPR	14.9	25.8%
Cao-2 no rinse — TPR	17.9	31.0%
Cao-2 rinse-TPR	2.5	4.3%
Cao-3 no resin-TPR	14.1	24.4%
Cao-3 rinse-TPR	2.8	4.9%
Cao-4 no resin-TPR	12.1	21.0%
Cao-4 rinse-TPR	10.1	17.5%

Figure 9. Measurement of CuO loading amount and evaluation on prepared oxygen carriers and evaluation of redox performance of prepared oxygen carriers using air-H<sub>2</sub> ChemiSorb

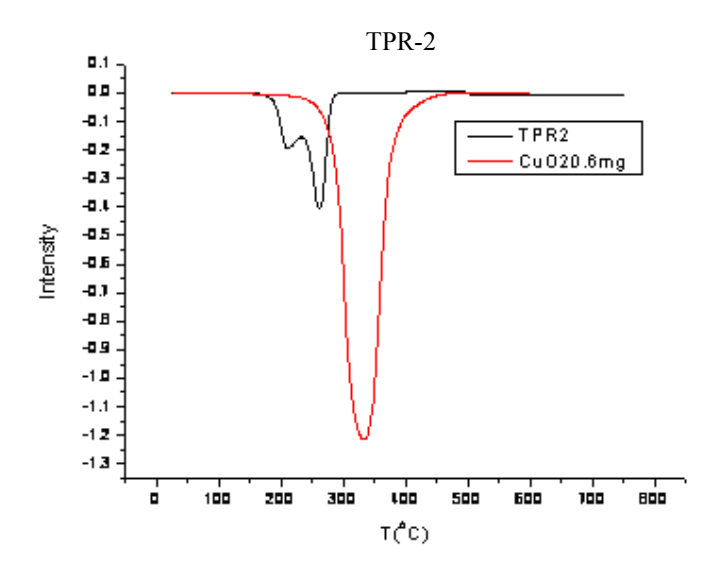
#### CA series samples.

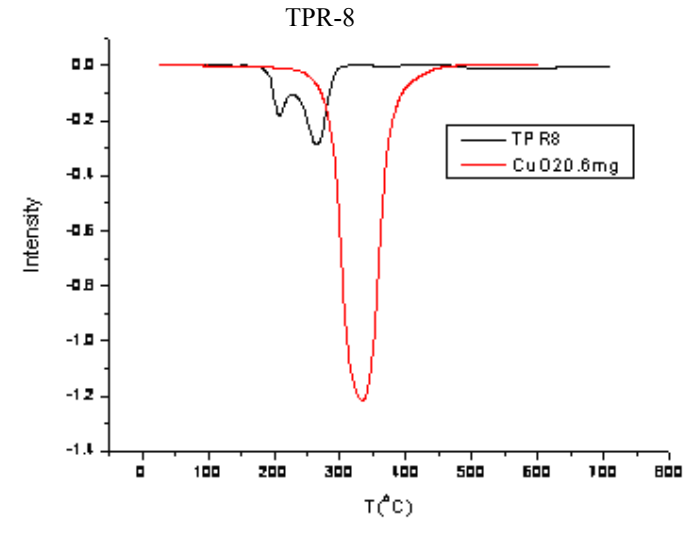
Sample ID	Sample weight (mg)	CuO Area	CuO mass (mg)	CuO content (%)
CA-TPR 1	20.9	15.2	4.31	0.21
CA-TPR 2	20.9	14.2	4.06	0.19
CA-TPR 3	20.9	13.5	3.89	0.19
CA-TPR 4	20.9	13.6	3.91	0.19
CA-TPR 5	20.9	13.2	3.81	0.18
CA-TPR 6	20.9	13.3	3.84	0.18
CA-TPR 7	20.9	13.5	3.89	0.19
CA-TPR 8	20.9	13.9	3.99	0.19
CA-TPR 9	20.9	11.6	3.41	0.16
CA-TPR 10	20.9	11.9	3.49	0.17
CA-TPR 11	20.9	11.9	3.49	0.17
CA-TPR 12	20.9	11.8	3.46	0.17
CA-TPR 13	20.9	11.4	3.36	0.16
CA-TPR 14	20.9	11.6	3.41052	0.16
CA-TPR 15	20.9	11.7	3.43559	0.16
CA-TPR 16	20.9	12.6	3.66122	0.18
CA-TPR 17	20.9	13.5	3.88685	0.19
CA-TPR 18	20.9	13.5	3.88685	0.19
CA-TPR 19	20.9	13.3	3.83671	0.18
CA-TPR 20	20.9	14.3	4.08741	0.2



# CCA series samples.

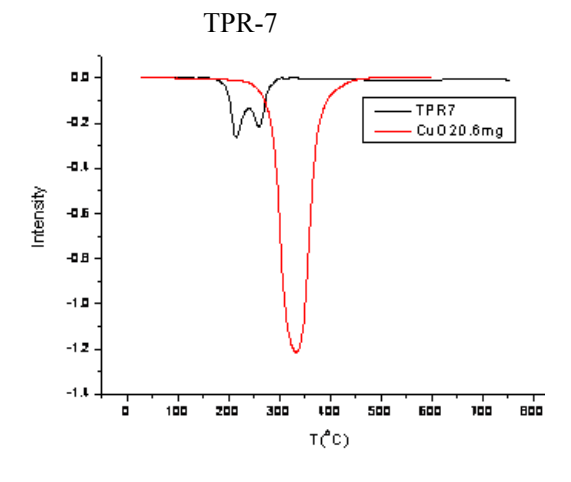
Sample ID	Sample weight	CuO area	CuO weight (mg)	CuO content (%)
CCA-TPR 1	20.7	21.1	5.7	27.8
CCA-TPR 2	19.5	18.7	5.1	26.5
CCA-TPR 3	19.5	16.6	4.6	23.8
CCA-TPR 4	19.5	16.8	4.7	24.1
CCA-TPR 5	19.5	16.6	4.6	23.8
CCA-TPR 6	19.5	15.8	4.4	22.8
CCA-TPR 7	19.5	16.6	4.6	23.8
CCA-TPR 8	19.5	16.3	4.5	23.4
CCA-TPR 9	19.5	16.8	4.7	24.1
CCA-TPR 10	19.5	15.9	4.4	22.9

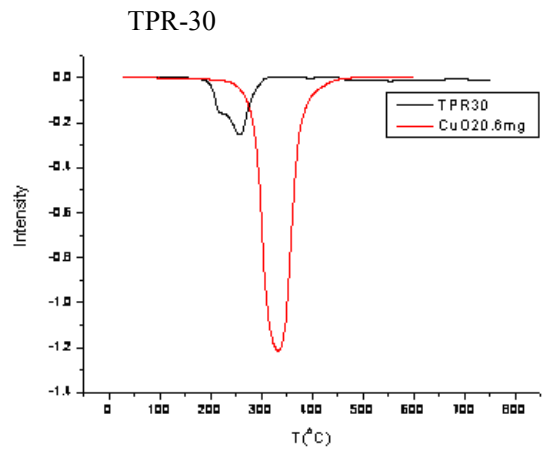


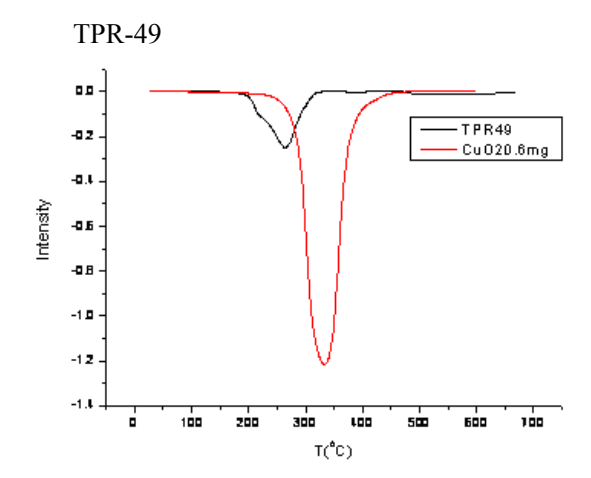


## LCA series samples.

Sample ID	Sample weight	CuO area	CuO weight (mg)	CuO content (%)	Sample ID	Sample weight	CuO area	CuO weight (mg)	CuO content (%)	Sample ID	Sample weight	CuO area	CuO weight (mg)	CuO content (%)
LCA-TPR 1	20.9	18.7	5.2	24.8	LCA-TPR 21	20.9	14.6	4.1	19.8	LCA-TPR 41	20.9	15.8	4.4	21.2
LCA-TPR 2	20.9	24.5	6.7	31.78	LCA-TPR 22	20.9	15.1	4.2	20.4	LCA-TPR 42	20.9	15.6	4.4	21.1
LCA-TPR 3	20.9	16.1	4.6	21.7	LCA-TPR 23	20.9	15.9	4.4	21.4	LCA-TPR 43	20.9	15.1	4.3	20.4
LCA-TPR 4	20.9	15.5	4.4	20.9	LCA-TPR 24	20.9	15.4	4.3	20.8	LCA-TPR 44	20.9	15.2	4.3	20.5
LCA-TPR 5	20.9	15.6	4.5	21.1	LCA-TPR 25	20.9	15.4	4.3	20.8	LCA-TPR 45	20.9	15.9	4.4	21.4
LCA-TPR 6	20.9	13.7	3.95	18.8	LCA-TPR 26	20.9	15.2	4.2	20.5	LCA-TPR 46	20.9	15.6	4.4	21.1
LCA-TPR 7	20.9	14.8	4.2	20.1	LCA-TPR 27	20.9	15.9	4.4	21.4	LCA-TPR 47	20.9	15.5	4.3	20.9
LCA-TPR 8	20.9	14.8	4.2	20.1	LCA-TPR 28	20.9	15.7	4.4	21.1	LCA-TPR 48	20.9	15.2	4.2	20.5
LCA-TPR 9	20.9	15.6	4.4	21.1	LCA-TPR 29	20.9	15.7	4.4	21.1	LCA-TPR 49	20.9	15.7	4.4	21.2
LCA-TPR 10	20.9	14.7	4.2	19.9	LCA-TPR 30	20.9	15.1	4.2	20.4	LCA-TPR 50	20.9	15.5	4.3	20.9
LCA-TPR 11	20.9	14.9	4.2	20.2	LCA-TPR 31	20.9	15.6	4.4	21.1					
LCA-TPR 12	20.9	14	3.9	19.1	LCA-TPR 32	20.9	16.1	4.5	21.6					
LCA-TPR 13	20.9	15.4	4.3	20.8	LCA-TPR 33	20.9	15.1	4.2	20.1					
LCA-TPR 14	20.9	15.1	4.2	20.4	LCA-TPR 34	20.9	15.6	4.4	21					
LCA-TPR 15	20.9	15.6	4.4	21.1	LCA-TPR 35	20.9	14.8	4.1	20					
LCA-TPR 16	20.9	15.3	4.3	20.6	LCA-TPR 36	20.9	15.3	4.3	20.6					
LCA-TPR 17	20.9	15.2	4.2	20.5	LCA-TPR 37	20.9	15	4.2	20.3					
LCA-TPR 18	20.9	15	4.2	20.3	LCA-TPR 38	20.9	15.5	4.3	20.9					
LCA-TPR 19	20.9	15.2	4.3	20.6	LCA-TPR 39	20.9	15.8	4.4	21.2					
LCA-TPR 20	20.9	15	4.2	20.3	LCA-TPR 40	20.9	15.6	4.4	21.1					







ICSET, WKU 56 December, 2012

Figure 10: TGA results of copper-based oxygen carrier – totally 864 cycles (H<sub>2</sub> as fuel)

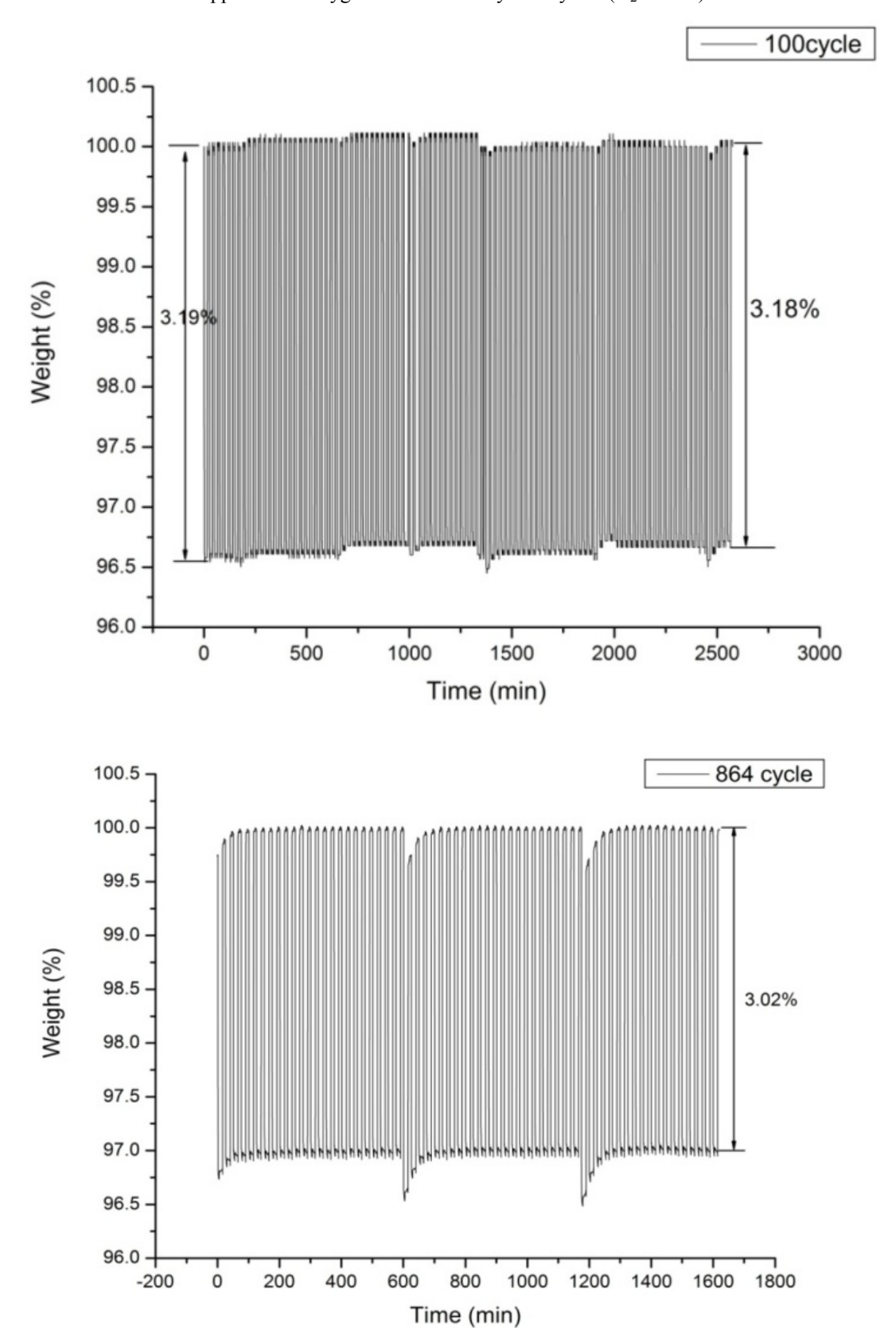
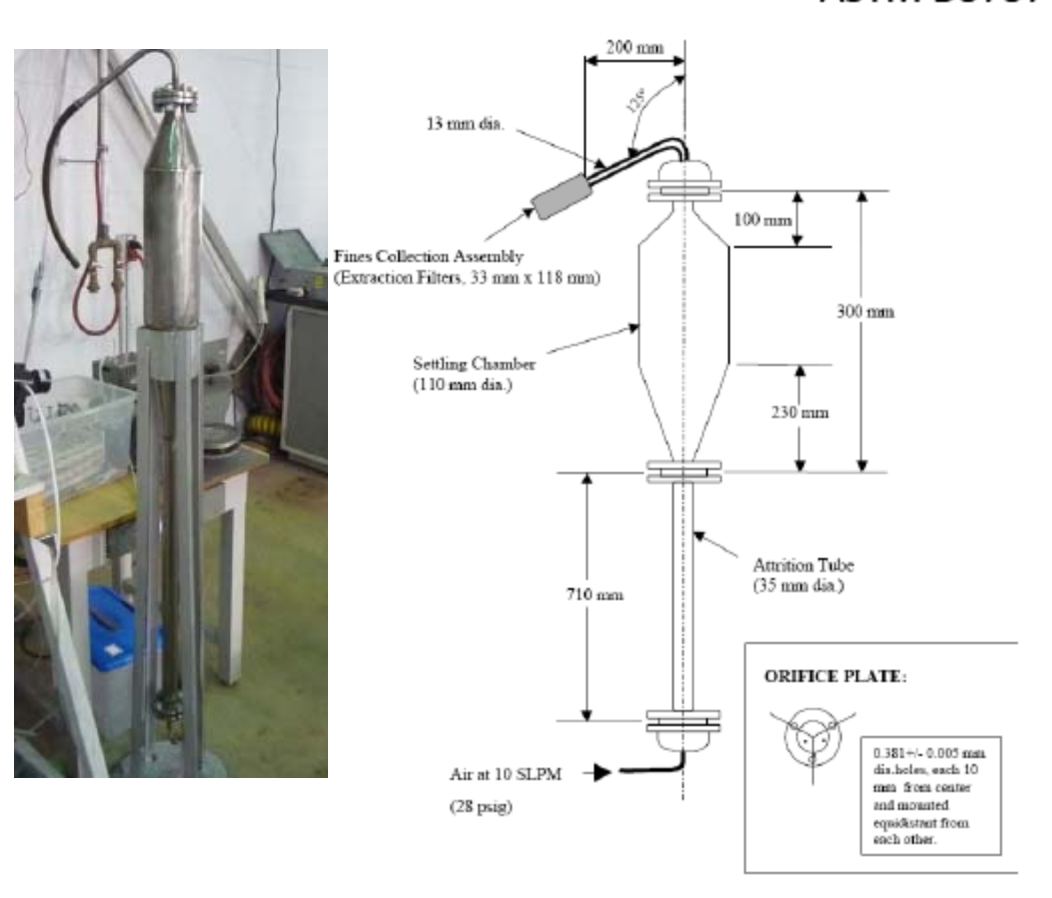


Figure 11. Strength tests of oxygen carrier using attrition test facility and preliminary results

#### ASTM D5757-95 attrition test



## Conditions

1.Particle size: 10~18 micrometer

2.Skeletal Particle density :2.4~3.0 g/cm3

3.Particle amount: 50 grams

4.Temperature and pressure: 273.15 K, 101.325 kPa

5.Air flow rate: 10 l/min(28 psig) 6.Tester material Stainless steel

#### Procedure

- 1. Pour the particles through the top
- 2. Make particle settle down on the bottom of attrition tube
- 3.Close the top
- 4. Measure and Assemble fines Collection Assembly
- 5.Supply air
- 6.After 5hour test measure the weight of Fines collection Assembly
- 7.Calculate collected weight of fines
- 8.Calculate AJI(5)
  - \*\*\*AJI(5)% = collected fines weight /initial weight
- 9. Disassemble and clean

	Original Al2O3	CA	CCA	Original LCA	LCA after tests
Runs	3	2	Х	2	4
Attrition rates,	3.36, 4.44, 4.94	1.79 2.43	x	1.13, 2.38	0.0052, 0.064,
%	3,30, 4,44, 4,34	1.75, 2.45	^	1.13, 2.30	0.26, 0.51

ICSET, WKU 58 December, 2012

#### 2.3. Evaluation of Prepared Oxygen Carriers in 100W CLC Facility

#### 2.3.1 Preparation and Characterization of Selected Coals and Their Ash

In this project, three coals were used in the coal-fired chemical-looping combustion process, including two Kentucky bituminous coals, and one sub-bituminous coal from the Powder River Basin (PRB). Two Kentucky coals were collected from local utilities (EKPC-East Kentucky Power Cooperation), and PRB coal was collected from a utility in Illinois. The collected coal samples were pulverized and air-dried at 80 °C overnight prior to analysis and subsequent feeding to test facilities. Properties of coal and ash are shown in Table 2. One of the Kentucky bituminous coals (#1) has higher ash content, thus, lower heating value (10396 Btu/lb) and carbon content (63.37 wt%). Another Kentucky bituminous coal (#2) presents lower ash (7.57 wt%) and moisture content (1.9 wt%), thus, higher heating value (13527 Btu/lb) and carbon content (72.94 wt%). The volatile content of both Kentucky coals are comparable, averaging 33 wt%. By contrast, PRB coal has higher volatile content (45.06 wt%), but medium heating value at 11090 Btu/lb because of its higher moisture content (11.26 wt%). There are no major significant differences between ashes of both Kentucky coals, except content levels of iron oxides (Fe<sub>2</sub>O<sub>3</sub>). Kentucky Coal #1 presents slightly higher iron oxides in ash, compared to Kentucky coal #2 and PRB coal. PRB coal presents higher CaO in its ash than those of the two Kentucky coals. Oxides of Cu, Cr and Ni, which are potentially oxygen carriers, could be ignored in all three coals. Kentucky bituminous coal #1 was selected as a major tested coal in this study.

The evaluation of combustion and gasification kinetics of selected coal samples was conducted using thermogravimetic analysis (TGA) under an air atmosphere for combustion conditions and a CO<sub>2</sub> atmosphere for gasification conditions. Results, as shown in Figure 12-1 for the air combustion conditions and Figure 12-2 for CO<sub>2</sub> gasification conditions, indicate that there are significant differences in reactivity during pyrolysis, combustion and gasification among the three selected coal samples. Generally, pyrolysis of all selected coals occurred very quickly when coal was heated, and combustion of coal char approximately followed the trend, but this was not the case for gasification coal chars, whose reactivity was subject to significant decreases for two Kentucky coals. The two Kentucky coals have both lower combustion and gasification reactivity than that of low-rank PRB coal because there are no significant decreases of gasification reactivity compared to the pyrolysis process. This might imply that a longer

residence time was necessary for the full conversion of the two Kentucky bituminous coals, than that of low-rank PRB coal.

The particle-size distributions of the prepared oxygen carriers and tested coals are shown in Figure 13-1. The prepared oxygen carrier had narrow particle-size distribution, and average about 262 µm. The majority of particle sizes were around 250 µm. This particle size with a narrow-size distribution makes the selected supporting material an excellent candidate for preparation of oxygen carriers being operated in fluidization modes. The average size of the three tested coals is around 750 µm as prepared. The average size of char, which was collected after tests, was found to be about 680 µm, but its particle density decreased significantly, from about 1300 kg/NM<sup>3</sup> for coals to 770 kg/NM<sup>3</sup> for their chars. These two physical parameters (sizes and densities) were very important in determining their fluidization behaviors, which could be grouped into the Gerldart fluidization chart, as shown in Figure 13-2. The two parameters of all tested particles were organized and marked in the Gerldart fluidization chart, which shows all tested particles are located in Group B, in which a smooth fluidization could be expected. The follow-up mixing tests, using coal char and oxygen carriers under fluidization conditions at U=5U<sub>mf</sub>, indicated a better mixture status could be achieved between the coal char and the oxygen carrier of their selected sizes. This was not the case when switching coal-char samples with the prepared coal samples under similar fluidization conditions, where serious segregation between coal and oxygen carriers was found. Because of the quick pyrolysis of coal under testing temperatures, the initial segregation of coal and oxygen carriers at their selected sizes in the fluidization conditions, will soon be replaced by the better mixing status of the coal char and oxygen carrier.

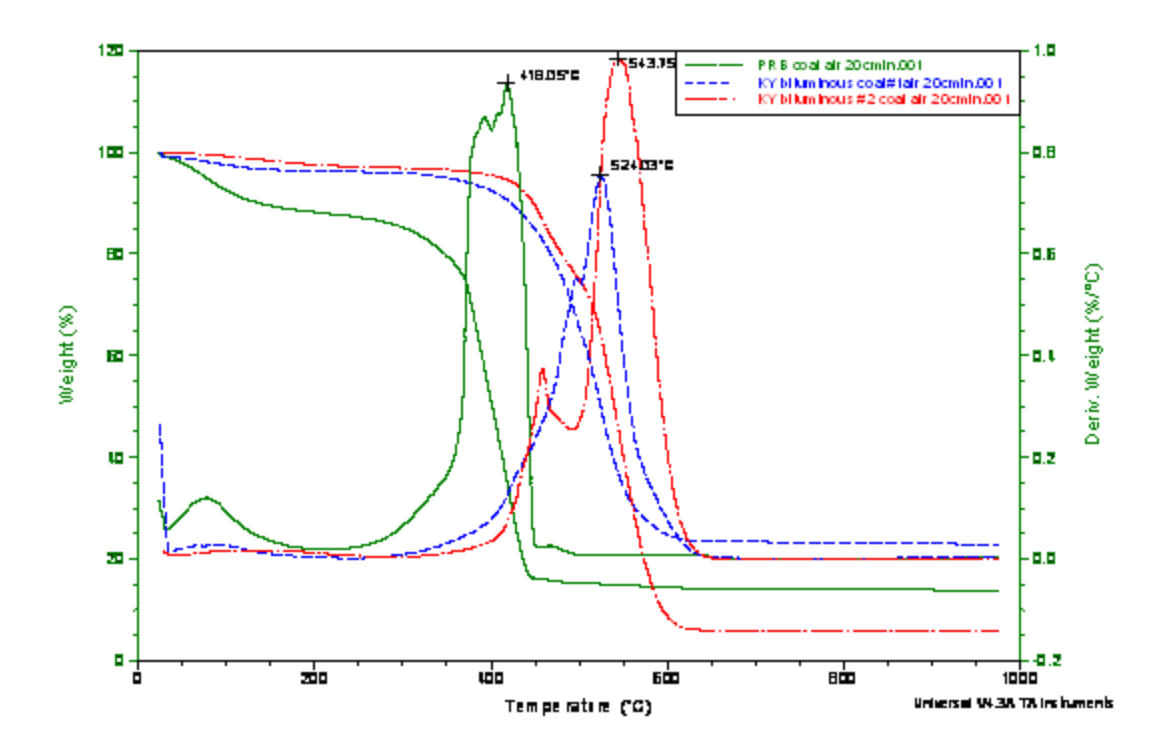
Table 2. Properties of coal and ash

		Dry Basis							
	Moisture	Ash	Vol. Mat	Sulfur	Btu	Carbon	Hydrogen	Nitrogen	Oxygen
SampleName	%	%	%	%	BTU/lb	%	%	%	%
Kentukcy Bituminous Coal #1	3.00	23.08	31.18	3.71	10396	63.37	4.56	1.16	4.12
Kentukcy Bituminous Coal #2	1.90	7.57	34.83	0.08	13527	72.94	5.00	1.46	12.95
Sub-bituminous Coal	11.26	9.47	45.06	0.78	11090	64.37	4.81	1.03	19.55
	Chloride	Fluoride	Bromide	Mercury					
	ppm	ppm	ppm	ppm					
Kentukcy Bituminous Coal #1	1506	102	ND	0.20					
Kentukcy Bituminous Coal #2	1185	40	ND	0.01					
Sub-bituminous Coal	129	62	ND	0.11					
	$Al_2O_3$	Fe <sub>2</sub> O <sub>3</sub>	SiO <sub>2</sub>	CaO	Na <sub>2</sub> O	K₂0	SrO	MgO	TiO <sub>2</sub>
	%	%	%	%	%	%	%	%	%
Kentukcy Bituminous Coal #1	20.576	15.357	51.456	2.166	0.482	2.482	0.055	1.075	1.095
Kentukcy Bituminous Coal #2	25.743	4.226	51.654	7.476	0.382	2.025	0.150	1.480	1.941
Sub-bituminous Coal	18.129	5.574	36.875	17.477	0.523	0.631	0.196	3.153	1.638
	SO <sub>3</sub>	BaO	P <sub>2</sub> O <sub>5</sub>	MnO	Cr <sub>2</sub> O <sub>3</sub>	CuO	V <sub>2</sub> O <sub>5</sub>	ZnO	NiO
	%	%	%	%	%	%	%	%	%
Kentukcy Bituminous Coal #1	2.106	0.092	2.750	0.193	0.018	0.007	0.043	0.035	0.009
Kentukcy Bituminous Coal #2	2.160	1.271	1.227	0.160	0.023	0.011	0.046	0.008	0.017
Sub-bituminous Coal	11.022	2.346	2.204	0.114	0.014	0.018	0.067	0.011	0.008

ICSET, WKU 61 December, 2012

Figure 12. Characterization of combustion and gasification reactivity of tested coal

## 12-1. combustion reactivity



## 12-2. gasification reactivity

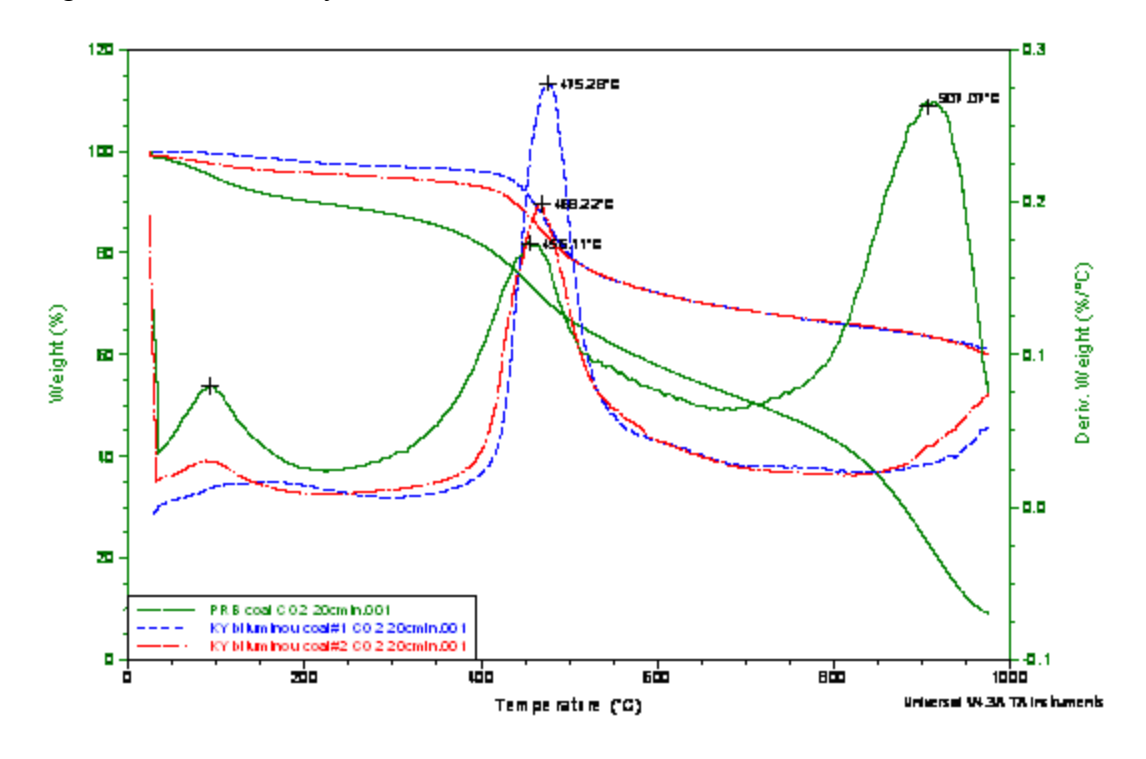
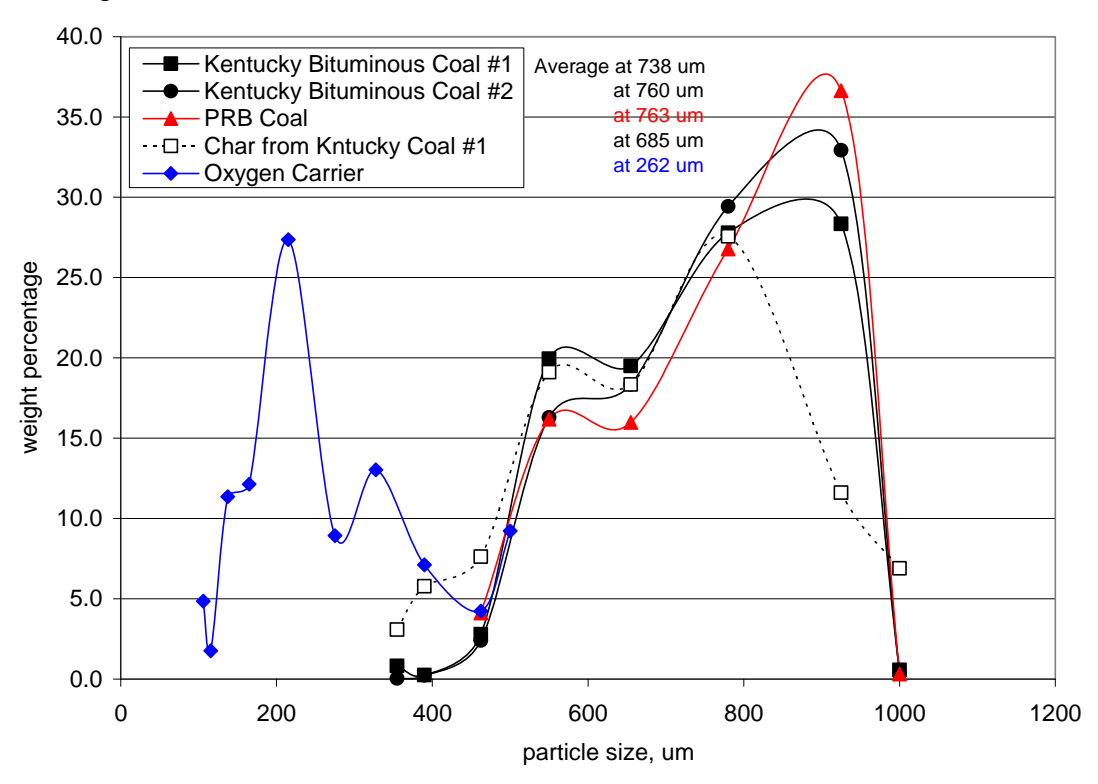
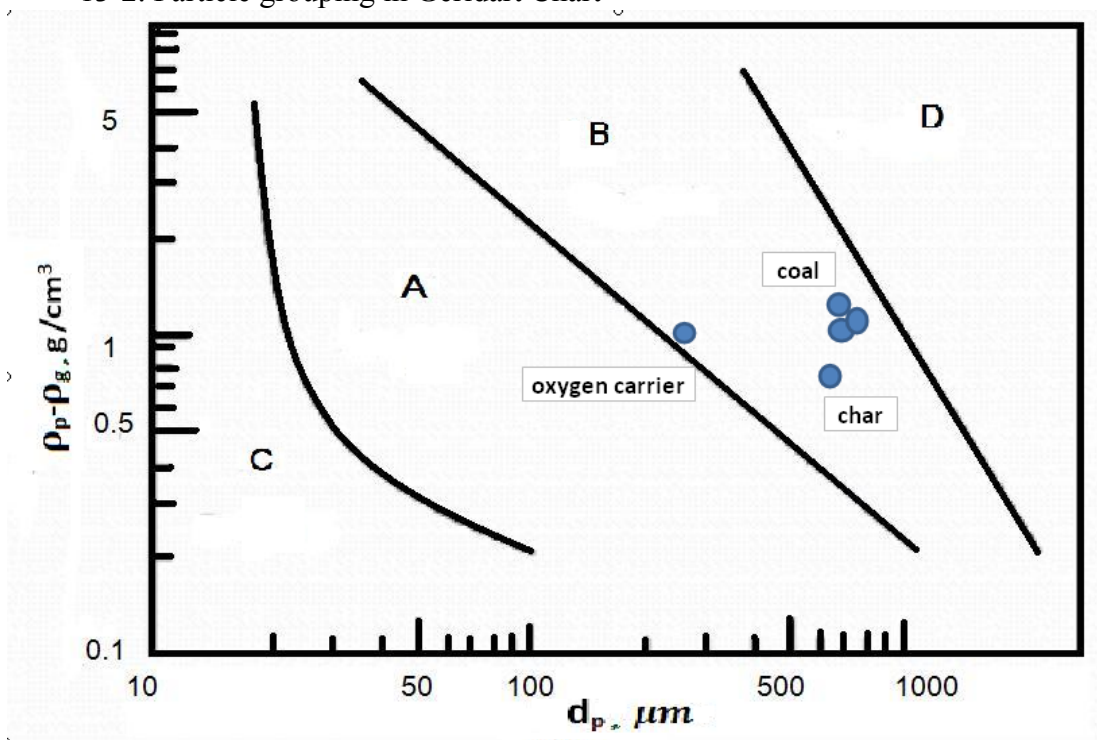


Figure 13. Particle size distribution of selected coal samples and oxygen carriers

## 13-1. particle size distribution



## 13-2. Particle grouping in Gerldart Chart



#### 2.3.2 Lab-scale fluidized bed CLC facility.

A fluidized bed coal-fired chemical looping combustion facility was used in this study. The schematic of this setup is shown in Figure 14-1, and the picture of the entire setup system is shown in Figure 14-2. It includes several major components: an electrically heated main body of the fluidized bed reactor; one hopper for storage of the coal and oxygen carrier mixture, one screw feeder; a steam generator and a gas switch system (between air, N2 and steam) and their metering system; a bed material discharging pipe and a collecting hopper; a synthesis gas cleanup unit mainly including a high temperature metal filter and water cooling tube, and a wet scrubber. The inside diameter (ID) of the low part of the facility is about 20 mm. There is a plate gas distributor at its bottom with a percentage of its total opening at 1% in order to achieve good fluidization performance. The facility's temperatures are monitored by a platinum-rhodium thermocouple, which is sealed into a stainless steel tube. The thermocouple could be movable inside this tube to monitor temperature variation along the height of the facility. The temperatures of the facility were found to be evenly distributed along the height of the gasifier except for the coal feeding area, where the temperature was generally 50 °C lower than those at other parts of the facility due to coal fed at room temperature. The pressure drop between the bottom and top of the facility is monitored by a U-shaped water column tube.

The air under oxidation conditions or the mixture of nitrogen and steam under reduction conditions were preheated and continuously fed into the facility through the gas distributor. Flow meters were used for controlling flow rates of air and nitrogen injection, which were calibrated before tests began. Air supply was obtained from a compressed air line. The steam was generated by a steam-carrying bath using nitrogen as the carrying gas with temperatures controlled to the desired carrying rates of saturated steam at setting temperatures into the facility. The nitrogen stream from an  $N_2$  cylinder was used for system start-up and shut-down and conditions when switching between oxidation and reduction. The nitrogen also functioned as a trace gas to calculate flow rates generating gas under both oxidation and reduction conditions. The fluidized-bed facility was generally operated at a velocity of about 5  $U_{\rm mf}$  (the minimum fluidization velocity under local operational temperatures). Coal feeding was controlled by a volumetric screw feeder, which was calibrated prior to tests. There were two outlets for mixture collection. There was a special port for the overflow of the mixture of coal ash (or char) and oxygen carriers on the top of the dense phase of the fluidized bed. During tests, the mixture of

coal and oxygen carriers was continuously fed in and the mixture of coal char or ash and oxygen carriers was continuously discharged through this overflow port to maintain the height of the dense phase of the bed material in the facility. It was used to control residence time of the oxygen carrier and coal ash in the facility. The adjustability of the mixture's residence time in the facility could be achieved by changing the mixture feed rate, since the amount of coal char and oxygen carrier inside the facility remained constant during the test. The minimum amount of the mixture that was entrained at the top outlet of the facility was collected by a high temperature porous metal filter. The cleaned and cooled gas was directly delivered into a micro-GC analyzer for gas analysis.

The reactor was initially filled with a desired amount of fresh-oxygen carriers and was electrically heated to the desired temperature under the air atmosphere to simulate oxidation conditions. This was followed by feeding prepared coal samples to start the reaction between coal and oxygen carriers under the N<sub>2</sub>/H<sub>2</sub>O atmosphere to simulate reduction conditions. During and after this step, the mixture of reduced oxygen carriers and coal ash or char in the reactor as well as those in the collection hopper was again fed back to the reactor using the screw feeder under air oxidation conditions. This cyclic operation continued until over 20 cycles were achieved. During these cyclic operations, a fresh oxygen carrier was not supplied. Offgas was analyzed by a Micro-GC instrument and solid samples were collected for characterization.

Figure 14-1. Schematic of lab-scale test facility on chemical looping combustion

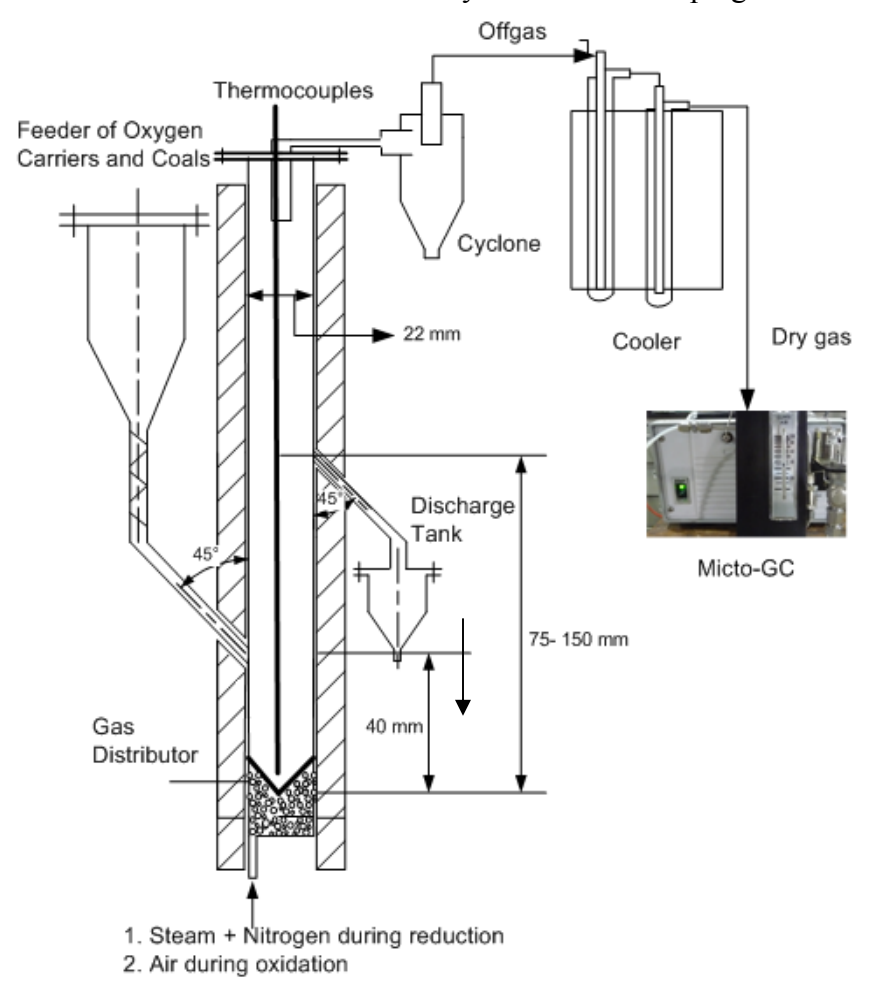
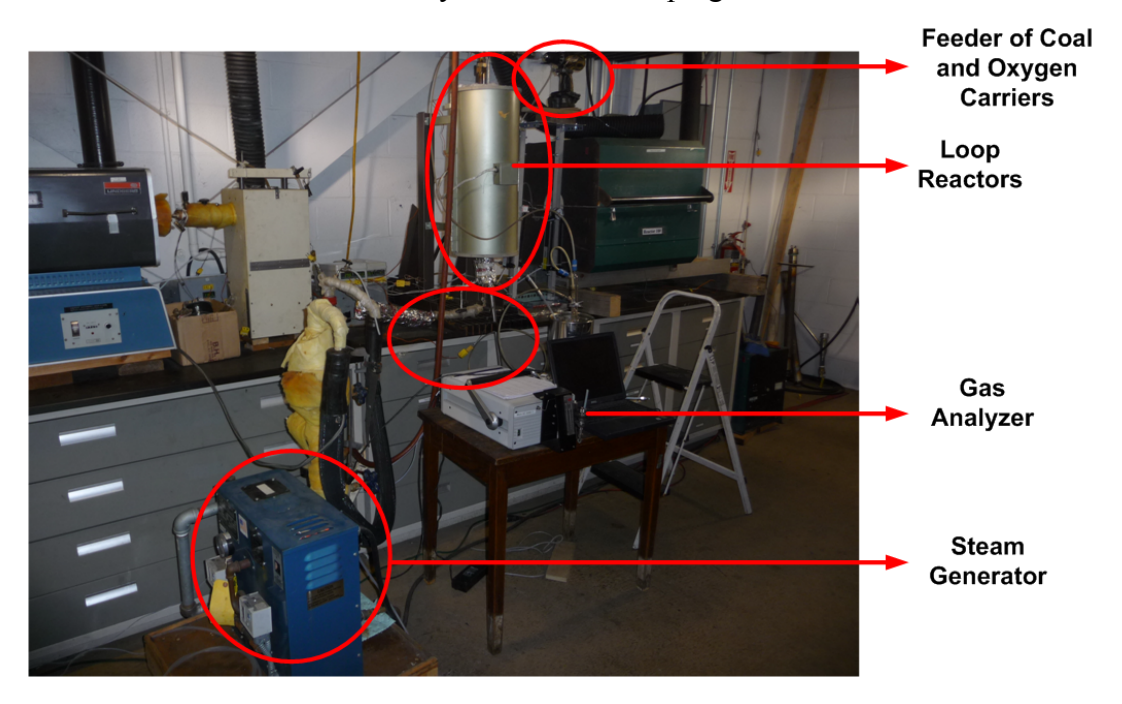


Figure 14-2 Picture of lab-scale test facility on chemical looping combustion



#### 2.3.3 Cyclic Operations of Coal-fired Chemical Looping Combustion (20 cycles)

Cyclic operations of coal-fired chemical looping-combustion were conducted in the aforementioned lab-scale fluidized bed CLC facility. Major parameters and key results are summarized in Table 3. Results show that various solid fuels of differing reactivity may be adapted to achieve the varied carbon conversion efficiency in a range between 50-100 % under optimal utilization temperatures of CuO at 900-950 °C. Depending on solid residence time, which was typically 8 to 15 minutes, the carbon conversion of low-rank coal (PRB coal) in high reactivity was over 90%, contrasting with 50% (8 minutes of solid residence time) and close to 90% (15 minutes of solid residence time) for typical Kentucky bituminous coal (Kentucky bituminous coal #1). A gas-residence time close to 1 second seemed enough to convert all combustible gas (CH<sub>4</sub>+CO+H<sub>2</sub>) in the fuel reactor, which was from the gasification of coals. This test also identified that CLC of solid fuel is more comparable to the gasification process of solid fuel. Like gasification of solid fuel, CLC of solid fuel yields less reactive char residue, which needs more severe operational conditions to use it. This causes CLC of solid fuel to face both technical and economic challenges. Based on the kinetics of combustion and gasification of solid fuels, partial coal gasification and combustion using the chemical looping technology and partial residue char combustion in existing boilers can solve this issue and resolve these challenges within one process cycle.

Figure 15 shows a gas concentration profile at the exit of the fuel reactor using Kentucky bituminous coal #1 as fuel in over 20 cycles of cyclic operation. During the initial 30 hours over 15 redox cycles, 100 % of CO<sub>2</sub> was found at the exit of the fuel reactor on an SO<sub>2</sub>-free basis, which was removed prior to sequestrating CO<sub>2</sub>. There was no H<sub>2</sub>, CO or CH<sub>4</sub> found at the exit of the fuel reactor during these 15 cycles. The only exception was that the H<sub>2</sub> concentration increased slightly at the end of each cycle, where oxygen was totally consumed. As redox cycles exceeded 20 and the accumulated time of oxygen carriers in redox cycles achieved over 38 hours, it was identified that the failure occurred in the pre-heater, which caused a temperature decrease at the lower portion of the reactor, where some SO<sub>2</sub> may have reacted with copper in the oxygen carrier, resulting in a loss of oxygen-carrying capability. In all, this test successfully demonstrated the feasibility of obtaining pure CO<sub>2</sub> for sequestration in the proposed process, as well as the importance of maintaining temperatures in the fuel reactor.

A higher sulfur content of 3.5 wt% was found in one Kentucky coal (Kentucky bituminous

coal #1). This could potentially create fast degradation of oxygen carrier because of interaction between oxygen carriers and sulfur. Coal was only fed in the fuel reactor to reduce oxygen carriers. Therefore, sulfur in coal will firstly be resealed as H<sub>2</sub>S or SO<sub>2</sub>, and subsequently react with copper-based oxygen carrier to form potential sulfur-loading solid products under desired temperatures, such as the CuS or Cu<sub>2</sub>S, CuSO<sub>4</sub>. Thus, as mentioned in the last paragraph, sulfur is not only a major concern as an air pollutant in the coal-fueled chemical looping combustion process, but also leads to the degradation of oxygen carriers by their sulfurization. This will become even worse when sulfurization of oxygen carriers in the fuel reactor likely releases sulfur as diluted SO<sub>2</sub> in the subsequent air reactor because oxygen carriers always re-circulated between air and fuel reactors within the chemical looping process. From the perspective of chemical-reaction engineering, the diluted SO<sub>2</sub> is more difficult to remove. This makes a large control facility is and high energy penalty necessary. Ideally only the gas-phase sulfur compounds (such as H<sub>2</sub>S or SO<sub>2</sub>) are formed in the concentrated CO<sub>2</sub> stream at the outlet of the fuel reactor. In this case, only the higher H<sub>2</sub>S or SO<sub>2</sub> concentration was generated in lower amounts of the total gas output, which was easily controlled economically. The depletion of copper-based oxygen carrier fine particles, which are a good sulfur adsorbent, was proposed to be used downstream of the chemical looping combustion process to capture gas phase sulfur species.

The thermodynamics study, as shown in Figure 16, indicated that the temperatures and atmospheres were two major factors in creating sulfur transformation between the sulfur compounds in the solid phase and those in the gas phase in the fuel reactor. Using the example of the CH<sub>4</sub>-fueled chemical looping combustion process, with an excessive supply of CH<sub>4</sub> and H<sub>2</sub>O, the system will be under a reducing atmosphere with the availability of H<sub>2</sub>, CO and CH<sub>4</sub>. In this case, the solid Cu<sub>2</sub>S will be the major sulfur compound when equilibrium is achieved. When decreasing the supply of CH<sub>4</sub> and H<sub>2</sub>O, but keeping CH<sub>4</sub> excessive, we found that the solid Cu<sub>2</sub>S remains the major sulfur compound. The occurrence of Cu<sub>2</sub>S will exist in a wider temperature range from 200 °C to 700 °C (at least). This means that Cu<sub>2</sub>S will most likely enter the air reactor, followed up by SO<sub>2</sub> emissions at its outlet. The amounts of Cu<sub>2</sub>S generated inside the reducer is dependent on its sulfurization kinetics.

Generally, the oxygen carrier (CuO herein) was excessively supplied inside the reducer to prevent leakage of combustible constituents (pyrolysis and gasification products of coal under

 $H_2O$  and  $CO_2$ ) out of the fuel reactor as secondary air pollutants. In this case, the thermodynamics study proved that the solid-sulfur compounds, such as  $Cu_2S$ ,  $CuSO_4$  and  $Cu_2SO_4$ , are major products only under a lower-temperature range below 300 °C. Starting at 300 °C, increasing temperatures will significantly increase the occurrence of  $SO_2$  in the offgas stream. Theoretically, gaseous  $SO_2$  will be the only sulfur compound when operational temperatures exceed 600 °C.

Table 3. Summary of test condition and results

Gas velocity Umf (cm/s)	Geradart A type Particle			
3.43				
Expansion factor	Packing density (kg/NM³)	Density in fluidization (kg/NM³)		
1.34	947.80	708.13		
. Test conditions				
2.1 Facility - 1				
ID (cm)	Bed Height (cm)	Reactor temperature (°C)	Steam Temp (°C)	Vapor content
2.20	7.50	900-950 Fuel reactor 800-850 Air reactor	150.0	95.2%
2.20	7.50	900-950 Fuel reactor 800-850 Air reactor	80 (nitrogen carryover)	50.0%
	U/Umf	Average solid residence time (mins)	Average gas residence time (mins)	
Test 1 - 21 cycles	5.26	8.08	0.42	
Test 2 - 20 cycles	5.28	8.08	0.41	
2.2 Facility - 2 (modified)				
ID (cm)	Bed Height (cm)	Reactor Main Temp	Steam Temp (°C)	Vapor content
2.14	15.00	900-950 Fuel reactor 800-850 Air reactor	80 (nitrogen carryover)	50.0%
	U/Umf	Average residence time (mins)	Average gas residence time (mins)	
Test 2 - 20 cycles	5.58	15.28	0.78	
. Major Results				
3.1 Facility - 1_	Carbon conversion (%)	CO2 purity (%)	The total of CO+H <sub>2</sub> +CH <sub>4</sub> (%)	
Test 1 - 21 cycles	65%	90-95	< 10	
Test 2 - 20 cycles	50%	> 99.9	undr detection limit	
2.2 Facility 2 (modified)				
2.2 Facility - 2 (modified) Test 2 - 20 cycles	68%	>99.9	underdection limit	

Figure 15. Profiles of gas concentrations at the exit of fuel reactor

## Gas concentrations at exit of fuel reactor

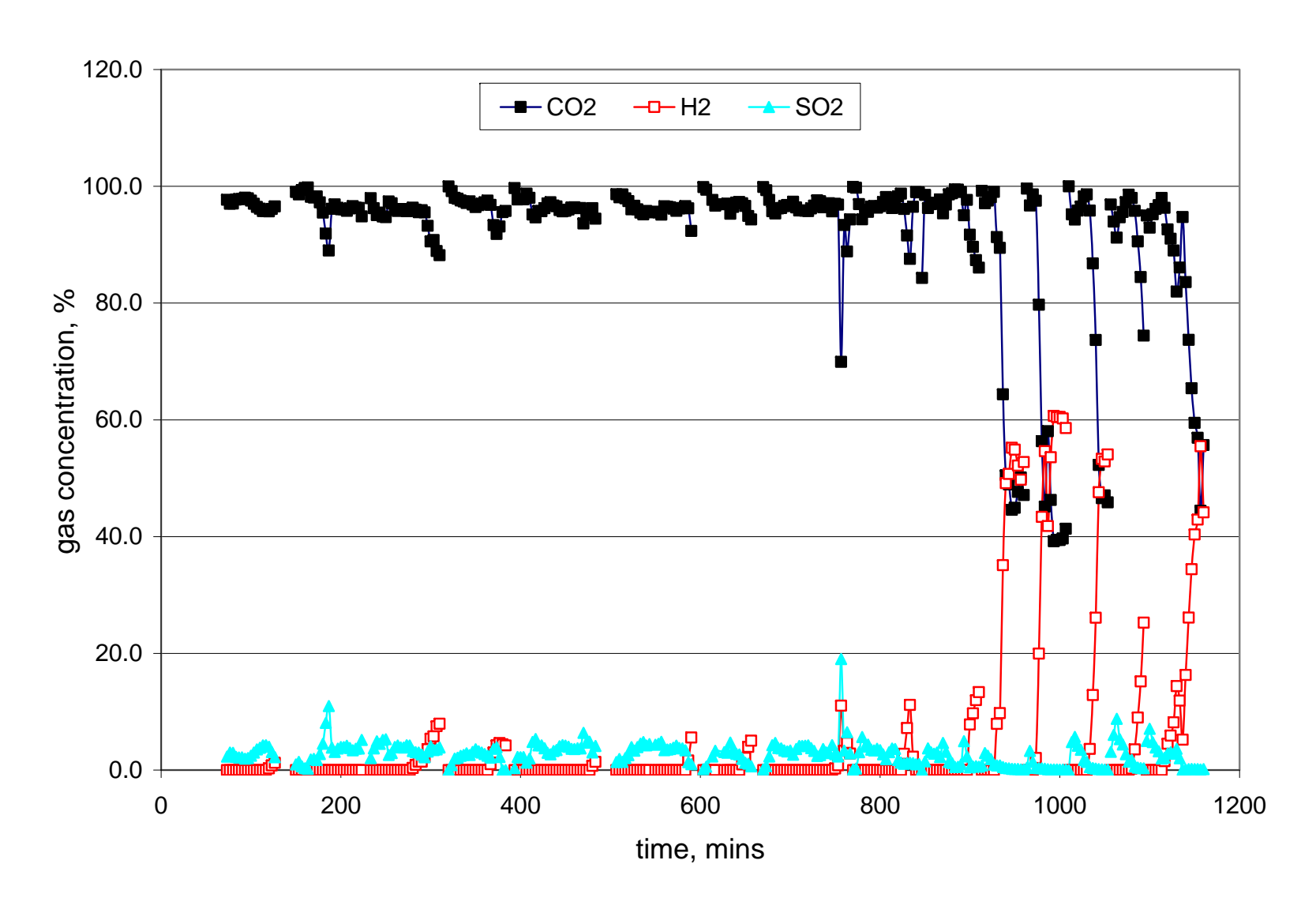
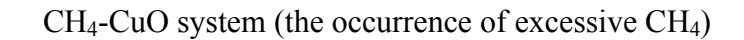
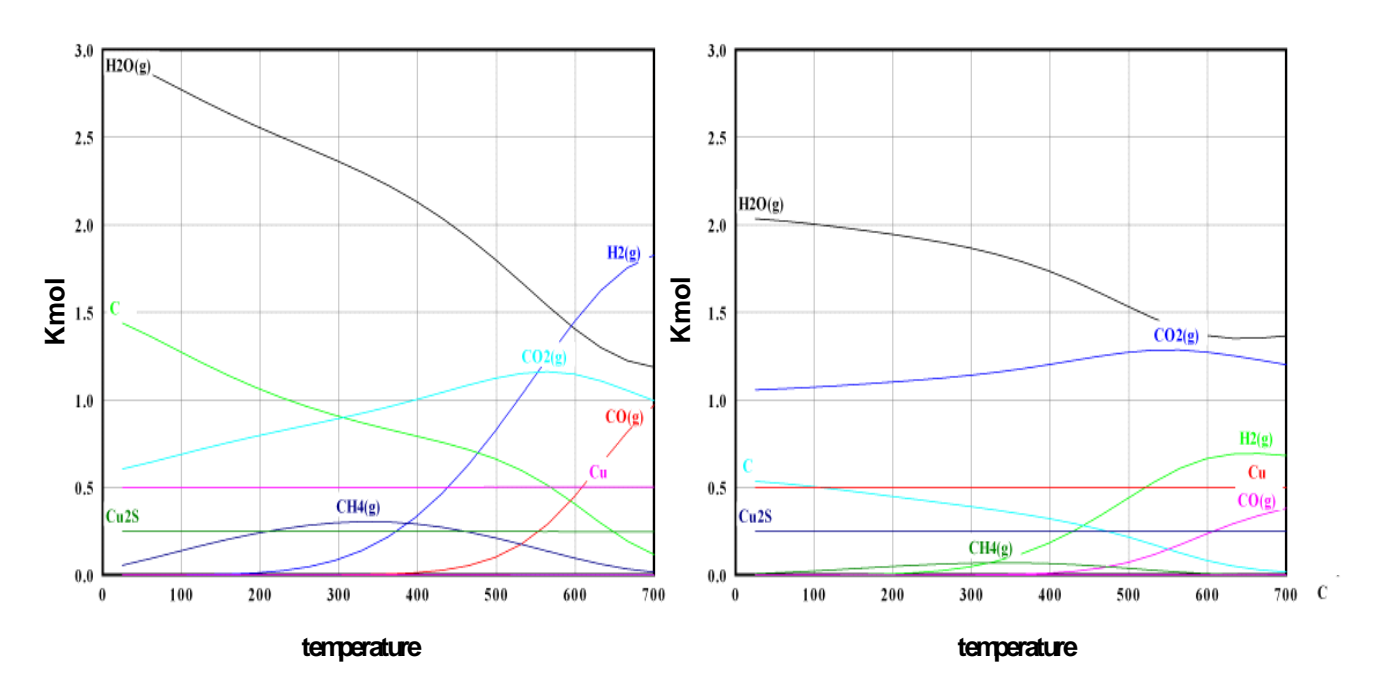
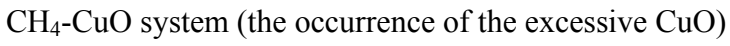
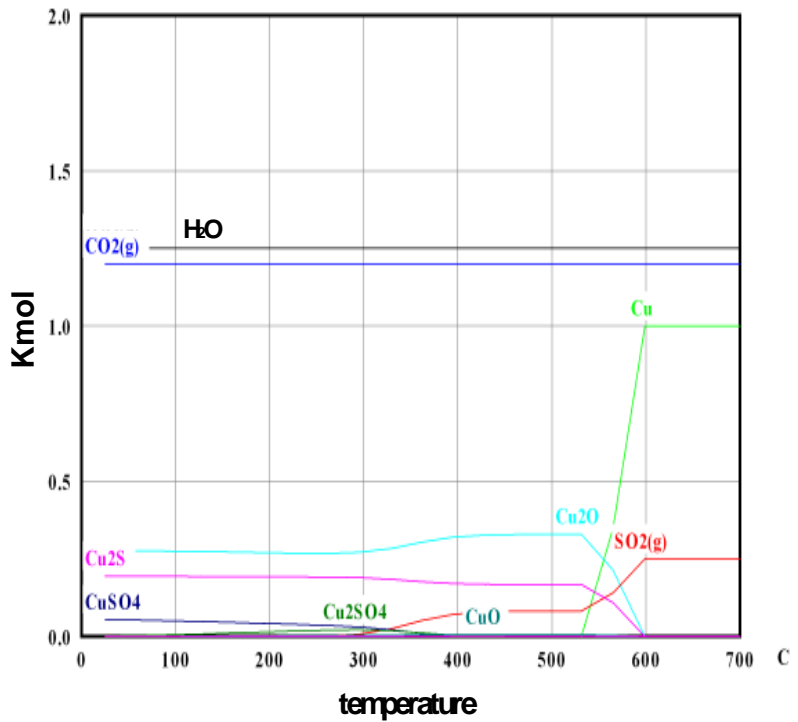


Figure 16. Thermodynamics analysis of interaction of CuO-Cu and sulfur









#### Characterization of Used Oxygen Carriers from Coal-fired CLC Combustion

The CuO-Cu oxygen carriers selected for chemical looping can achieve auto-thermal heat balance, and generate a high purity CO<sub>2</sub> with favorable kinetics. The balance of heat release in both air and fuel reactors makes the proposed process an elegant way of oxidizing solid fuels. Favorable kinetics could be achieved by oxygen-releasing properties through the path of partial conversion of CuO to Cu<sub>2</sub>O, which makes process kinetics more favorable. This was confirmed by the analysis of the crystal structure of used oxygen-carrier samples, which showed the available Cu<sub>2</sub>O crystal on oxygen carrier samples. This was shown in SEM pictures in Figure 17. The phase diagram relative to Cu-Cu<sub>2</sub>O-CuO is shown in Figure 18. The equilibrium line divides the 2 D area into two zones, which correlates the temperature with the partial pressure of oxygen. Above the equilibrium line the CuO could have a stable existence. Under this equilibrium line, Cu<sub>2</sub>O could have a stable existence. It could be found that CuO started to decompose into Cu<sub>2</sub>O when temperatures were above 900 °C, depending on actual atmospheres in the fuel reactor.

Compared to two other popular oxygen carriers, such as nickel-based and iron-based, the copper-based oxygen carrier could generate high purity CO<sub>2</sub> under less severe conditions and less secondary emissions. A The prepared copper-based oxygen carriers performed well in 20 cyclic operations under severe conditions of reduction (900-950 °C) and oxidation (750-850 °C) using Kentucky coal as a fuel. Significantly, there was no agglomeration of the copper constituent found on the used oxygen carriers, as indicated in Figure 19. This contrasts with the severe agglomeration that occurred in the first generation copper-based oxygen carrier, which lasted six cycles, as indicated in Figure 20. Therefore, the major constituents and chemical formula used to stabilize the performance of copper-based oxygen carriers, have been confirmed. However, further studies indicated structure change occurred at the molecular level under the nanometer dimension based on pore structure analysis, as indicated in Figure 19. Thus, this necessitates the continued investigation of the interactions between molecules inside oxygen carriers.

Figure 17. Crystal analysis of fresh and used oxygen carrier samples

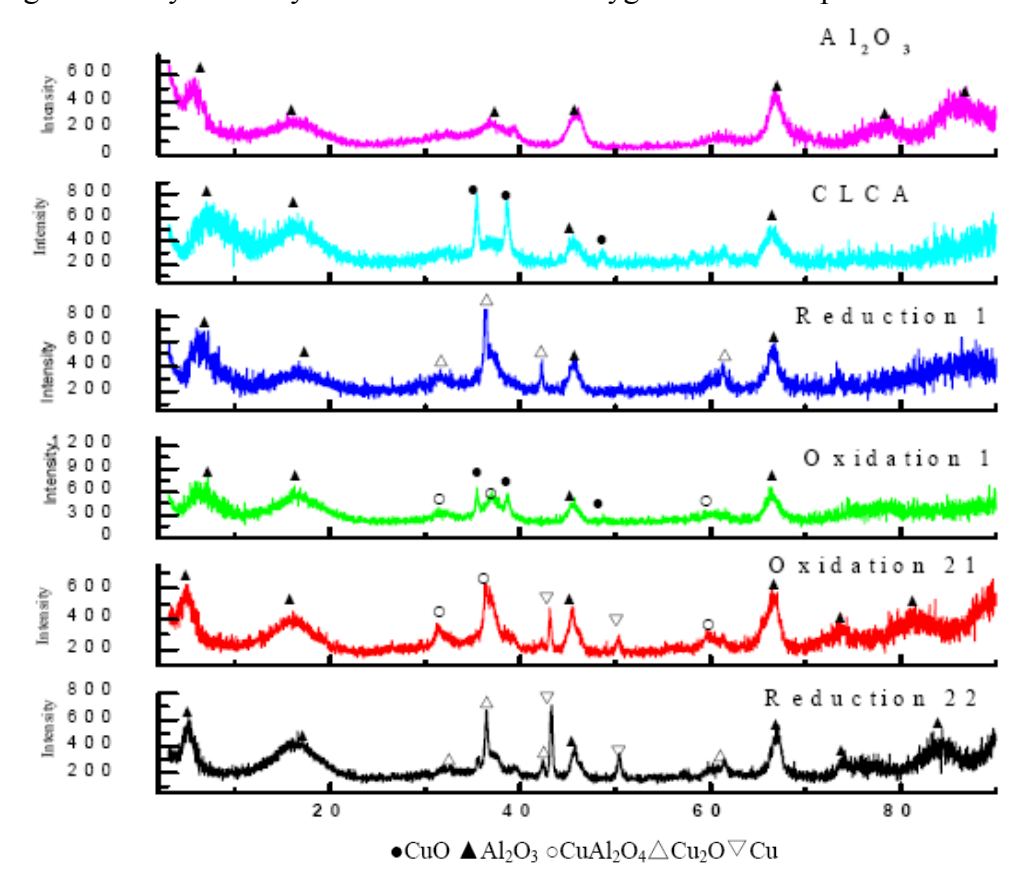


Figure 18. The phase diagram for CuO and  $Cu_2O(P_{O2}-T)$ .

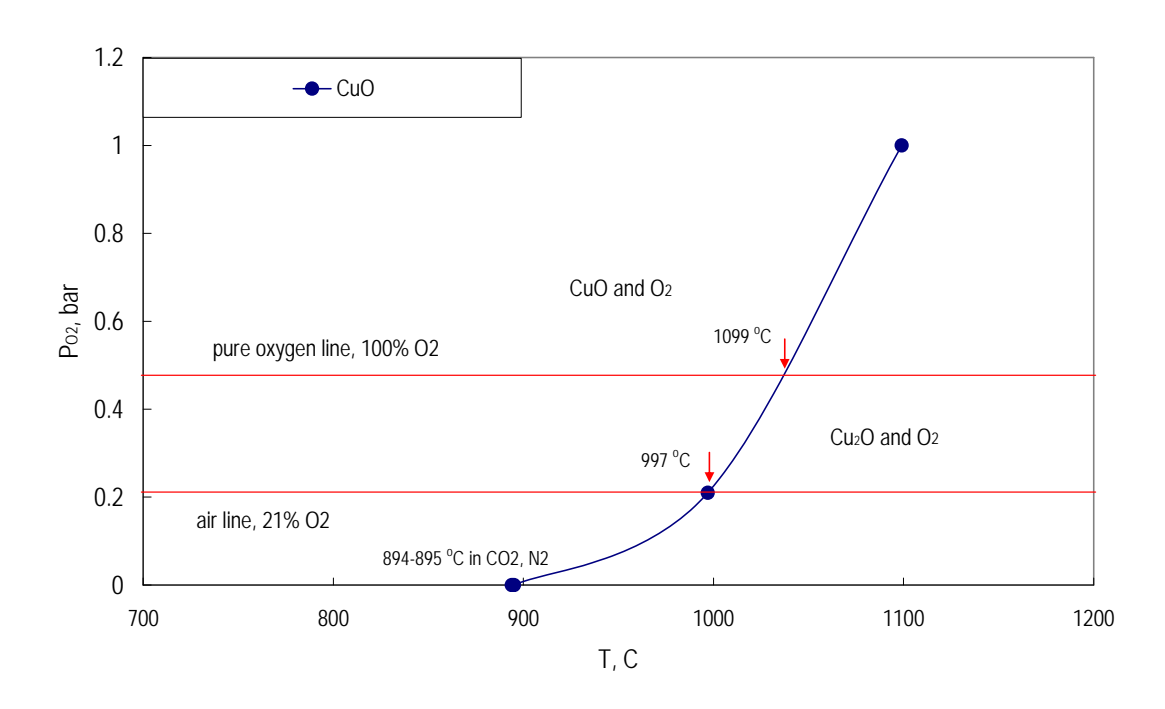


Figure 19. SEM pictures of performance-improved oxygen carriers (after 20 cycles operation)

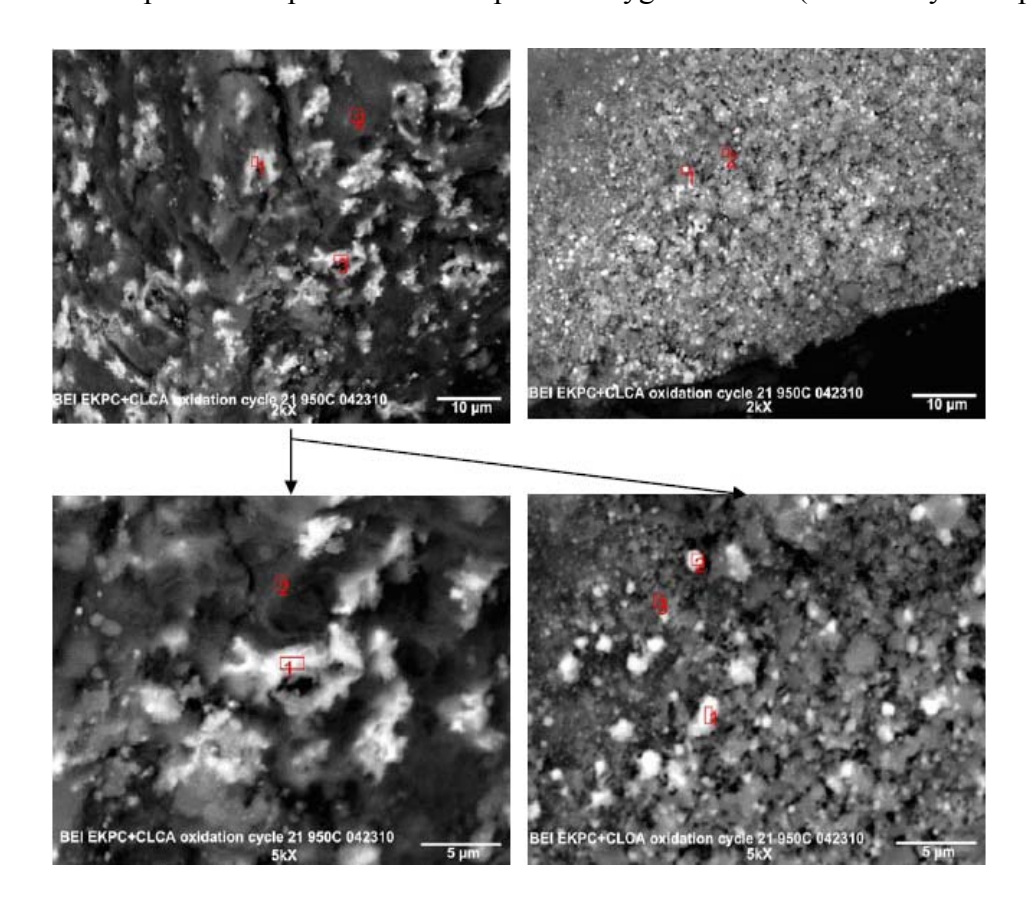
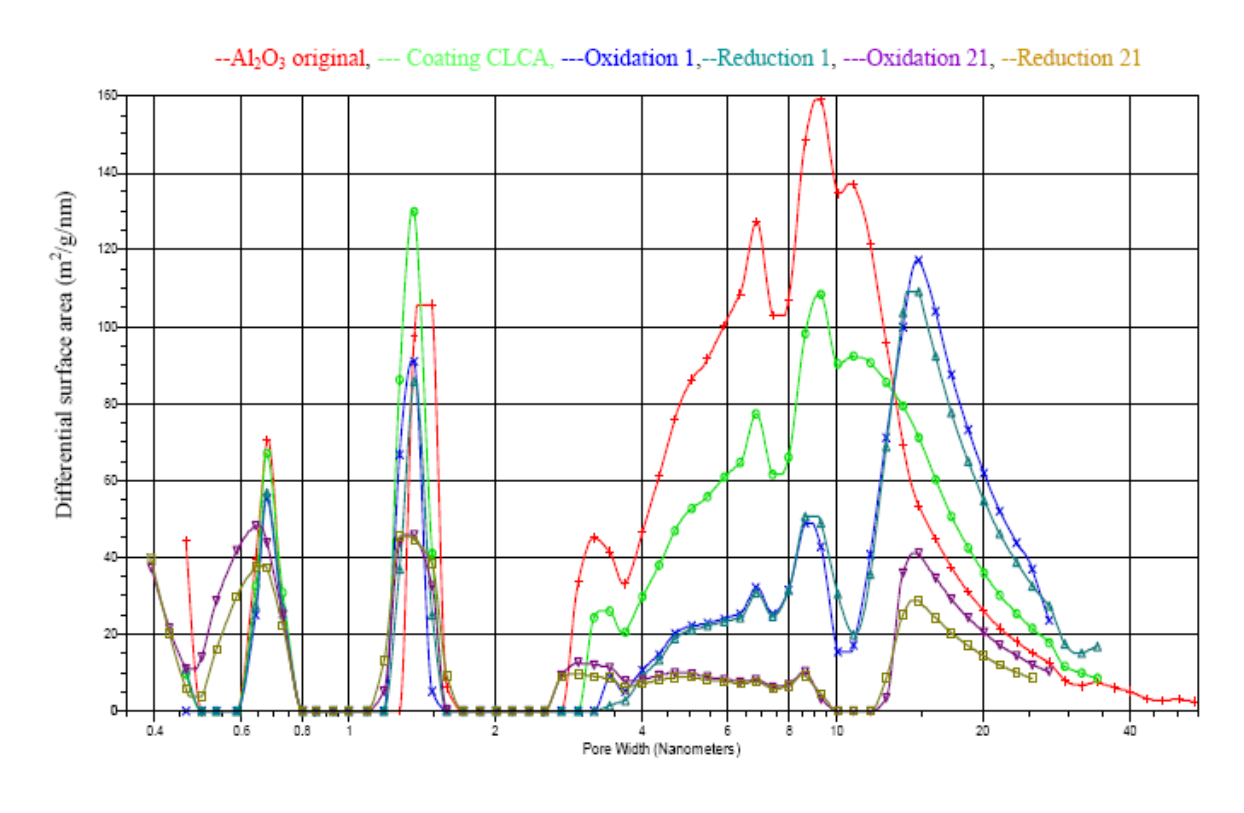
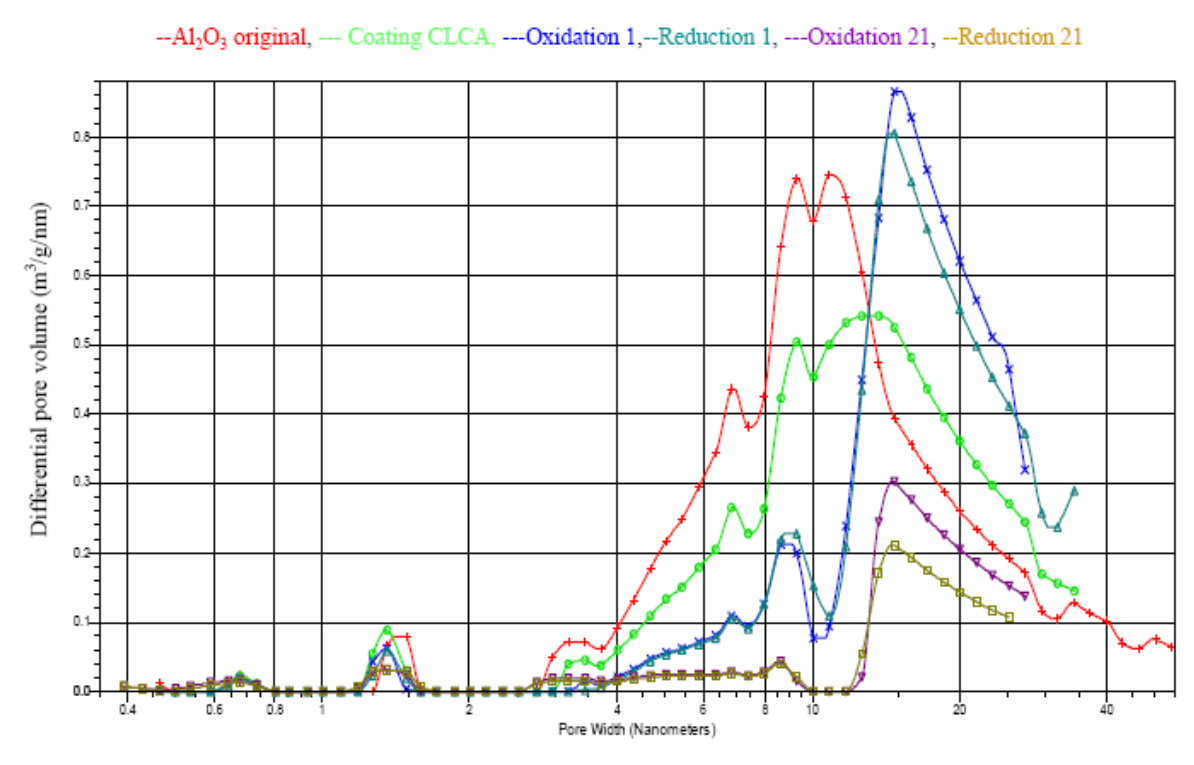


Figure 20. Analysis of pore surface and pore structure in nanometer level (fresh and used oxygen carriers)





# 2.4 Evaluation of Prepared Oxygen Carrier in 10 kW CLC Facility

A cold chemical looping pilot to test the solid circulation between air and fuel reactors, based on the concept of circulating fluidized bed with loop seals, was successfully set up and tested. After extensive tests following several major modifications as indicated in Figure 21, the final design, i.e., Version f. of the cold model pilot showed that it could be operated under high solid circulation rates, and it had no gas leakage between air and fuel reactors. This was followed by build-up of a 10 kW hot-model CLC facility based on cold-model version f. Successful setup of a cold chemical looping facility to achieve the solid recirculation between air and fuel reactors, based on a concept of circulating fluidized bed with loop seals. After extensive tests following several major modifications, the most updated setup of the cold model facility could be operated under higher solid recirculation rates, and simultaneously prevent gas leakage between air and fuel reactors. This setup could also be operated modes to adapt to different change residence times of oxygen carriers as a function of their kinetics.

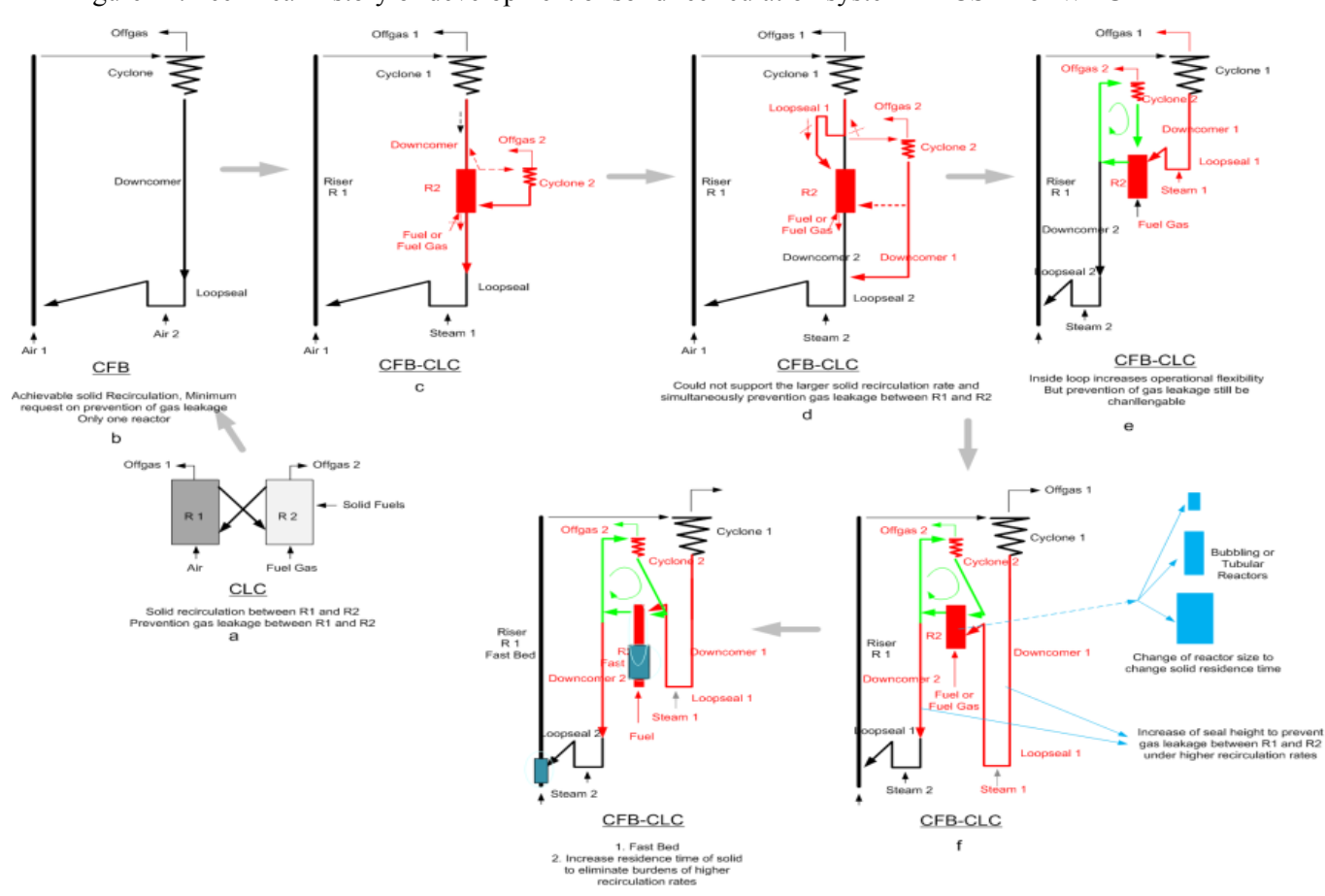


Figure 21. Technical history of development of solid recirculation system in ICSET of WKU

Major components of the 10 kW CLC pilot include a fast fluidized bed air reactor, two stage cyclones connected to top of the air reactor, a bubbling fluidized bed fuel reactor, one cyclone connected to the top of the fuel reactor, one loop seal each for the air reactor and the fuel reactor respectively, two downcomers connecting to LP1 and LP2, oxygen carriers coming out from the fuel reactor one-way upward into a buffle tank (BT), which is followed-up by the fuel-reactor cyclone, second-way downward LP 2, which is connected to the air reactor, and two filter bags (maximum temperatures at 150 °C) with cooling towers connected to each of the two cyclone outlets. This 10 kW hot model CLC system has been successfully operated using natural gas, liquid-fuel pyrolysis syngas for 3 days at 8 hours each day.

The demonstration test used a gas mixture of natural gas and pyrolyzed asphalt. The gas product composition of asphalt pyrolysis using natural gas as carrying gas is shown in Table 5. Within an 2-hour firing of the pilot at 7.4 - 12.6 kW of the mixed-fuel supply, the system exhibited stable operation, no gas leakage between the air and fuel reactors, and 100 % conversion of the mixed fuels with only CO<sub>2</sub> in the dry clean flue gas. During this operation, there was minimal operator intervention. Through the view port located just above the dense bed of the air reactor, a continuous up-flowing of oxygen carrier could be clearly observed and maintained throughout the demonstration period. Switching from the 100 % natural gas firing to the mixed fuel gas including the syngas from pyrolyzed asphalt injection was smooth. The demonstration test seemed very successful. This 2-hour demonstration test was extended into an 8-hour continuous firing with the 100 % natural gas at the capacity of 11 kW, after a 1.5-hour temporary shut down. During this shut down period, a little air was supplied into the whole system (including both air and fuel reactor and two LPs) for the oxidation of oxygen carrier back to its fresh status. At the beginning of the 8-hour run at a capacity of 11 kW, 100% conversion of the supplied natural gas was accomplished for about 20 mins. This was followed by a drop of the conversion efficiency until the solid recirculation was increased. This was possibly due to a shift of the oxygen content in the oxygen carrier during normal operation, when the oxygen carrier may not be 100% oxidized in the air reactor. The issue is that the residence time of the oxygen carrier in the dense bed of the air reactor may not be enough, considering the fixed kinetics property of the prepared oxygen carriers. In the current 10 kW pilot, the flexibility adjustment for the matching of both fluidization conditions and circulation rate via the adjustment of the air flow rates were restricted as the system capacity changed. This was a critical point for the air

reactor dense bed modification in the future. The current solution to increase the solid re-circulation rate was to increase the air flow rate, such that more oxygen carrier was available in the fuel reactor to satisfy the 100 % conversion of fuel. This seemed to have worked as shown in Figure 22-1. The conversion efficiency of the supplied fuel was gradually improved and was finally close to 100 % for another 7-hour continuous run. During this period of firing, the major critical temperatures of system, for example, temperatures of dense beds of both the air and fuel reactors were maintained constantly.

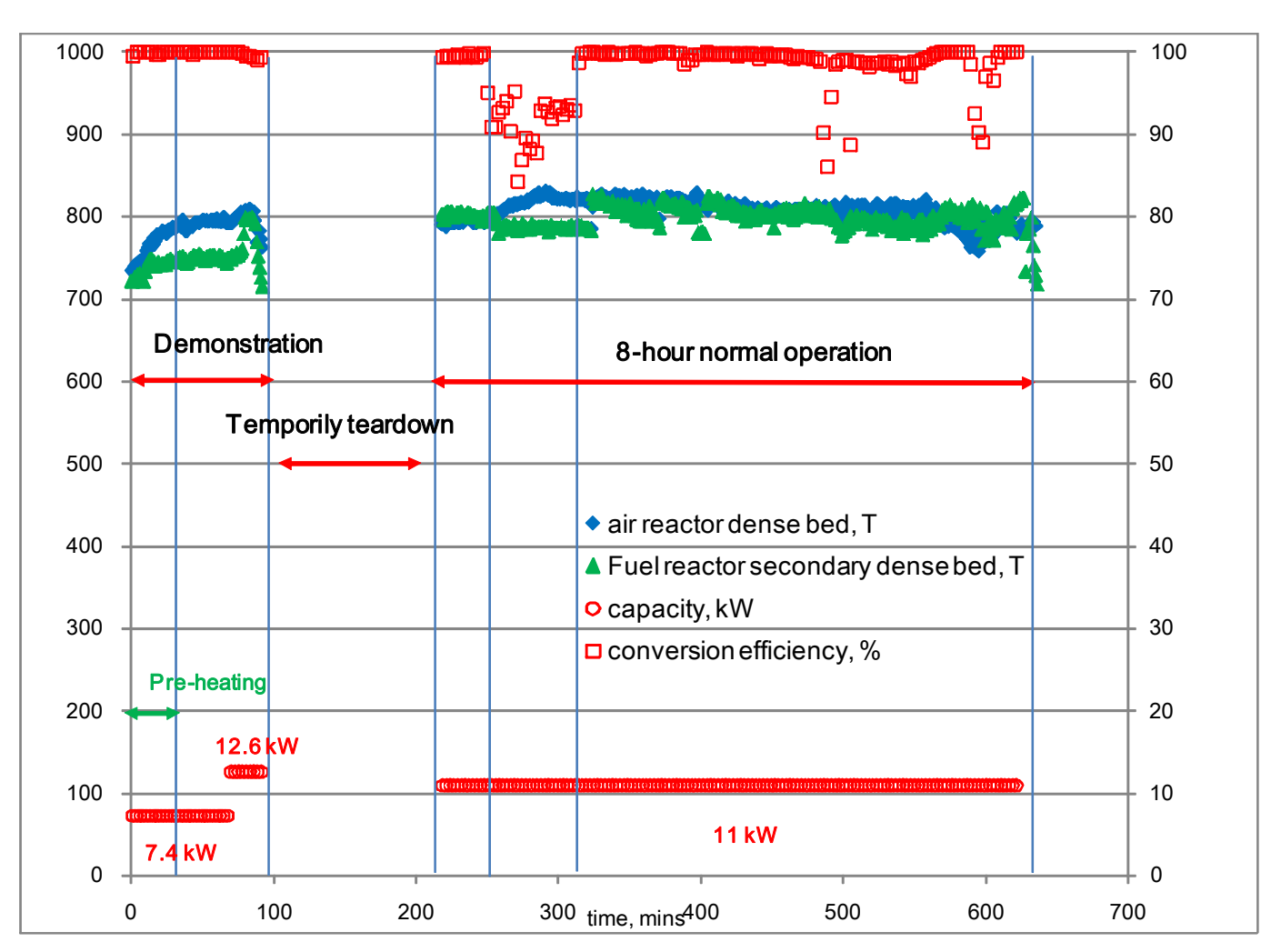


Figure 22-1 1st-8-hour run in 10 kW CLC facility

On the second day, the second 8-hour continuous firing of the CLC pilot was resumed. Result was shown in Figure 22-2. The system temperature was raised by natural gas injection at 7.4 kW after the initial electrical-heating. It could be observed that the fuel conversion efficiency

was directly correlated to temperatures of both the air and fuel reactors. At around 780 °C in this case, 100% of the fuel conversion was achieved. Maintaining the constant supply of natural gas, the temperatures of system was continuously raised until a little above 800 °C, when the heat balance was achieved. Increasing the fuel supply to 8.8 kW continued to raise the temperature, and the decrease of the fuel supply would drop temperatures to its original status at the same system capacity. It seemed that a better load adjustment could be achieved in the current system. This phenomenon was repeated as the fuel supply load was adjusted back to 8.8 kW. Again, during this second 8-hour of firing, the major critical temperatures and the fuel conversion efficiency of the CLC pilot could be maintained constantly.

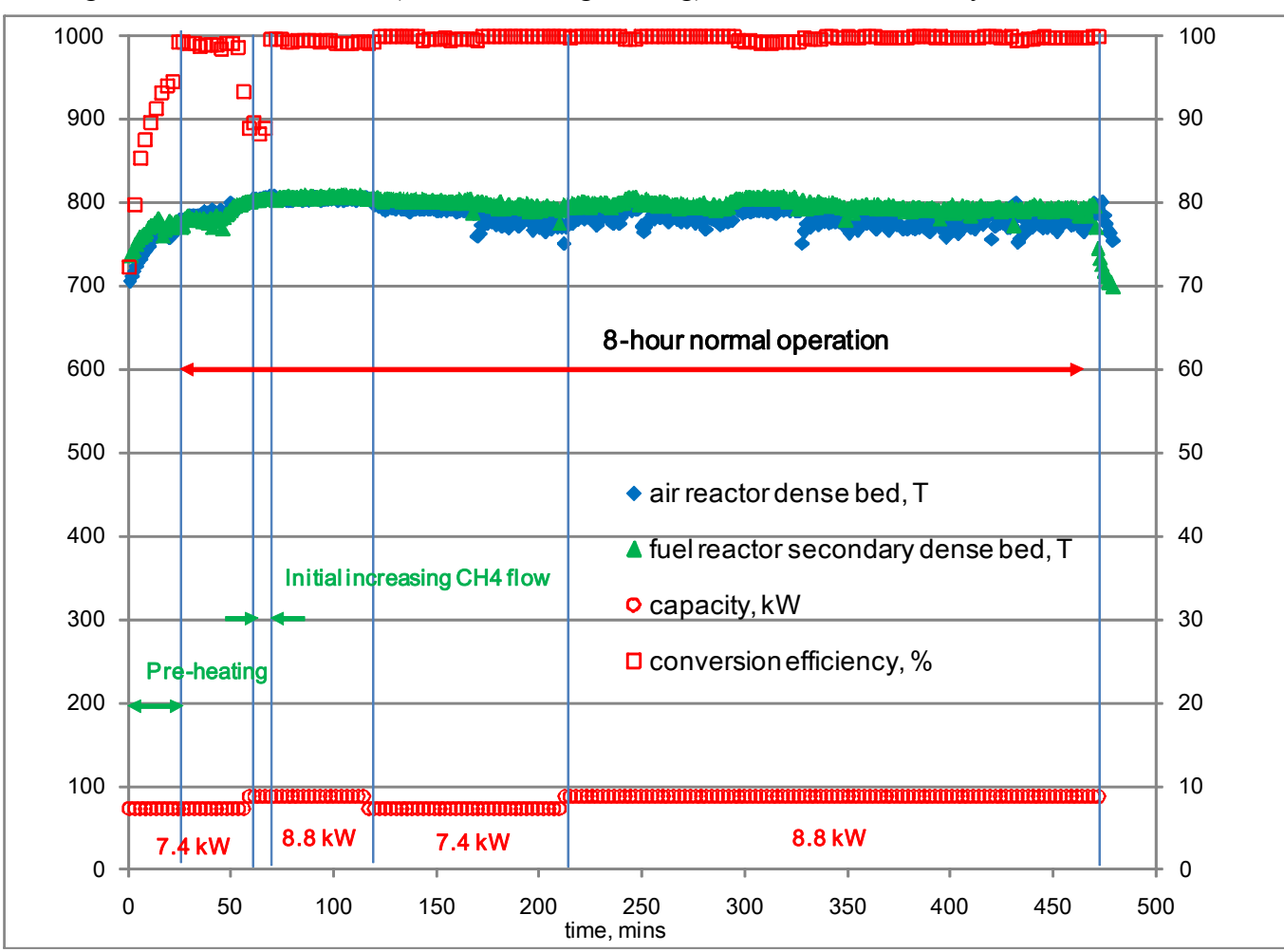


Figure 22-2 2<sup>nd</sup>-8-hour run (100 % natural gas firing) in 10 kW CLC facility

This was followed up the third 8-hour run of the pilot using the same procedure, but at

slightly higher fuel supply of 9.2 kW following step increase of 8.1 and 8.9 kW. Results are shown in Figure 22-3. Except for an interruption during the switch over of empty to full natural gas cylinders, the major critical temperatures and the fuel conversion efficiency of the CLC system could be maintained constantly. However, the fuel conversion efficiency averaged 99%, and some natural gas was not fully consumed. There was H<sub>2</sub> in the fuel reactor off gases, because of the reforming and the water-shift-reaction of unreacted natural gas. These long-term evaluation tests demonstrated the integrity of the each component of the 10 kW CLC pilot, acceptable properties of Cu-based oxygen carrier prepared including its kinetics, maintaining oxygen transfer capability and agglomeration tendency. There was no tendency of agglomeration found during this long-term evaluation of oxygen carrier, which demonstrated the successful formula was obtained in this study. Test results were shown in Figure 23-1, 23-2.

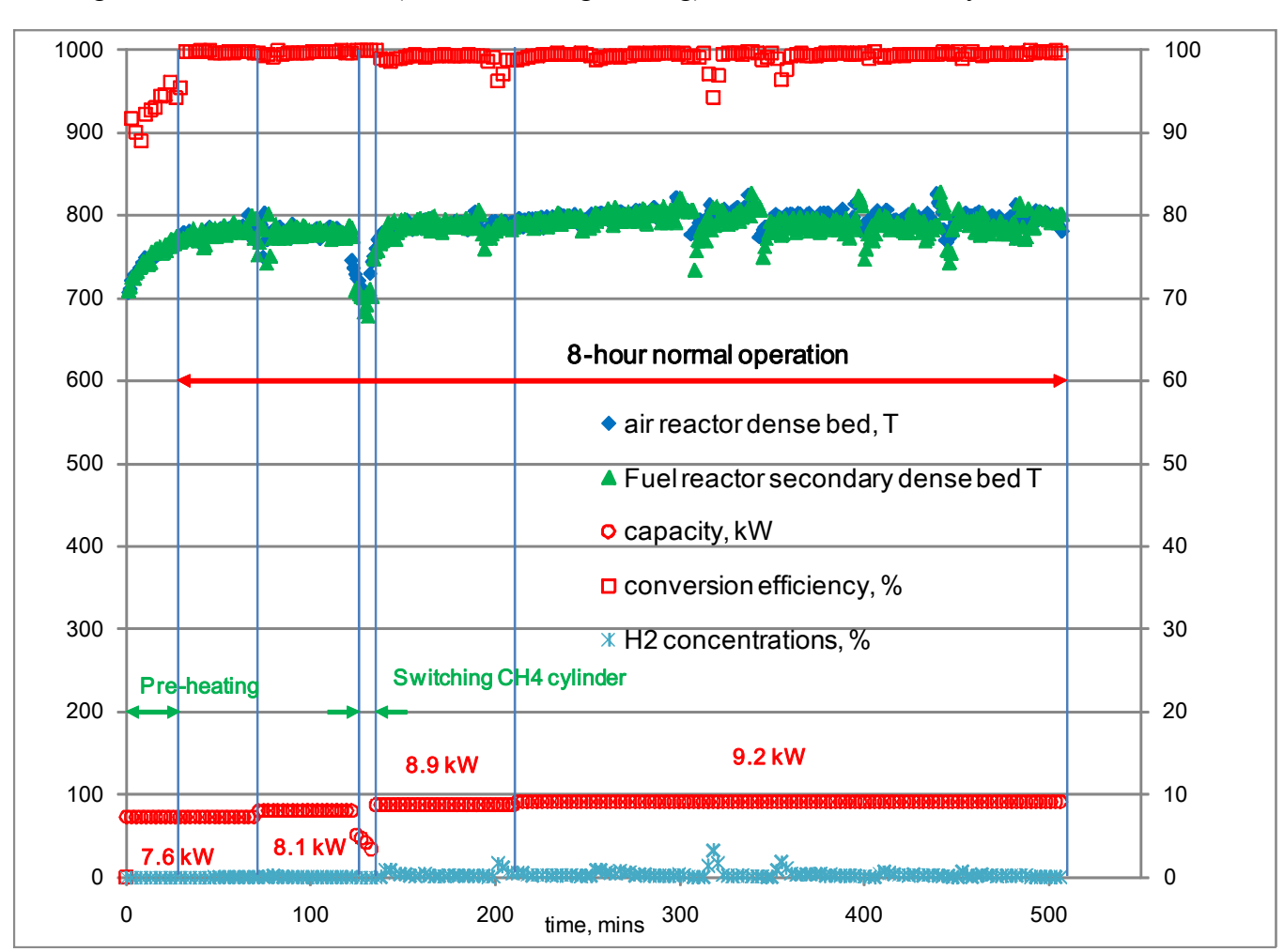
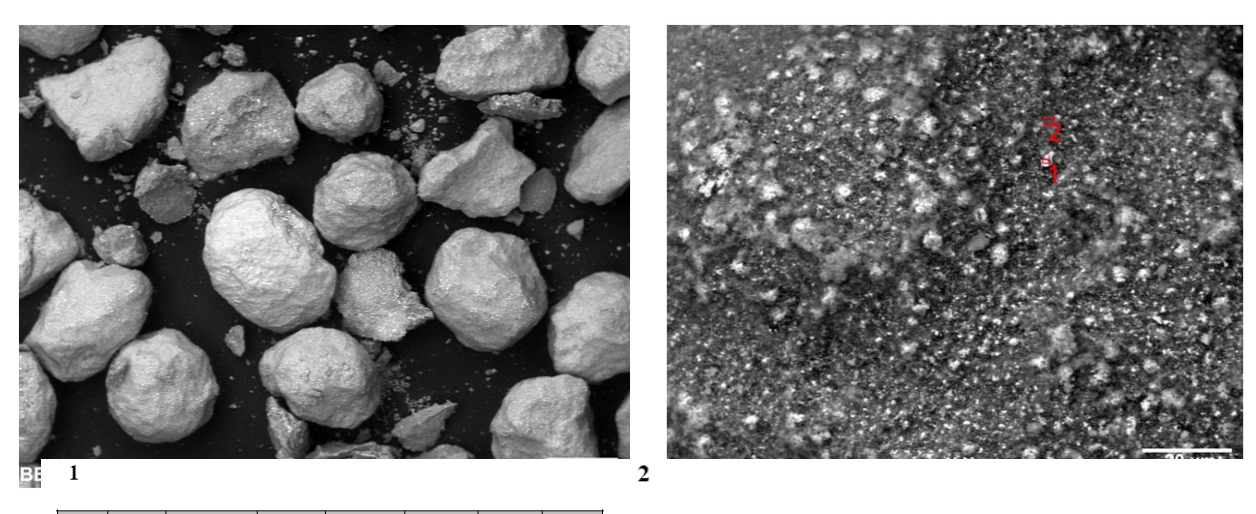


Figure 22-3 3<sup>rd</sup>-8-hour run (100 % natural gas firing) in 10 kW CLC facility

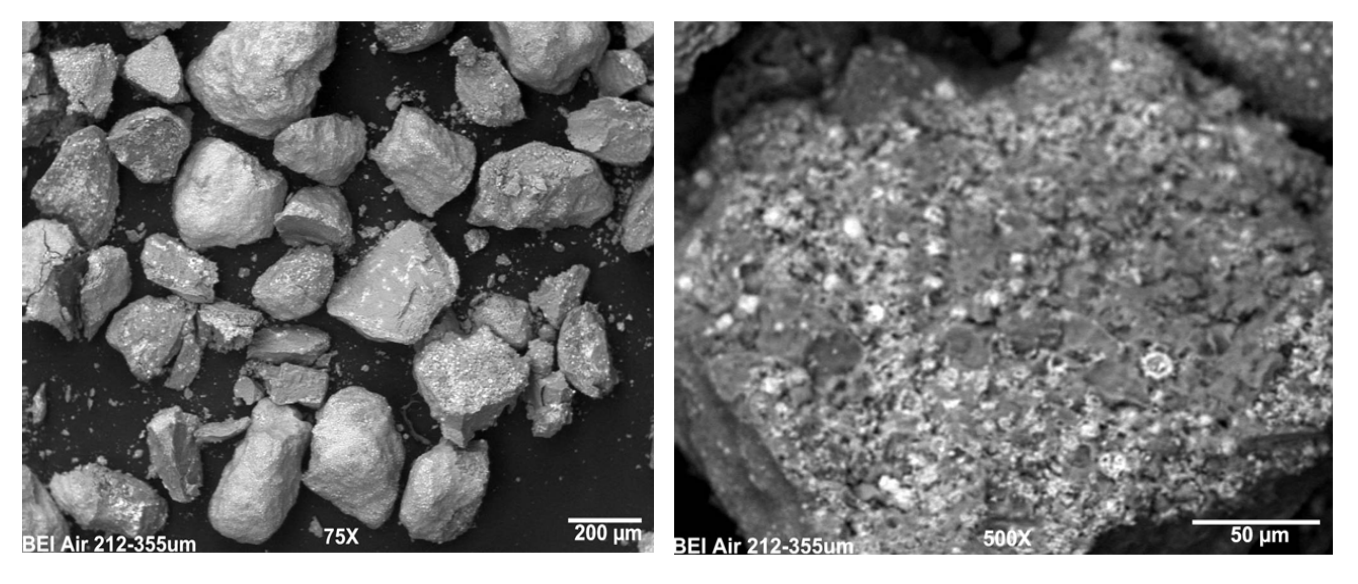
Figure 23-1 SEM pictures of used oxygen carriers firing in for 3 day totally 24-hour (Fuel reactor)



Elt.	Line	Intensity	Error	Atomic	Conc	Units	
		(c/s)	2-sig	%			
0	Ka	131.66	4.322	58.78	41.47	wt.%	
Al	Ka	372.54	7.174	36.19	43.06	wt.%	
Cu	Ka	42.69	2.537	4.62	12.95	wt.%	
La	La	6.98	1.516	0.41	2.52	wt.%	
				100.00	100.00	wt.%	Total

Elt.	Line	Intensity	Error	Atomic	Conc	Units	
		(c/s)	2-sig	%			
0	Ka	186.34	5.126	62.98	47.06	wt.%	
Al	Ka	457.13	7.972	33.34	42.02	wt.%	
Cu	Ka	43.37	2.555	3.68	10.92	wt.%	
				100.00	100.00	wt.%	Total

Figure 23-2 SEM pictures of used oxygen carriers firing in for 3 day totally 24-hour (Air reactor)



The major issue found in this long-term evaluation test was the attrition loss of active ingredient, i.e., copper in the ICSET oxygen carrier. Unlike those tests in TG where oxygen carrier was kept in static status for the testing period, high circulation rates of oxygen carrier was maintained during the continuous operations of the 10 kW CLC pilot. Collisions of oxygen carrier particles against themselves and the reactors and cyclones were constant, resulting in the breakage of oxygen carrier particles. Because of our preparation method in this study, the active ingredient of Cu-CuO remained in the surface shells of the oxygen carriers, where attrition occurred as a result of the particle-particle and particle-wall collisions. The outcome was the loss of the active ingredients which were collected in the filter bags and not returned to participate in the recirculation inside the reactors. This resulted in the loss of oxygen transfer capability of oxygen carriers inside the fuel reactor, which was found in the final stage of extended runs. The significant difference of CuO content in oxygen carrier samples, collected at different location inside the 10 kW CLC pilot was shown in Table 4. It could be observed that the CuO contents (oxygen capacity) of fine particles collected in the baghouse were 40 wt%, which was generally much greater than those samples staying in the reactors. It seemed that the CuO-rich fine particles resulted from the attrition of the original oxygen carriers, which were CuO-rich on their outside surface. The initial CuO content of the fresh oxygen carrier was about 25%. After 3 day 8-hour for each day firing of CLC, the average CuO-content in used oxygen carriers varied between 14.5 wt% to 17.5%, losing 40 wt% of its original oxygen transfer capacity.

Table 4. Copper oxide contents on the collected oxygen carrier samples

1.1			-	
Experime	ent date	2011-11-2 (during the 1st-8-hour firing)		
Sample	Name	weight change in TG	CuO %	
air reactor	sample	5.196%	26.0%	
fuel reactor	fuel reactor sample		14.1%	
Experime	ent date	2011-11-3 (during the 2nd-8-hour firing)		
Sample	Name	weight change in TG	CuO %	
air reactor	sample	3.565%	17.8%	
fuel reactor	sample 1	4.206%	21.0%	
Experime	ent date	2011-11-4 (during the 3rd-8-hour firing)		
Sample	Name	weight change in TG	CuO %	
aiı	r	5.417%	27.1%	
fue	fuel		15.3%	
Experime	ent date	2011-11-7 (after total 3-8-hour firing)		
Sample	Sample Name		CuO %	
	125um down	7.119%	35.6%	
Particle sizing	125-212 um	3.328%	16.6%	
Farticle Sizing	212-355 um	3.161%	15.8%	
	355um up	3.499%	17.5%	
	125um down	3.361%	16.8%	
Particle sizing	125-212 um	2.827%	14.1%	
i article sizing	212-355 um	3.144%	15.9%	
	355um up	3.444%	17.2%	
Air reactor baghouse		8.718%	43.6%	
Fuel reactor baghouse		8.072%	40.4%	

The evaluation of used oxygen carrier samples, collected after the extended tests (3-day, 8-hour for each day), indicated only trace-amount of coke or carbon deposits on the copper-based oxygen carriers in the fuel Reactor. This indicated there was a tendency of carbon deposits under current operational conditions, but the carbon deposits had been controlled by the system tuning (system temperatures for achieving higher fuel conversion efficiency). There was also no evidence to show the sulphidization of oxygen carriers in the system by using the high-sulfur-laden asphalt fuels, only the trace-amounts of sulfur on samples in two baghouses, where temperatures were as low as 150 °C. This matched well with theoretical thermodynamics calculation that temperatures are a critical parameter to control the reaction between copper and sulfur species in fuel gas. If the system temperature is controlled above 750-800 C, there should be no sulfur reaction with copper-based oxygen carrier. This was not true when temperature dropping to as low as 150 °C, when copper could react with sulfur.

Table 5. The carbon and sulfur contents in the used oxygen carriers

ICSET#	Sample ID	Carbon (%)	Sulfur (%)
18056	Air < 125 microns	0.04	< 0.01
18057	Air 125-212 microns	0.03	< 0.01
18058	Air 212-355 microns	0.03	< 0.01
18059	Air > 355 microns	0.04	< 0.01
18060	Fuel Rxt & Storage < 125 microns	0.07	< 0.01
18061	Fuel Rxt & Storage 125-212 microns	0.03	< 0.01
18062	Fuel Rxt & Storage 212-355 microns	0.04	< 0.01
18063	Fuel Rxt & Storage > 355 microns	0.04	< 0.01
18064	Baghouse Air	0.04	0.01
18065	Baghouse Fuel Rxt	0.03	0.06
18066	Fresh	0.01	< 0.01

# 2.5 Oxygen Carrier Uncoupling

Chemical looping combustion (CLC) is an innovative combustion concept, which could totally negate the necessity of pure oxygen by using oxygen carriers. Its disadvantage is that it is less mature in terms of technological commercialization. In the conventional chemical looping combustion coupling process, fuels are oxidized by metal oxides in a fuel reactor to generate pure CO<sub>2</sub> stream for sequestration after steam is condensed. The reduced metal is re-oxidized by air in an air reactor. In order to improve the process kinetics, a concept called chemical looping combustion oxygen uncoupling (CLOU) has been put forwarded<sup>38-41</sup>. In this uncoupling process, specific metal oxides are selected to directly release free oxygen for the combustion of fuels, which is similar to the conventional combustion using pure oxygen. The major oxygen releasing metal oxides include copper oxide (CuO) and manganese oxides (Mn<sub>2</sub>O<sub>3</sub>). The equations are presented below, where CuO is used as uncouping oxygen carrier and carbon (C) as example of fuel sources:

$$CuO = Cu_2O + 1/2O_2$$
 (1)

$$2(1/2O_2) + C = CO_2, 1/2O_2 + H_2 = H_2O$$
 (2)

$$Cu_2O + 1/2O_2 = CuO \tag{3}$$

$$CuO + C = CO_2 + Cu (4)$$

$$Cu + 1/2O2 = CuO$$
 (5)

In the CLOU process, highly active free oxygen is produced for the reduction of fuel (Equations 1 & 2), especially desirable in case of hard to oxidize high-carbon content fuels such as asphalt or bitumen (C in Equation 2). CLOU would overcome the difficulty of oxidizing solid fuel with solid oxygen carrier in regular CLC oxygen coupling as represented by Equation 4. Equations 3 and 5 are the respective oxidation reactions in the Air Reactor for CLOU and CLC coupling.

Early in 2005, Cao et al proposed a concept concerning direct oxygen production based on chemical looping scheme using metal oxides or peroxides<sup>42</sup>, to solve the potential interference between coal ash and oxygen carriers and issues of slow kinetics of direct coal-fueled chemical looping combustion<sup>41-42</sup>. Similar concept could be found elsewhere<sup>43</sup>, for example, Moghtaderi performed a detailed analysis of a similar concept (the CLAS process). The preliminary results confirmed the feasibility of the CLAS process for air-separation applications. It showed that the

specific power consumption of the CLAS process is about 0.045 kWh per cubic meter of oxygen produced, which is approximately 11% of the specific power consumption of conventional cryogenic air-separation systems. This technology option features low energy demand, inexpensive manufacture, and simplicity, which would substitute for oxy-combustion of solid fuels without ASU or gasification.

In this study, we paid special attention to the performances of an Al<sub>2</sub>O<sub>3</sub>-supported CuO oxygen carrier (CLCA) in coupling and uncoupling conditions.

In this study, commercial CuO powder (Fisher Scientific) is used as a reference standard for CLOU investigation.

The  $O_2$  release during CuO decomposition (fresh CLCA sample) was not recognized in many parallel tests using the fixed bed reactor made of stainless steel. Continuous several parallel tests using the used CLCA sample (re-oxidized CLCA after initial reduction) and commercial CuO sample, again, did not find significant  $O_2$  (<0.2% vol) in the reactor offgas in tests using the fixed bed reactor made of stainless steel.

Characterization of all three samples, from tests using the stainless steel fixed bed reactor (fresh CLCA sample, commercial CuO powder and commercial CuO powder collected on filter paper during the fixed bed tests), under N<sub>2</sub> or air atmosphere were shown in Figure 24 and the XRD spectrum of filter paper sample is showed in Figure 25.

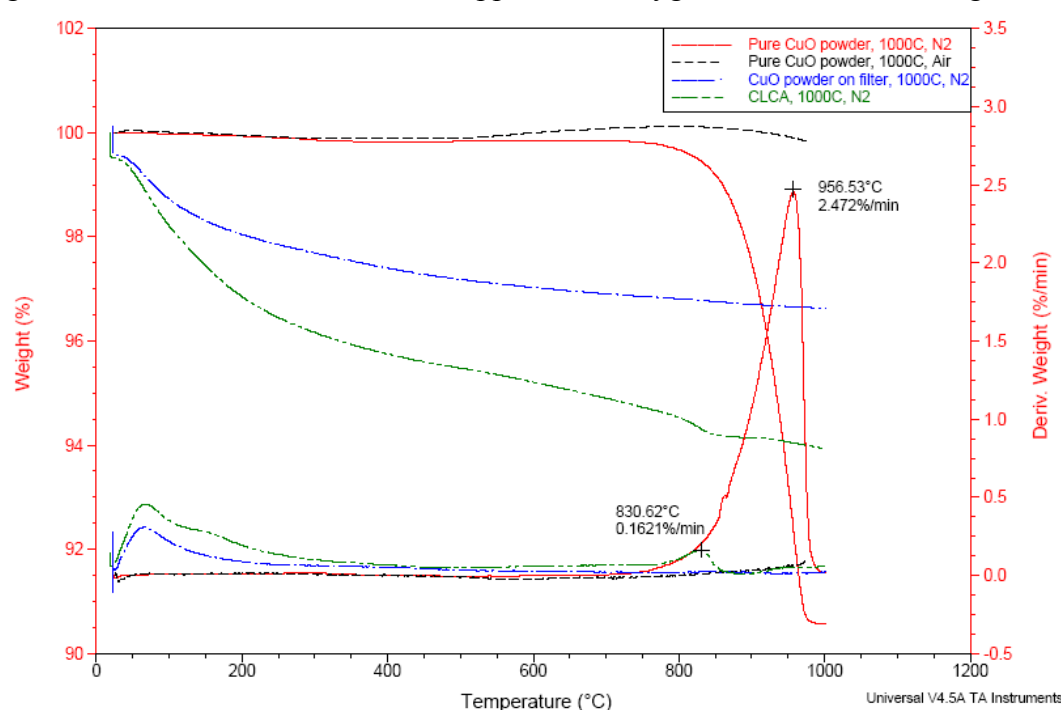
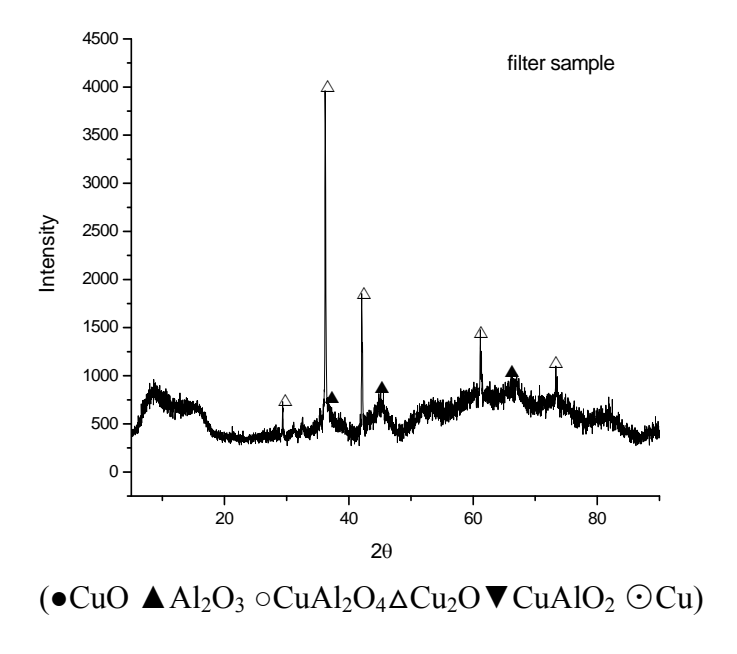


Figure 24: TGA curves for the three copper oxide oxygen carriers under nitrogen flow.

ICSET, WKU 86 December, 2012

The weight loss of fresh commercial CuO powder under N<sub>2</sub> atmosphere (red line) is slightly below the weight loss of theoretical complete CuO decomposition to Cu<sub>2</sub>O (about 10 wt%). Because of the higher O<sub>2</sub> partial pressure (about 21%) under an air atmosphere, no weight loss was attributed to the commercial CuO powder decomposition (black line). A slight weight increase in this test was likely attributed to impurity in the commercial CuO powder, likely to be Cu<sub>2</sub>O. This would explain the under-predicted theoretical decomposition of the same sample under N<sub>2</sub> atmosphere. There was also no significant weight loss (< 4 wt%) for the sample collected on the filter papers from the entrained commercial CuO emitted from the fixed bed reactor (blue line). This indicated the major decomposition of CuO of this sample had already been accomplished inside the fixed bed reactor under N<sub>2</sub> atmosphere. This was evidenced by the XRD characterization showing that only Cu<sub>2</sub>O was present as the copper constituent in this sample (see Figure 25). The decomposition of the fresh CLCA oxygen carrier (green line) occurred at lower peak temperature (825 °C) than that of the commercial CuO powder (958 °C) although their temperatures of initializing decomposition were similar. Differences in peak decomposition temperatures indicated differences in active energies of CuO deposition under different CuO occurrence on those samples. One assumption is the particle size of CuO in the commercial CuO powder is different than that in the CLCA oxygen carrier. The CLCA oxygen carrier, which was prepared by the "dry" impregnation method using dispersion additives, would better maintain its smaller granule size of CuO on Al<sub>2</sub>O<sub>3</sub> supporting material. For the CLCA oxygen carrier, a larger weight loss was found before its decomposition, which seemed to be attributable to not only the moisture loss (before reaching 200 °C), but also incomplete decomposition of Cu(NO<sub>3</sub>)<sub>2</sub> during the sample preparation (above 200 °C). The previous procedure, regarding CLCA sample preparation, resulted in questions on an incomplete decomposition of Cu(NO<sub>3</sub>)<sub>2</sub>.2H<sub>2</sub>O under 500 °C for just half hour. It seemed that longer residence times and higher temperatures were necessary as a modification of future preparation of oxygen carrier.

Figure 25: XRD analysis of the entrained commercial CuO powder on the filter paper



A fixed bed reactor made of quartz material was used to repeat all the previous tests conducted in the stainless steel reactor. The results were presented in Figure 26-1. Oxygen was found in all these tests, which were different than the previous tests in the stainless steel reactor. This was direct evidence of CuO decomposition to Cu<sub>2</sub>O and O<sub>2</sub> of both commercial CuO powder and CLCA samples from the off gas analyses. After tests, agglomerates were found in the decomposed solid residues when the commercial CuO powder was used. The agglomeration may also restrict the O2 release, and consequently in different O2 releasing curves. This was not the case when the CLCA sample was used, which showed the stable O2 release, and no agglomeration tendency. Tests also indicated that the kinetics of the O2 release (CuO decomposition) may be slow and temperature dependent, regardless of the origin of CuO (there were no any O<sub>2</sub> release peaks). The important point to note in this study was that O<sub>2</sub> releasing process may be kinetics-limited, unless the available O<sub>2</sub> would be consumed by the fuel. The XRD analysis of sample residue after tests was shown in Figure 26-2. There was no significant evidence on agglomeration of Al<sub>2</sub>O<sub>3</sub>-supported CuO oxygen carriers, shown in Figure 26-3. This contrasted the severe agglomeration of commercial CuO powder. The absence of agglomeration indicated the supporting material, Al<sub>2</sub>O<sub>3</sub>, may significantly improve the oxygen-releasing performance and thermal stability of the Al<sub>2</sub>O<sub>3</sub>-supported CuO, comparing to the commercial CuO powder. The quick formation of a new crystal phase (CuAl<sub>2</sub>O<sub>4</sub>)

cross-linking CuO and  $\gamma$ -Al<sub>2</sub>O<sub>3</sub> may be the major reason to contribute both the stability of copper-based oxygen carrier under severe uncoupling condition (close to melting point of copper), but slow kinetics of O<sub>2</sub> release.

This study also clearly demonstrated that  $O_2$  released through the decomposition of CLCA sample reacted with iron in the reactor material. A quartz reactor is necessary to show the  $O_2$  release during the CuO decomposition as it did not react with the  $O_2$ . But the current study did not clarify how the reactor material competes against the fuel in the reactor for reacting with the released  $O_2$ , which deserves a further investigation.

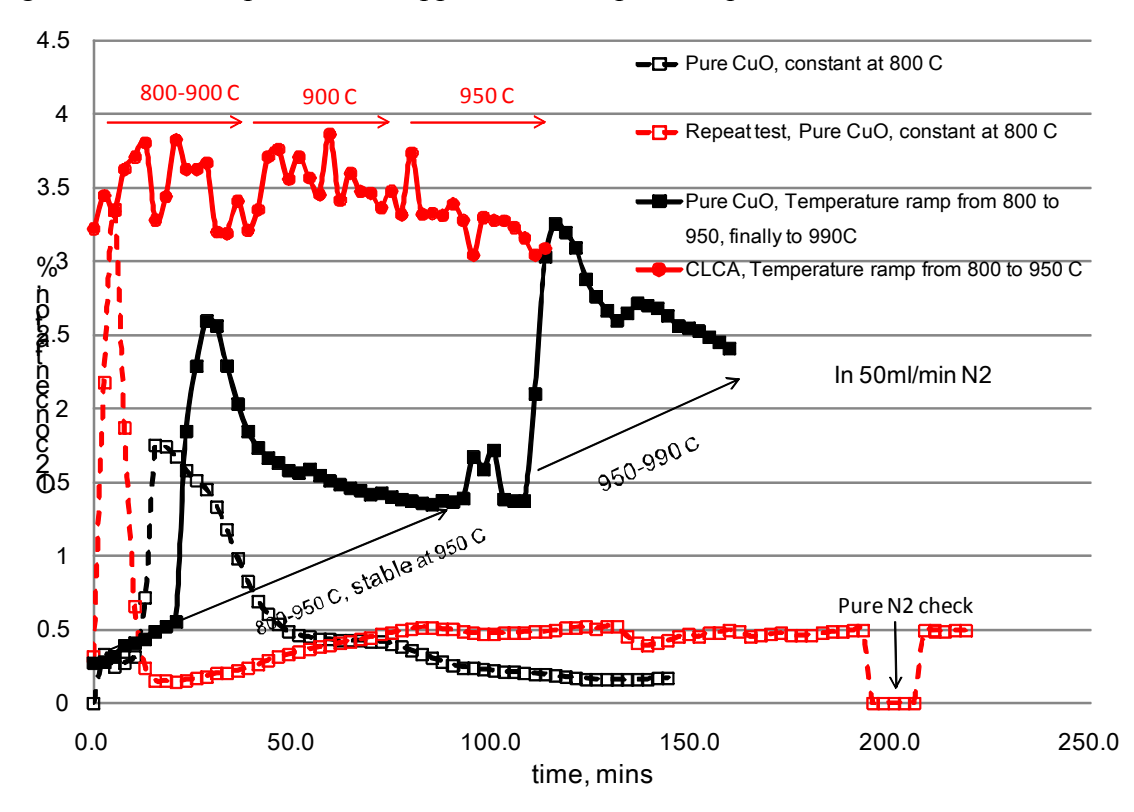
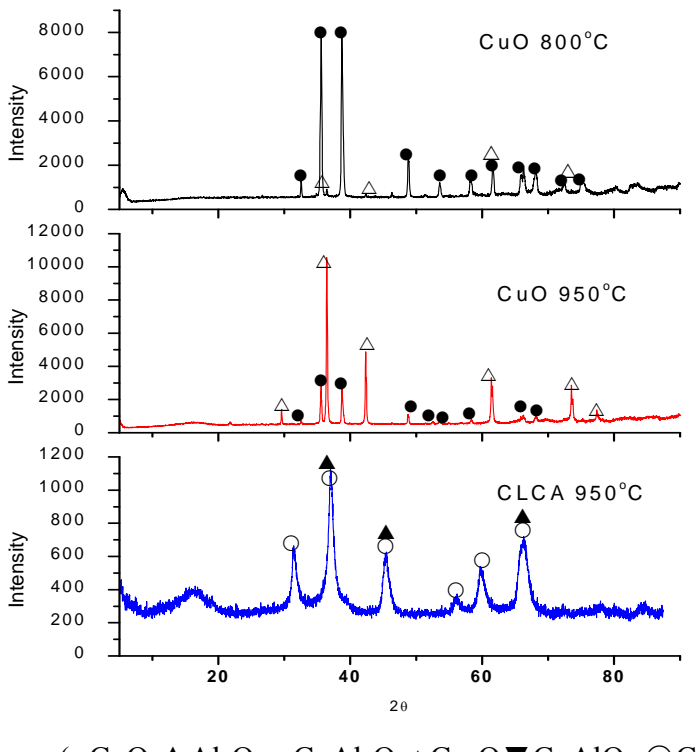


Figure 26-1 Decomposition of copper oxide sample in a quartz reactor

Equilibrium calculation of CuO decomposition was shown in Figure 27. Thermal decomposition of CuO under N<sub>2</sub> atmosphere could begin at as low as 700 °C (O<sub>2</sub> partial pressure starts to rise from zero). As in actual fuel reactor condition, O<sub>2</sub> partial pressure should be zero. Thus, the uncoupling condition using CuO as oxygen carrier would start approximately at 700 °C. Both tests using TGA and the fixed bed reactor, confirmed that both commercial CuO and CLCA samples could be close to 100 % decomposition under 800-950 °C although their respective kinetics may vary. The evidence is directly from tests of the commercial CuO powder and CLCA

samples in the quartz tube reactor, when temperatures of reactor were above 800 °C (800 °C to 990 C), and indirectly from solid residue sample of the fixed bed reactor made of stainless steel. Thermodynamics accurately predict performance of CuO decomposition, but complicated phenomena may occur under different conditions. The experimental skills played major role in success and failure of obtaining the direct evidence of free oxygen release under uncoupling conditions.

Figure 26-2 Commercial CuO and CLCA sample 800 °C through 990 °C



 $(\bullet CuO ▲ Al<sub>2</sub>O<sub>3</sub> ∘ CuAl<sub>2</sub>O<sub>4</sub> △ Cu<sub>2</sub>O <math>\blacktriangledown CuAlO<sub>2</sub> ∘ Cu)$ 

Figure 26-3. SEM image of CLCA

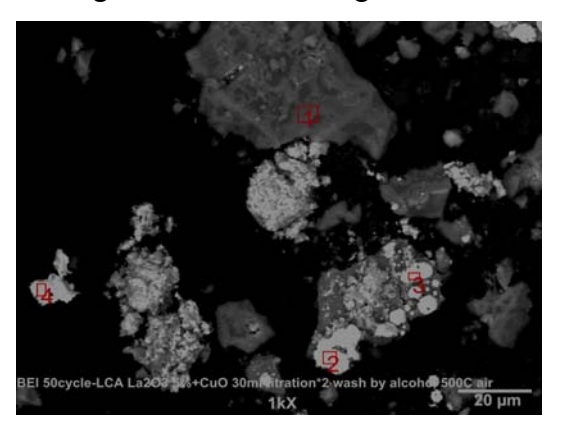
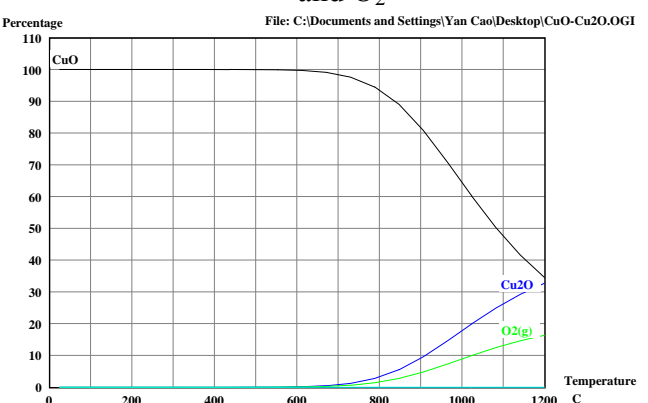


Figure 27. Equilibrium curves of CuO, Cu<sub>2</sub>O and O<sub>2</sub>



#### 2.6 Conclusion

Institute for Combustion and Environmental Technology (ICSET) of Western Kentucky University (WKU), has been working on the development of chemical looping combustion technology (CLC) over 10 years. The initialization of this research focus started in 2002 with exploring the feasibility of the coal-fueled CLC system under US DOE grant (DE-FG02-04ER84036). Copper-based materials were applied as oxygen carriers, and a circulating fluidized bed was applied as the prototype CLC system. The application of fuels have covered gas fuels (syngas and natural gas), liquid fuels (bitumen and asphalt), and solid fuels (biomass and coals). Copper was chosen as oxygen carrier because of their relatively, low toxicity and larger oxygen transfer capability. Most importantly, its exothermic reduction reaction can provide heat for the endothermic gasification of a solid fuel to form synthesis gas, as well as capability to produce free oxygen for the promoted combustion reaction kinetics.

Under joint financial supports from the Kentucky Energy and Environmental Cabinet (*PO2 127 0900025004 1*), Canada (Cenuvos) and US DOE grant (*DE-FE0001808*), the optimized chemical formula of the copper-based oxygen carrier has finally been confirmed for the prevention of agglomeration, while still maintaining the basic benefits of copper material, such as the higher redox reactivity and the near completeness of fuel conversion efficiencies. Results also indicated the supporting material, Al<sub>2</sub>O<sub>3</sub>, significantly impact the oxygen releasing performance and thermal stability of the Al<sub>2</sub>O<sub>3</sub>-supported CuO, comparing to the commercial CuO powder. The Al<sub>2</sub>O<sub>3</sub>-supported CuO presented a slow release of oxygen. However, there was no serious agglomeration of the copper constituent found on Al<sub>2</sub>O<sub>3</sub>-supported CuO. This contrasted the severe agglomeration that occurred in the commercial CuO powder. The quick formation of a new crystal phase (CuAl<sub>2</sub>O<sub>4</sub>), cross-linking CuO and γ-Al<sub>2</sub>O<sub>3</sub>, maybe a major reason for the stability of copper-based oxygen carrier and the slow oxygen release under high temperature uncoupling condition.

The cost-Effective and practical coal-based chemical looping combustion process has been developed in a 100 W fluidized bed chemical looping facility. Tests indicated that higher temperatures and longer residence times enhance carbon conversion of fed coals under 900-950 °C in the fuel reactor. The carbon conversion of U.S. Bituminous coal could be 50% when the solids residence time was controlled at about 8 minutes; and it increased to about 68% when the

solid residence time was increased to 15 minutes. The prepared copper-based oxygen carriers performed well in 20 cyclic redox operations. Significantly, there was no agglomeration of the copper constituent found on the used oxygen carriers.

The flow dynamics of solids recirculation without gas leakage between the air and fuel reactors have been investigated in a 10 kW equivalent cold-model CLC facility. Mastering the controls of constant solids recirculation, the prevention of gas leakage and the finalized formula of oxygen carrier moves forward the 10 kW hot model CLC system. This facility has been successfully operated using natural gas and liquid-fuel pyrolysis syngas for two years, and finally demonstrated for a continuous operation for 3 days. The evaluation of used oxygen carrier samples, collected after tests, indicated that only trace amounts of sulfur or carbon deposited on the copper-based oxygen carriers. During the normal operation period, less intensive manual handling of the system was necessary except for the initial period to the building-up the optimized solid-recirculation. There was absolutely the prevention of no gas leakage between the air and fuel reactors, which was independent on operation conditions. The evaluation of used oxygen carrier samples, collected after tests, indicated that only trace-amount of coke or carbon deposit on the copper-based oxygen carriers in the fuel Reactor, indicting the tendency of carbon deposits under current operational conditions, but has been maximized controlled by system tuning. There was also no evidence to show the sulphidization of oxygen carriers in the system by using the high-sulfur-laden asphalt fuels, the trace-amounts of sulfur on samples at two baghouses, where temperatures were as low as 150 °C.

The next step would be the system modification of the currently available 0.6 MW CFBC (DE-FC26-03NT41840) into a 1 MW CLC, as well as a new concept on the chemical-looping pure-oxygen production for replacing the ASU process.

# 2.7 Acknowledgement

Financial support for this project was provided by the U. S. Department of Energy National Energy Technology Laboratory (Cooperative Agreement NO. DE-FE0001808). Finally, the contributions of the project team members who actually executed the project work are greatly appreciated.

## 3. References

- [1] Final Report, "Advancing Oxycombustion Technology for Bituminous Coal Power Plants: An R&D Guide," DOE/NETL-2010/1405, Page 18, Exhibit 2-8, <a href="http://www.netl.doe.gov/energy-analyses/refshelf/PubDetails.aspx?Action=View&Source=Main&PubId=416">http://www.netl.doe.gov/energy-analyses/refshelf/PubDetails.aspx?Action=View&Source=Main&PubId=416</a>
- [2] McGlashan, N. R. (2008), Chemical-looping combustion a thermodynamic study, Proc. IMechE Vol. 222 Part C: J. Mechanical Engineering Science, pp.1005-1019. DOI: 10.1243/09544062JMES790
- [3] Sempuga, B. C.; Hausberger, B.; Patel, B.; Hildebrandt, D.; Glasser, D. (2010), Classification of Chemical Processes: A Graphical Approach to Process Synthesis To Improve Reactive Process Work Efficiency, *Ind. Eng. Chem. Res.* 49, pp. 8227–8237.
- [4] Anheden, M.; Svedberg, G. (1998), Exergy Analysis of Chemical-looping Combustion System, Energy Convers. Mgmt 39 (16-18), pp. 1967-1980.
- [5] Sempuga, B. C.; Hildebrandt, D.; Patel, B.; Glasser, D. (2010), Work to Chemical Processes: The Relationship between Heat, Temperature, Pressure, and Process Complexity. Ind. Eng. Chem. Res. 50, pp. 8603–8619.
- [6] Abad, A.; Mattisson, T.; Lyngfelt, A.; Ryd\_en, M. (2006), <u>Chemical-looping combustion</u> in a 300 W continuously operating reactor system using a manganese-based oxygen carrier, Fuel 85 (9), pp. 1174–1185.
- [7] Lyngfelt, A.; Kronberger, B.; Ad\_anez, J.; Morin, J.-X.; Hurst, P. (2004), In Seventh International Conference on Greenhouse Gas Control Technologies, Vancouver, Canada, Elsevier Science: Oxford, U.K.
- [8] Ryu, H. J.; Jin, G. T.; Yi, C. K. (2004), In Seventh International Conference on Greenhouse Gas Control Technologies, Vancouver, Canada, Elsevier Science: Oxford, U.K.
- [9] Kolbitsch, P.; Pr€oll, T.; Bolhar-Nordenkampf, J.; Hofbauer, H. (2009), Performance of a NiO-based oxygen carrier for chemical looping combustion and reforming in a 120 kW unit. Energy Proc. 1 (1), pp. 1465–1472.
- [10] Jin, H. G.; Ishida, M. (2004), A new type of coal gas fueled chemical-looping combustion Fuel 83, pp. 2411–2417.
- [11] Siriwardane, R.; Tian,H. J. George Richards. (2008), Chemical-Looping Combustion of Coal with Metal Oxide Oxygen Carriers, TWENTY FIFTH ANNUAL INTERNATIONAL PITTSBURGH COAL CONFERENCECOAL ENERGY, ENVIRONMENT AND SUSTAINABLE DEVELOPMENT, Pittsburgh, PA, USA.
- [12] Dennis, J. S., Scott, S. A. (2010), In situ gasification of a lignite coal and CO<sub>2</sub> separation using chemical looping with a Cu-based oxygen carrier Fuel 89, pp. 1623–1640.
- [13] Song Q., Xiao R., Deng Z., Shen L., Xiao J., Zhang M. (2008), Effect of temperature on reduction of CaSO<sub>4</sub> oxygen carrier in chemical-looping combustion of a simulated flue gas in a fluidized bed reactor. Ind Eng. Chem. Res. 47, pp. 8148–59.
- [14] Scott S. A., Dennis J. S., Hayhurst, A.N., Brown T. (2006), In situ gasification of a solid fuel and CO<sub>2</sub> separation using chemical looping. AIChE J. 52, pp. 3325–3328.
- [15] Leion H., Mattisson T., Lyngfelt A. (2007), The use of petroleum coke as fuel in chemical looping combustion. Fuel 86, pp.1947–58.
- [16] Leion H, Mattisson T, Lyngfelt A. (2008), Solid fuels in chemical looping combustion. Int. J. Greenhouse Gas Control 2, pp.180–93.
- [17] Lyon R. K., Cole J. A. (2000), Unmixed combustion: an alternative to fire. Combust

- Flame 121, pp. 249-61.
- [18] Dennis J. S., Scott S. A, Hayhurst A. N. (2006), In situ gasification of coal using steam with chemical looping: a technique for isolating CO<sub>2</sub> from burning a solid fuel. J. Energy Inst 79, pp.187–90.
- [19] Berguerand N., Lyngfelt A. (2008), Design and operation of a 10 kWth chemical-looping combustor for solid fuels testing with South African coal. Fuel 87, pp.2713–26.
- [20] Rubel, A.; Zhang, Y.; Neathery, J. K.; Liu, K. L. (2009), Comparative study of the effect of different coal fly Ashes on the performance of oxygen carriers for chemical looping combustion. Fuel, 88, p. 876.
- [21] Cuadrat, A.; Abad, A.; de Diego, L. F.; García-Labiano, F.; Gayán, P.; Adánez, J. (2012), Prompt considerations on the design of Chemical-Looping Combustion of coal from experimental tests. Fuel, 6(4), pp.153-163.
- [22] Gao, A. P.; Shen, L. H.; Xiao, J.; Qing, C. J. Song, Q. L. Use of Coal as fuel for chemical-looping combustion with Ni-based oxygen carrier. (2008), Ind. Eng. Chem. Res. 47, pp. 9279–9287.
- [23] Lewis, W. K.; Gilliland, E. R. (1954), Production of pure carbon dioxide. US Patent No: 2665972.
- [24] Cao, Y.; Pan, W. P. (2006), Investigation of Chemical Looping Combustion by Solid Fuels. 1. Process Analysis. Energy Fuels 20 (5), pp.1836–1844.
- [25] Pan, W. P.; Cao, Y.; Liu, K. L.; Wu, W. Y.; Riley, J. T. (2004), Abstr. Pap. Am. Chem. Soc. 228, U676–U676.
- [26] Wang, J. S.; Anthony, E. (2008), Clean combustion of solid fuels. J. Applied Energy 85, pp. 73–79.
- [27] Shen, L. H.; Wu, J. H.; Xiao. (2009), Experiments on Chemical Looping Combustion of Coal with a NiO based Oxygen Carrier. J. Combust. Flame 156 (3), pp. 721–728.
- [28] Shen, L. H.; Wu, J. H.; Gao, Z. P.; Xiao. (2009), Reactivity Deterioration of NiO/Al2O3 Oxygen Carrier of Chemical Looping Combustion of Coal in A 10 kW Reactor. J. Combust. Flame 156 (7), pp. 1377–1385.
- [29] Shen, L. H.; Wu, J. H.; Xiao, J.; Song, Q. L.; Xiao, R. (2009), <u>Chemical-Looping Combustion of Biomass in a 10 kW<sub>th</sub> Reactor with Iron Oxide As an Oxygen Carrier</u>. Energy Fuels 23, pp. 2498–2505.
- [30] Forret, A.; Hoteit, A.; Gauthier, Th. (2010), Chemical Looping Combustion Processes Applied to Liquid Fuels. The 1st International Conference on Chemical Looping Combustion IFP-Lyon, France.
- [31] Cao, Y.; Li, B.; Zhao, H. Y.; Lin, C. W.; Sit, S. P. Pan, W. P. (2011), Investigation on Asphalt (Bitumen)-Fueled Chemical Looping Combustion Using Durable Cu-based Oxygen Carriers. Energy Procedia 4, pp. 457–464.
- [32] Shen, L.H.; Wu, J.; Gao, Z.; Xiao. (2010), J. Combust. Flame.15, pp. 934-942.
- [33] Linderholm, C.; Cuadrat, A.; Lyngfelt, A. (2011), Chemical-looping combustion of solid fuels in a 10 kWth pilot batch tests with five fuels. Energy Procedia 4, pp. 385-392.
- [34] Kolbitsch, P.; Pröll, T.; Bolhar-Nordenkampf, J.; Hofbauer, H. (2009), Operating experience with chemical looping combustion in a 120kW dual circulating fluidized bed (DCFB) unit. Energy Procedia, 1(1), pp.1465-1472.
- [35] Li, F.; Kim, H. R.; Sridhar, D.; Wang, F.; Zeng, L.; Chen, J.; Fan, L. S. (2009), Syngas Chemical Looping Gasification Process: Oxygen Carrier Particle Selection and Performance. Energy Fuels 23, pp. 4182-4189.

- [36] Adanez, J.; Abad, A.; Garcia-Labiano, F.; Gayan, P.; de Diego, L.F. (2012), Progress in Chemical-Looping Combustion and Reforming Technologies. A review. Prog. Energ. Combust. *38*, pp. 215-282.
- [37] Cuadrat, A.; Abad, A.; Garcia-Labiano, F.; Gayan, P.; de Diego, L. F.; Adanez. (2011), The use of ilmenite as oxygen-carrier in a 500 Wth Chemical-Looping Coal Combustion unitJ. Int. J. Greenhouse Gas Control *5*, pp.1630-1642.
- [38] Mattisson, T., Lyngfelt A. Leion H. Chemical-looping with oxygenuncoupling for combustion of solid fuels, International Journal of Greenhouse Gas, 2009, 3(1), 11-19.
- [39] Shulman, A., Cleverstam, E., Mattisson, T., Lyngfelt, A. Manganese/Iron, Manganese/Nickel, and Manganese/Silicon Oxides Used in Chemical-Looping With Oxygen Uncoupling (CLOU) for Combustion of Methane, *Energy Fuels*, 2009, *23* (10), 5269–5275
- [40] Edward M., Eyring, Gabor Konya, JoAnn Lighty, Asad Sahir, Adel F. Sarofim, Kevin Whitty. Chemical Looping with Oxygen Uncoupling. 2010 NETL CO<sub>2</sub> Capture Technology Meeting, Pittsburgh, PA. September 15, 2010
- [41] Lyngfelt, A. Chemical Looping Combustion of Solid Fuels Status of Development, 2012 2<sup>nd</sup> International Conference on CLC, 26-28 September 2012, Darmstadt, Germany.
- [42] Cao, Y.; Pan, W. P. Investigation of Chemical Looping Combustion by Solid Fuels. 2. Redox Reaction Kinetics and Product Characterization with Coal, Biomass, and Solid Waste as Solid Fuels and CuO as an Oxygen Carrier, Energy Fuels 2006, 20 (5), 1845–1854.
- [43] Moghtaderi, B. Application of Chemical Looping Concept for Air Separation at High Temperatures, Energy Fuels 2010, 24, 190–198.